A Technical and Economic Assessment of Geothermal Aided Power Generation

Masters by Research Thesis

Jiyun Qin

THE UNIVERSITY of ADELAIDE

The University of Adelaide

The School of Mechanical Engineering

May 2013

Abstract

With the increase in demand for energy and the need for environmental protection, geothermal energy, as a renewable resource, is receiving growing attention. Stand alone geothermal power stations have been established all over the world. However these systems predominantly harvest volcanic resources, which have limited availability, while the more widespread deep resources are still expensive to access. Integrating the geothermal resources into a conventional fuel fired Rankine cycle power plant, through the so called “geothermal aided power generation” (GAPG) concept. In so called GAPG technology, geothermal fluid is used to replace parts of extraction steam in regenerative Rankine cycle power plant to preheat feedwater of power plant. The GAPG technology can significantly increase the efficiencies and reduce the costs of geothermal energy for power generation purposes.

The general aim of this research is to comprehensively study the advantages and disadvantages of geothermal aided power generation by developing and validating a simulation model that can be used as a tool for the technical and economic analysis of a GAPG system. The developed modelling simulates the steam Rankine power plant so as to assess the technology and to provide an economic analysis of GAPG technology for a variety of structural types of power plant. Two case studies are carried out with modelling. A 500 MW subcritical power plant is used as case study to study the technical performance of GAPG technology for both power boosting mode and fuel

saving mode. Two coal fired power plants, a 580 MW subcritical coal fired power plant and a 580 MW supercritical coal fired power plant, are selected as study cases to demonstrate the economic advantages of the GAPG technology with medium to low temperature geothermal resources. Cost of electricity (COE) of GAPG technology in two cases is used to compare with that in a flash cycle geothermal power plant and a binary cycle geothermal power plant.

The results indicate that the GAPG technology has higher thermodynamic first law efficiency than the geothermal alone power plant and the efficiency of the GAPG technology is no longer limited by the temperature of geothermal fluid, but rather by the maximum temperature of the Rankine cycle power plant. It is also found that utilization of the existing infrastructure of conventional fossil fired power plants can demonstrate the economic advantages of the GAPG technology as the lower COE than the geothermal alone power plant.

Chapter one of this thesis defines the concept, aims and scope of this study. Chapter two details the previous research in the field of this study. The functions and structure of modelling for GAPG technology are described in chapter three. Chapter four presents the operational method and the modelling validation. Two case studies are carried out by modelling, with the technical and economic performance of GAPG technology presented in chapters five and six.

Declarations

This work contains no material which has been accepted for the award of any other degree or diploma in any university or other tertiary institution and, to the best of my knowledge and belief, contains no material previously published or written by another person, except where due reference has been made in the text.

I give consent to this copy of my thesis, when deposited in the university Library, being made available for load and photocopying, subject to the provisions of the Copyright Act 1968.

Jiyun Qin

Acknowledgments

The author would like to express my gratitude to my principal supervisor Associate Professor Eric Hu for the opportunity for me to work on this project. He gave to me kind encouragement and useful and instant instructions all through my project. A special acknowledgement to my co-supervisor Graham Nathan, from whose suggestions I benefited greatly. Finally, I extent my greatest thanks to my parents whose support has enabled me to continue working on the project to completion.

Table of Contents

Abstract……..i

Declarations……..iii

Acknowledgements……..iv

List of figures……...ix

List of tables……..xiii

List of symbols and abbreviations……..xv

1 Introduction

1.1 Background……..……..……1

1.2 Geothermal Aided Power Generation…….……6

1.2.1 Regenerative rankine cycle…….……..6

1.2.2 Geothermal Aided Power Generation……..……9

1.3 Aims of this study……..13

1.3.1 General aims……...…….……...13

1.3.2 Specific objectives…….....……..13

1.4 Scope and limitations of this study……..……..15

1.4.1 Scope of technical sub model…….……15

1.4.2 Scope of economic sub model……17

2 Literature Review

2.1 Geothermal power generation…..……..…….……...18

2.2 Hybrid geothermal fossil electricity power generation…….22

2.3 Integrating other thermal resources into power generation……...25

2.4 Previous models of the use of geothermal fluid to preheat feedwater for power generation……28

3 Modelling Descriptions

3.1 Introduction……...30

3.2 The physical model of GAPG technology…….33

3.3 Technical sub model of GAPG technical……...36

3.3.1Steam turbine module …….38

3.3.2 Feedwater heater modules……..……41

3.3.3 Deaerator module...……43

3.3.4 Condenser module……..45

3.3.5 Boiler module…….47

3.3.6 Geothermal aided module……...49

3.3.7 Assessment of GAPG technology……...62

3.4 Economic sub model…….66

3.4.1 Cost of electricity (COE)……67

3.4.2 Capital cost of GAPG technology……..68

3.4.3 Capital cost of Geothermal alone power plant……...70

4 Programming and Model Validation

4.1 Programming of the mathematical modelling……...75

4.1.1 Introduction……75

4.1.1.1 Structure of GAPGEM……76

4.1.1.2 Steam cycle Structure type…….……78

4.1.2 Operation layout and usage……..……..78

4.1.2.1 List of sheets of GAPGEM programming…….……78

4.1.2.2 An example case for GAPGEM…….……80

4.2 Model validation of mathematical modelling……....90

5 Technical Case Study

5.1 Introduction…….……..95

5.2 First law analysis of GAPG in this case study…….101

5.3 Second law analysis of GAPG technology……..107

6 Economic Case Study

6.1 Introduction……..112

6.1.1 Geothermal well field and geothermal power plant……..112

6.1.2 Coal fired power plant…..……114

6.1.3 Scenarios of case study…….119

6.2 Results……..121

6.2.1 Technical performance of GAPG……..121

6.2.2 Cost of GAPG geothermal power plant……122

6.2.3 Cost of GAPG technology ……..125

6.2.4 COE of four scenarios ……...……...126

7 Conclusion……..129

8 Future Work……...…….132

References…….134

List of Figures

Figure 1.1 T-S diagram of a basic Rankine steam cycle.....7

Figure 1.2 T-s diagram of a typical regenerative and reheating Rankine steam cycle…..8

Figure 1.3 Typical schematic diagram of a feedwater heater with a geothermal fluid (heat exchanger) by-pass…….10

Figure 1.4 Two operational modes of a GAPG plant……..…….12

Figure 2.1 Simplified diagram of a single-flash power plant schematic (DiPippo 2008)……20

Figure 2.2 Simplified schematic diagram of a double-flash power plant schematic (DiPippo 2008)……....20

Figure 2.3 Simplified schematic flow diagram of a dry steam plant (DiPippo 2008)……21

Figure 2.4 Simplified schematic diagram of a basic binary geothermal power plant (DiPippo 2008)……21

Figure 3.1 Structure of correlations of the technical sub model and the economic sub model……..…….32

Figure 3.2 Schematic diagram of a typical coal fired power plant (with two closed feedwater and one deaerator) with GAPG technology……34

Figure 3.3 Schematic diagram structure of the steam turbine with extraction points for steam used in mathematical model…….…….38

Figure 3.4 Schematic diagram of the model of the closed feedwater

heater……..…….……..……..42

Figure 3.5 Schematic diagram of the structure of the Open Feedwater Heater used in the mathematical model……..……..44

Figure 3.6 Schematic diagram of the condenser that is modelled…….…..…46

Figure 3.7 Schematic diagram of the boiler modelled here……..……...47

Figure 3.8 Schematic diagram of the model of the Closed Feedwater Heater with Geothermal preheater.....51

Figure 3.9 Typical schematic diagrams of one stage of steam turbine…….…..….55

Figure 3.10 Precipitation rate of amorphous silica as a function of temperature and silica concentration (Bhuana, Ashman & Nathan, 2009)……..59

Figure 3.11 Schematic diagram of a GAPG power generation with full replacement of all closed feedwater heaters (the dashed line indicates the boundary for exergy analysis).....64

Figure 4.1 Flow chart of the software program of GAPGEM…….…..……...77

Figure 4.2 Input sheet of GAPGEM……..…….……82

Figure 4.3 Geodata sheet of GAPGEM……...84

Figure 4.4 Input data regarding of geothermal wells……...85

Figure 4.5 Input data regarding of geothermal power plant……86

Figure 4.6 Input of combustion power plant and GAPG technology……..87

Figure 4.7 Technical output of Report sheet……88

Figure 4.8 Report sheet for the economic calculation…..…….…...88

Figure 4.9 Heat and steam balance of the 500 MW LOY YANG unit at design condition…….……..……91

Figure 4.10 Heat and steam balance of the supercritical unit at design condition……..92

Figure 5.1 Heat and steam balance of the 500 MW unit at design condition……..96

Figure 5.2 Schematic diagram of the subcritical power plant feedwater system with GAPG technology, scenario 1, replacing the extraction steam at point A…….…..98

Figure 5.3 Schematic diagram of the subcritical power plant feedwater system with GAPG technology, scenario 2, replacing the extraction steam at point B…….……..98

Figure 5.4 Schematic diagram of subcritical power plant feedwater system with GAPG technology, scenario 3, replacing all the extraction steam at point A, B, D, E, F……...99

Figure 5.5 Schematic diagram of subcritical power plant feedwater system with GAPG technology, scenario 4, replacing the extraction steam at point D, E and F……..100

Figure 5.6 Extra power output from the steam turbine for the scenario one and scenario two of different proportions of replacement of bled steam in the power boosting mode……..……....102

Figure 5.7 Saved fossil fuel of power plant at extraction point A and B in different proportion of replacement (fuel saving mode)……..102

Figure 5.8 Mass flow rate of geothermal fluid in different operational mode for four scenarios……103

Figure 5.9 Efficiencies of the geothermal component of the power in the GAPG system for different scenarios……105

Figure 5.10 Schematic diagram of LOY YANG power plant (the dotted line indicates

the boundary for exergy analysis, scenario 2)…….……..…108

Figure 6.1 Heat and steam balance of the 580 MW unit at design condition……....115

Figure 6.2 Heat and steam balance of the supercritical unit at design condition…..…117

Figure 6.3 Schematic diagram of the subcritical power plant feedwater system with GAPG technology in which FWH 4,3,2 are fully replaced by geothermal fluid ...…..120

Figure 6.4 Schematic diagram of supercritical power plant feedwater system with GAPG technology in which FWH 4,3,2 are fully replaced by geothermal fluid….….120

List of Tables

Table 1.1 OECD and non-OECD net electricity generation by energy source, 2008-2035 (trillion kilowatt-hours) (USEIA, 2011)……2

Table 1.2 OECD and non-OECD net renewable electricity generation by energy source, 2008-2035 (billion kilowatt-hours) (USEIA, 2011)……..3

Table 1.3 Variation in the installed capacity of geothermal power generation from 1975 to 2005 and the variation in electricity production from 1995 to 2005(Bertani 2005)……..4

Table 3.1 Temperature functions of the rate constants for silica-water reactions (Rimistidt and Barnes 1980)…….…….……..61

Table 4.1 Comparison result of operational parameters and simulated parameters of subcritical power generation……92

Table 4.2 Comparison result of operational parameters and simulated parameters of supercritical power generation…….....93

Table 5.1 Parameters of LOY YANG power plant……..……95

Table 5.2 Replacing scenarios and numbers of subcritical power plants……..…….97

Table 5.3 Exergy efficiency of power plant alone and four scenarios……...109

Table 5.4exergy input into the boiler……..……...109

Table 5.5 Exergy destruction of condenser…….…….……..109

Table 5.6 Exergy destruction of steam turbine…….…….……110

Table 5.7 Exergy destruction for each feedwater heater (without deaerator)…….…...111

Table 6.1 Technical performance of binary cycle power plant……..113

Table 6.2 Technical performance of flash cycle power plant……114

Table 6.3 Simulated technical performance of subcritical power plant…….114

Table 6.4 Capital cost of the 580MW subcritical power plant (NETL, 2007)……..…116

Table 6.5 Maintenance material Cost (O&M Cost) of subcritical power plant (NETL, 2007)…….116

Table 6.6 Calculated technical performance of supercritical power plant……..……..117

Table 6.7 Capital cost of 580MW supercritical power plant (NETL, 2007)…….118

Table 6.8 Maintenance material Cost (O&M Cost) of supercritical power plant (NETL, 2007)……..118

Table 6.9 Four scenarios of economic case study…….……119

Table 6.10 Technical performance of the GAPG technology for the subcritical power plant…….…….…….121

Table 6.11 Technical performance of GAPG technology for the supercritical power plant……..…122

Table 6.12 Costs of geothermal well fields (for the binary cycle power plant)…….…123

Table 6.13 Capital cost and O&M cost of binary cycle power plant…….124

Table 6.14 Costs of geothermal well fields (double flash cycle power plant)….……..124

Table 6.15 Capital cost and O&M cost of double flash cycle power plant……...124

Table 6.16 Costs of geothermal well fields (subcritical GAPG technology)……125

Table 6.17 Costs of geothermal well fields (supercritical GAPG technology…….…..126

Table 6.18 COE of four scenarios for economic case study……..128

List of Symbols and Abbreviations

Abbreviation

COE	Cost of Electricity
DEA	Deaerator
FWH	Feed Water Heater
GAPG	Geothermal Aided Power Generation
GAPGEM	Geothermal Aided Power Generation Evaluation Model
HPH	High Pressure Feedwater Heater
IPH	Intermediate Pressure Feedwater Heater
LPH	Low Pressure Feedwater Heater

Symbol

		Unit
H	Specific enthalpy	kJ/kg
M	Mass flow rate	Kg/s
Q	Heat flow	J/s
S	Specific entropy	kJ/kg.K
T	Temperature	℃
W	Work	J/s
X	Specific exergy	kJ/kg

Chapter 1

Introduction

1.1 Background

With rapid economic development, the consumption of electricity has supplied an increasing share of the world's total consumption of energy. The report from the U.S. Energy Information Administration (2011) shows that the increase of electricity demand has grown more rapidly than the demand for liquid fuels, natural gas and fossil fuels. The traditional fuels used to produce electricity are coal, natural gas, liquid fuels and nuclear power. Coal is the most widely used fuel to produce electricity. In 2008, coal fired power plants generated 40 percent of world electricity (U.S. Energy Information Administration 2011). However, with the increasing awareness of the negative environmental impacts from carbon dioxide, which is an emission from coal fired power plants, the use of other kinds of energy resources to produce electricity has become more attractive. Renewable resources, such as geothermal energy, solar energy and wind energy, are receiving growing attention for the production of electric power. The data from U.S Energy Information Administration (2011) shows that renewable energy is the

fastest growing energy source of electricity production in recent years and that the electricity production from renewable energy increases by 3.1 percent per year. Table 1.1, which shows net electricity generation by different kinds of energy source, shows that the average annual percent increase in renewable energy sources (3.1 percent) world-wide will be 1.2 percent greater than the average increase in coal (1.2 percent).

Table 1.1 OECD and non-OECD net electricity generation by energy source, 2008-2035 (trillion kilowatt-hours) (USEIA, 2011)

Region	2008	2015	2020	2025	2030	2035	Average annual percent change
OECD							
Liquids	0.4	0.3	0.3	0.3	0.3	0.3	-0.8
Natural gas	2.3	2.5	2.7	2.9	3.4	3.8	1.8
Coal	3.6	3.3	3.4	3.5	3.6	3.8	0.2
Nuclear	2.2	2.4	2.6	2.7	2.8	2.9	1.0
Renewables	1.8	2.3	2.7	2.9	3.1	3.2	2.2
Total OECD	10.2	10.9	11.6	12.4	13.2	13.9	1.2
Non-OECD							
Liquids	0.7	0.6	0.6	0.6	0.5	0.5	-1.0
Natural gas	1.8	2.4	3.0	3.5	4.1	4.6	3.4
Coal	4.1	5.2	5.6	6.7	7.9	9.1	3.0
Nuclear	0.4	0.7	1.2	1.5	1.7	2.0	6.0
Renewables	1.9	2.8	3.6	4.0	4.5	5.0	3.7
Total non-OECD	8.9	11.8	13.9	16.3	18.8	21.2	3.3
World							
Liquids	1.0	0.9	0.9	0.9	0.8	0.8	-0.9
Natural gas	4.2	4.9	5.6	6.5	7.5	8.4	2.6
Coal	7.7	8.5	8.9	10.2	11.5	12.9	1.9
Nuclear	2.6	3.2	3.7	4.2	4.5	4.9	2.4
Renewables	3.7	5.1	6.3	7.0	7.6	8.2	3.1
Total World	19.1	22.7	25.5	28.7	31.9	35.2	2.3

Table 1.2 predicts the OECD and non OECD new renewable electricity production

from different sources. It can be seen that from 2008 to 2035, the renewable energy generated from wind, geothermal and solar is extrapolated to grow at 7.5, 4.2, and 10.6 percent per year, respectively.

Table 1.2 OECD and non-OECD net renewable electricity generation by energy source, 2008-2035 (billion kilowatt-hours) (USEIA, 2011)

Region	2008	2015	2020	2025	2030	2035	Average annual percent change
OECD							
Hydroelectric	1,329	1,418	1,520	1,600	1,668	1,717	1.0
Wind	181	492	492	806	852	898	6.1
Geothermal	38	56	56	79	93	104	3.8
Solar	12	68	68	95	105	120	8.8
Other	217	268	268	362	381	398	2.3
Total OECD	1,778	2,302	2,302	2,941	3,099	3,236	2.2
Non-OECD							
Hydroelectric	1,791	2,363	2,946	3,224	3,536	3,903	2.9
Wind	29	219	347	426	499	564	11.6
Geothermal	22	56	58	61	70	81	5.0
Solar	0	19	48	60	65	71	22.8
Other	41	132	186	252	321	375	8.5
Total non-OECD	1,884	2,788	3,585	4,023	4,491	4,995	3.7
World							
Hydroelectric	3,121	3,781	4,465	4,823	5,204	5,620	2.2
Wind	210	710	1,035	1,232	1,350	1,462	7.5
Geothermal	60	112	125	139	163	186	4.2
Solar	13	87	134	155	170	191	10.6
Other	258	400	496	614	701	772	4.1
Total World	3,662	5,091	6,256	6,964	7,590	8,232	3.1

Renewable energy has the advantage of low environmental emissions and increased security. However, some of the renewable energy sources such as solar and wind energy have the disadvantage of being of an intermittent nature. Compared with

other renewable energy such as solar and wind energy, geothermal energy has the advantage of being non-intermittent, although its temperature is relatively low (typically 260℃). This limits its conversion efficiency. Stand alone geothermal power stations have been established all over the world. Table 1.3 shows the variation in the installed capacity of geothermal power generation from 1975 to 2005 and the variation in electricity production from 1995 to 2005 (Bertani, 2005).

Table 1.3 Variation in the installed capacity of geothermal power generation from 1975 to 2005 and the variation in electricity production from 1995 to 2005(Bertani 2005)

Year	Installed capacity (MWe)	Electricity generation (GWh/year)
1975	1300	N/A
1980	3887	N/A
1985	4764	N/A
1990	5832	N/A
1995	6832	38,035
2000	7972	49,261
2005	8933	56,786

For the low to medium temperature geothermal resources in the range of 90℃ -260℃, the common commercially available technologies for power plant are flash cycles and binary cycles including Organic Rankine Cycles (ORC). From the thermodynamic point of view, the efficiency of a geothermal power plant is capped by the temperature of the geofluid (out of ground) in a geothermal alone power plant. On the other hand, fossil-fuel combustion based power plant, which is presently the backbone of the global economy, has a better efficiency as the combustion temperature is much higher.

Properly integrating fossil fired power plants and geothermal energy sources is a practical way to efficiently use geothermal energy and reduce emission from power production. In this study a method of integrating geothermal energy into a conventional fossil fired power plant called geothermal aided power generation (GAPG) is analysed.

In order to promote thermal efficiency in a conventional fossil fired steam power cycle, part of the steam is bled from the turbine to pre-heat the feed-water in the so called regenerative Rankine cycle. The bled steam is also named extraction steam. Almost all power plants nowadays incorporate theses stages of regeneration. The GAPG technology uses geothermal resources to replace the extraction steam in a conventional regenerative Rankine power plant. Therefore in GAPG technology, the efficiency of geothermal energy (to power) is no longer capped by the temperature of the geothermal fluid.

1.2 Geothermal Aided Power Generation

1.2.1 Regenerative Rankine cycle

In a fossil fuel fired Rankine steam cycle power plant, the fuel is burned in the boiler to convert the chemical energy into heat energy and transfers heat into the water/steam. The steam is sent to a steam turbine where the mechanical energy is generated which is used to power the generator.

Four thermodynamic process are employed in a basic Rankine steam cycle, as shown in Fig.1.1:

1. Process 1-2: the working fluid (feedwater) is pumped from low pressure to high pressure.
2. Process 2-3: the working fluid (feedwater) is heated at constant pressure by an external heat source in the boiler. The working fluid in this process is heated to the dry saturated vapour.
3. Process 3-4: the working fluid (steam) is expanded in the steam turbine. In the ideal cycle, this process in the steam turbine is isentropic.
4. Process 4-1: the working fluid is cooled in the condenser to a saturated liquid at a constant temperature.

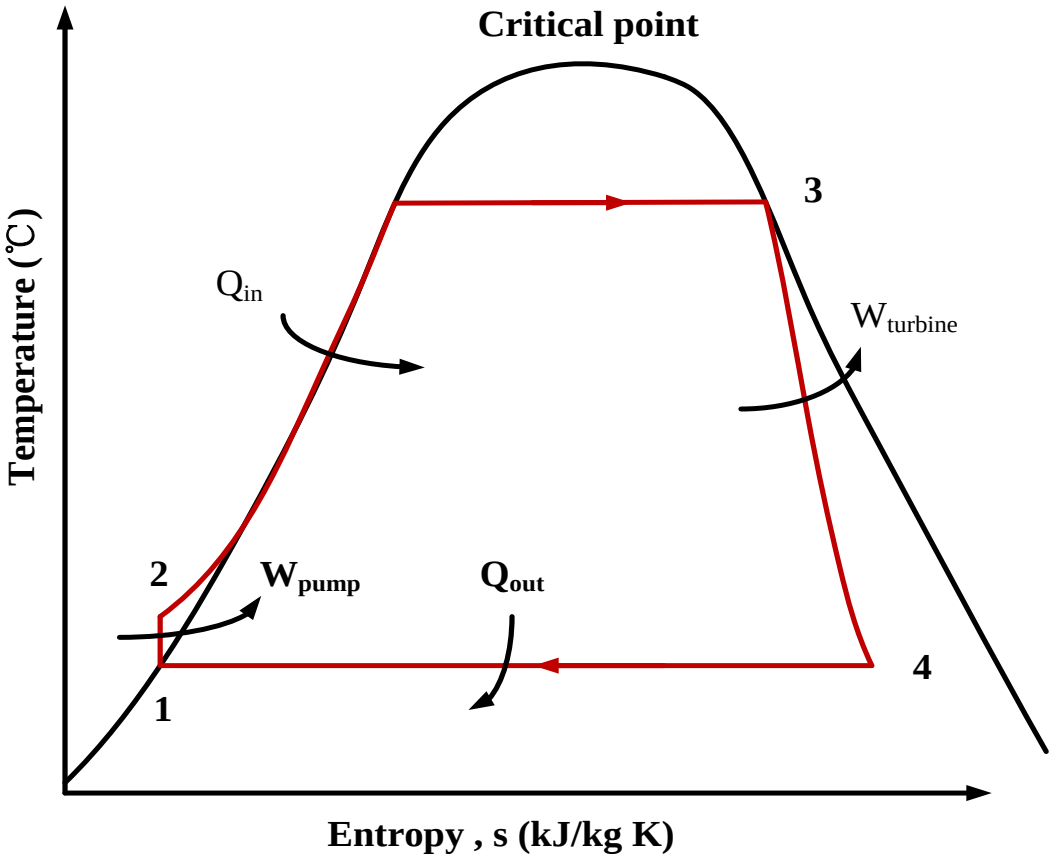

Figure 1.1 T-S diagram of a basic Rankine steam cycle

In order to improve the efficiency of the basic Rankine cycle the regenerative and reheating Rankine steam cycle is often used (Cengel, Boles 2000). Figure 1.2 shows the T-s diagram of a typical regenerative and reheating Rankine steam cycle.

Process 5-6 in Fig. 1.2 is the reheat process, in which the steam that has been partially expanded in the steam turbine is reheated in the reheater. Process 5-8 in Fig. 1.2 is regenerative. In the regenerative process, some of the steam is bled from the steam turbine and used to preheat the feedwater (from 2 to 8) in the feedwater heater (FWH). The bled off steam is also called the extraction steam. By so doing, the overall

steam cycle efficiency can be increased; however, the power generation by per unit of steam in the cycle and the work ratio of the cycle would decrease (Cengel, Boles 2000).

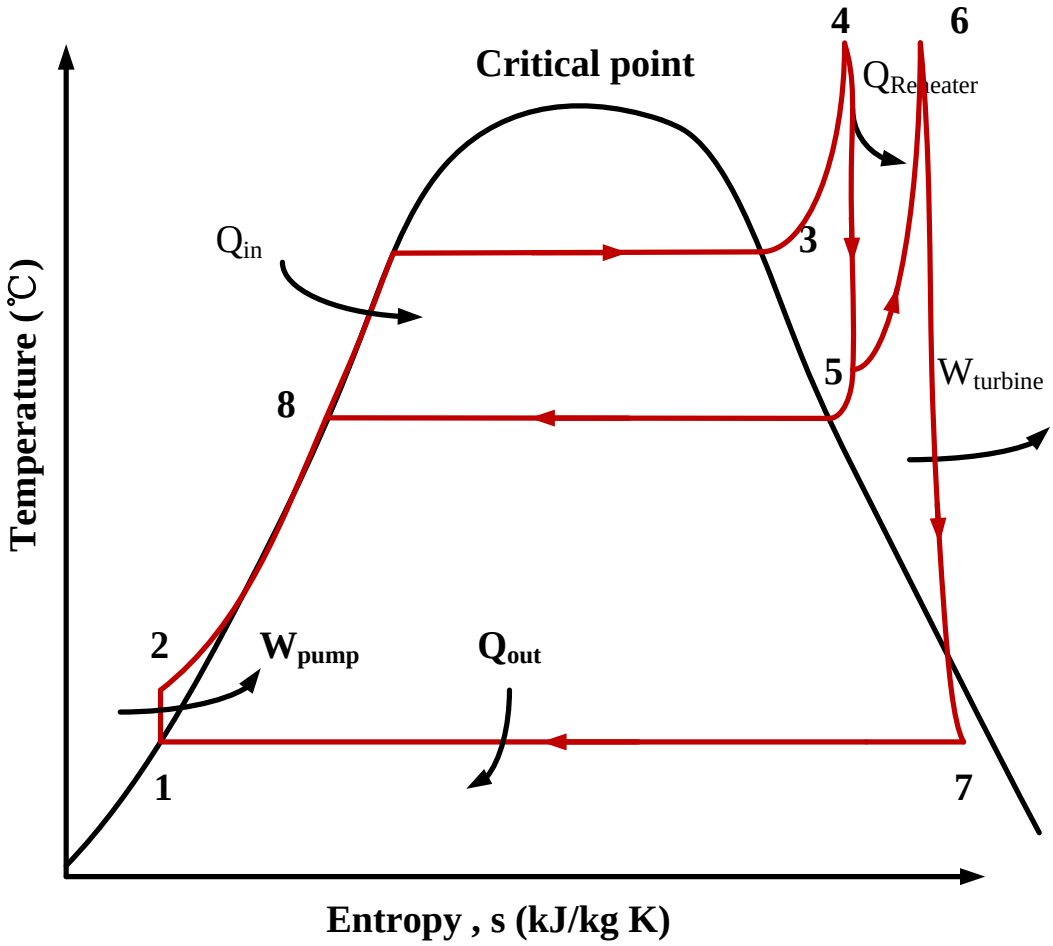

Figure 1.2 T-s diagram of a typical regenerative and reheating Rankine steam cycle

Types of feedwater heaters used in practice: open and closed feed heaters

The open feedwater heater

The open feedwater heater is a mixing chamber (Cengel, Boles 2000). The extraction steam from the steam turbine mixes directly with the feedwater from the

pump. In the ideal process of the open feedwater heater, the mixture feedwater leaves the feedwater as saturated liquid at the pressure of the feedwater.

The closed feedwater heater

The closed feedwater heater is a non-contact heat exchanger. The heat is transferred from the extraction steam to the feedwater heater without any mixing taking place. The ideal process for a closed feedwater heater involves the extraction steam leaving e the feedwater heater as a saturated liquid at the extraction pressure and moving to the other stages of the feedwater heater or condenser. During this process, the pressure of extraction steam and feedwater is kept constant.

A modern power plant can have up to 8 stages of regeneration, most of which are achieved with a closed feed heater. Typically only one open feedwater heater is used in a power plant, which doubles as a deaerator used for removing oxygen from saturated feedwater (Yan *et al.* 2010).

1.2.2 Geothermal Aided Power Generation (GAPG)

The GAPG technology is a way to integrate geothermal resources into the regenerative Rankine steam power cycle. In the GAPG, the geothermal fluid is used to replace the extraction steam to partially or fully preheat the feedwater. The extraction steam is replaced by geothermal heat, so that the saved steam can then expand further in the lower stages of the turbine to produce electricity. The key difference between the

GAPG and other multi-sources hybrid (boosting) power generation is that the geothermal energy (heat) does not enter the turbine directly.

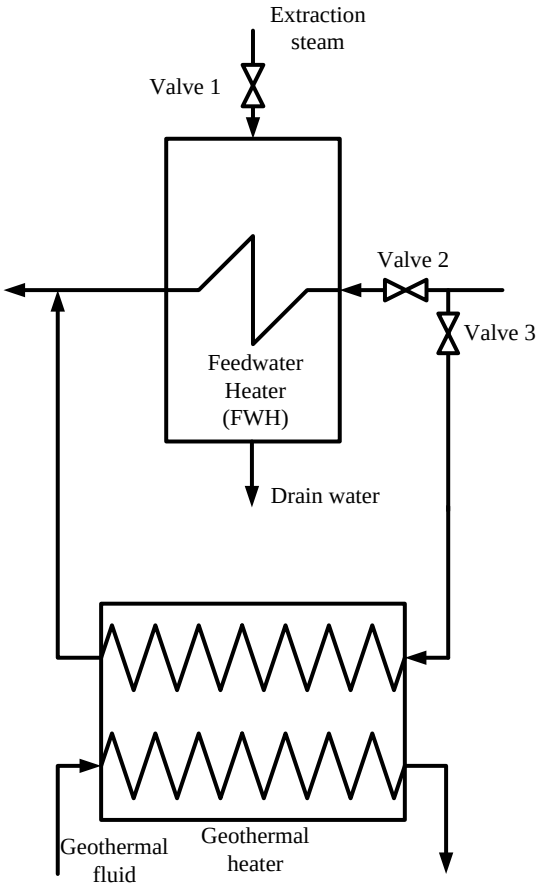

Figure 1.3 Typical schematic diagram of a feedwater heater with a geothermal fluid (heat exchanger) by-pass

In practice the geothermal fluid is integrated through a by-pass heat exchanger, called a geothermal heater in this thesis, as shown in Fig. 1.3. If the geothermal fluid is designed to partly replace the extraction steam, the feedwater flows entering the feedwater heater or by-pass heat exchanger can be controlled by valves (2 and 3 in Fig. 1.3). If the geothermal fluid is sufficient to replace all the extraction steam at this stage,

valves 1 and 2 would be closed to allow all the feedwater to pass through the geothermal heater to be preheated by geothermal fluid.

The concept of the geothermal aided power generation was presented in the late 1970s by DiPippo (Kestin, DiPippo & Kestin 1978). In recent years, the idea of using geothermal (or solar) resources to preheat the feedwater has been analysed by Bruhn (2002), Butcha (2010) and Hu (2010). Hu (2010) summarised the advantages of integrating geothermal resources into the fossil fired Rankine steam cycle power generation as follows :

- Compared with the fossil fuel fired Rankine steam cycle power plant and the geothermal alone power plant, the GAPG technology has higher thermodynamic first law and second law efficiencies.
- Integrating the geothermal resources into the power plant has relatively low capital costs and high social, environmental and economic benefits.
- The GAPG technology can be applied not only to the new power plant but also to existed power plants.
- The benefit from GAPG technology can come from two operational modes: power boosting and fuel saving. The schema of these two operational modes is shown in Fig. 1.4 (kolb 1978).

Power boosting mode: In the power boosting mode, the boiler consumes the

same amount of fuel and the mass flow rate of feedwater entering the boiler is kept constant. Therefore by using geothermal heat to replace the extraction steam (to preheat the feedwater), more steam passes through the lower stages of the turbine, thus generating more power.

Fuel saving mode: In the fuel saving mode, the power output of the steam turbine remains constant. Therefore, by using geothermal heat to replace the extraction steam (to preheat the feedwater), the flow rate of feedwater (entering the boiler) can be reduced. As a result, the fuel consumption (in the boiler) is reduced.

The power boosting mode of the GAPG system suits peak load operation when the electricity demand is high. On the other hand, the fuel saving mode suits off-peak generation when the electricity demand is low.

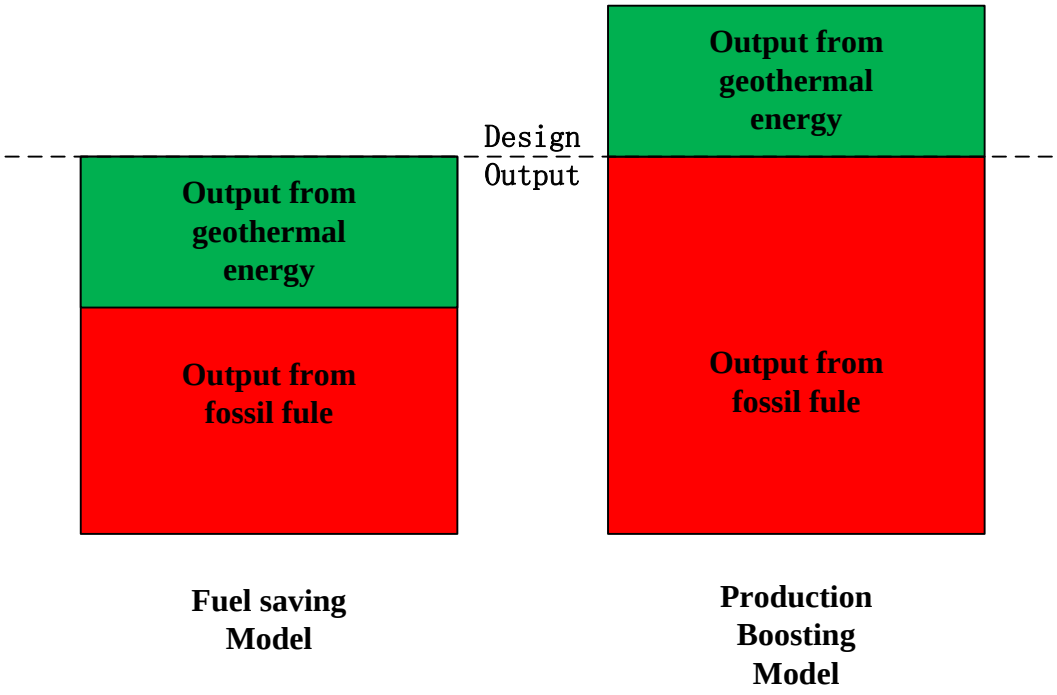

Figure 1.4 Two operational modes of a GAPG plant.

1.3 Aims of this study

1.3.1 General aim

The general aim of this research is to comprehensively study advantages and costs of geothermal aided power generation (GAPG) by developing and validating a simulation model that can be used as a tool for the technical and economic analysis of a GAPG plant. The simulation model consists of two sub models: the technical sub model, which simulates the steam power plant and analyses the technical benefits of GAPG, and the economic sub model, which analyses the economic benefit and costs of the GAPG technology.

1.3.2 Specific objectives

The specific objectives of the study are:

- To develop a simulation model (technical sub model) for the Rankine plant. The technical sub model has two functions. The first is to simulate the steam Rankine power plant, which is validated by a real power plant. The second is to provide a detailed energy and exergy analysis of geothermal aided power generation under different conditions of geothermal resources and options of replacement.
- To develop a mathematical model (economic sub model) of the cost-benefit performance of the GAPG technology.

- To integrate the sub models into a comprehensive GAPG simulation and evaluation package.

1.4 Scope and limitations of the study

1.4.1 Scope of the technical sub model

The basic design scope of the power plant includes three stages of the steam turbine, up to two reheaters of the boiler (between the two stages of steam turbines) and up to five feedwater heaters (alternatively the closed feedwater heater or the open feedwater heater) per stage of the steam turbine. The technical performance of the power plant and GAPG technology is simulated. The mass loss of the turbine, the pressure loss of extraction steam and pressure loss through a feedwater heater is the concern of the mathematical model.

When the geothermal fluid is integrated into the power plant to replace the extraction steam for the turbine, the steam flow rate through each stage of the steam turbine will change. The power plant in this condition is operated under a so-called off-design condition. In an off-design condition, the extraction pressure at each stage of the extraction point will change. Stodola's law is used in the technical sub model to calculate the changes of extraction pressure (Stodola 1927).

The technical sub model can be divided into two parts, the simulation of the coal fired steam Rankine power plant, and the simulation of the technical performance of the power plant when geothermal fluid is integrated into the power plant. The power boosting mode and the fuel saving mode can be calculated; with different mass flow

rates of geofluid and extraction steam being replaced at different percentages (from 0% to 100%), the performance of the GAPG technology can be calculated by a mathematical model. Some parameters of GAPG, which include thepower output of GAPG technology (power boosting mode), the amount of saved fossil fuel (fuel saving mode), the thermal efficiency of GAPG technology, and the exergy efficiency of GAPG technology, can be calculated with the mathematical model.

The outputs of the technical sub model are:

Before geothermal integration:

- Power output of the plant
- The boiler load
- Cycle first law efficiency
- Cycle second law efficiency
- Temperature of feedwater enter boiler

After geothermal integration:

- Additional power generated in the power boosting mode
- Annual carbon dioxide reduction in the fuel saving mode
- Efficiency of geothermal energy conversion to electricity in both modes
- Available temperature of geothermal fluid
- Pressure changes of the extraction steam

- Changes to boiler load
- Changes to power output;
- Cycle first law efficiency of the GAPG plant
- Cycle second law efficiency

1.4.2 Scope of economic sub model

The economic sub model estimates the capital costs of the geothermal wells and the related devices of the geothermal wells. The economic benefits from the two operational modes, power boosting and fuel saving, are calculated.

The economic sub model provides:

- Income from the additional power plant
- Income from the saved fossil fuel
- Payback time
- Cost of electricity power (COE)

Chapter 2

Literature Review

2.1 Geothermal power generation

The most common utilization of geothermal technologies are Single-flash Steam Power Plants, Double-flash Steam Power Plants, Dry-Steam Power Plants and Binary Cycle Power Plants (DiPippo 2008). In recent years, in order to meet the growing demand of renewable energy, the integration of renewable energy into the conventional energy source is becoming a more attractive proposition (Hu, Nathan and Battye 2010).

In the single-flash system the geothermal fluid undergoes a single flashing process. The geothermal fluid is separated into liquid and vapour in a cyclone separator and the vapour is used to produce the electricity. The single-flash steam plant is a common geothermal power plant that is often the first power plant built at a newly developed geothermal field (DiPippo 2008). As of 2007, about 32% of geothermal plants were single-flash plants (DiPippo 2008).

The double-flash steam plant is an improvement of the single-flash steam plant. In 2007 about 14% percent of geothermal plants were double-flash steam plants (DiPippo 2008). Double-flash steam plants utilise two stages of the flash process to increase efficiency (DiPippo 2008). Compared to a single-flash power plant, the double-flash power plant can produce 15%-20% more power by using the same geothermal fluid (DiPippo 2008).

The dry-steam power plants are the first type of commercially used geothermal power plants. The dry-steam power plants are simpler and less expensive than the single-flash power and double-flash power plants (DiPippo 2008). Because the geothermal fluid of dry-steam power plants is made up of liquid and is not mineral-laden, dry-steam geothermal plants have a low impact on the environment.

Binary cycle geothermal power plants are the most widely used type of geothermal power plants, although the average power rating per unit is only 2.3MW (DiPippo,2008). Binary cycle geothermal power plants are widely used where the geothermal fluid is 150℃ or less. In binary cycle geothermal power plants, the geothermal fluid from the production well is sent to a heat exchanger to heat the working fluid.

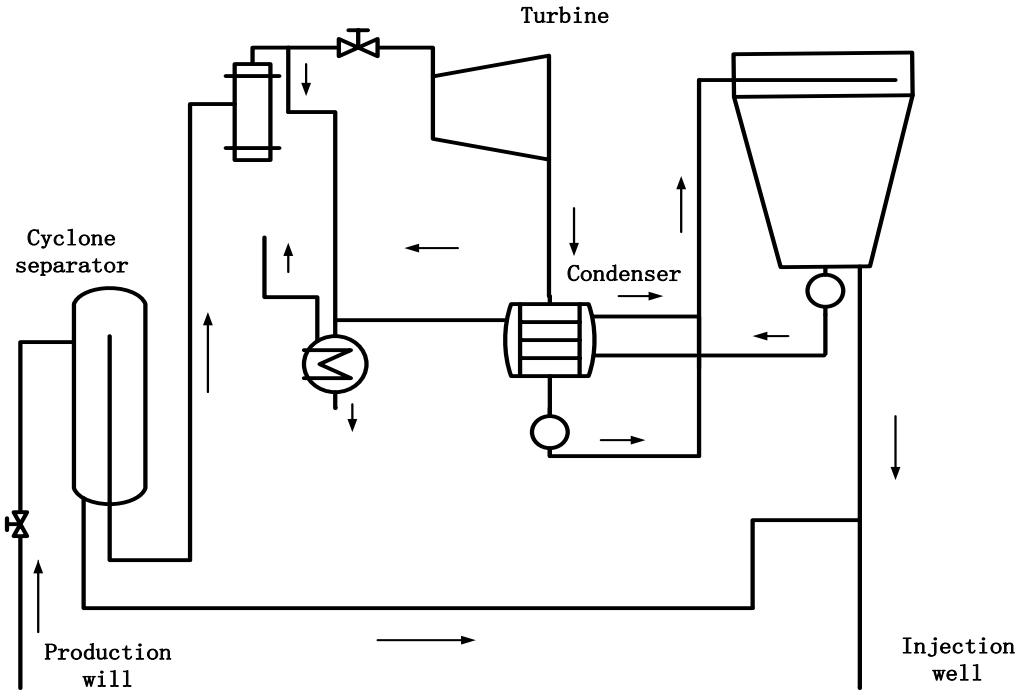

Figure 2.1 Simplified diagram of a single-flash power plant schematic (DiPippo 2008)

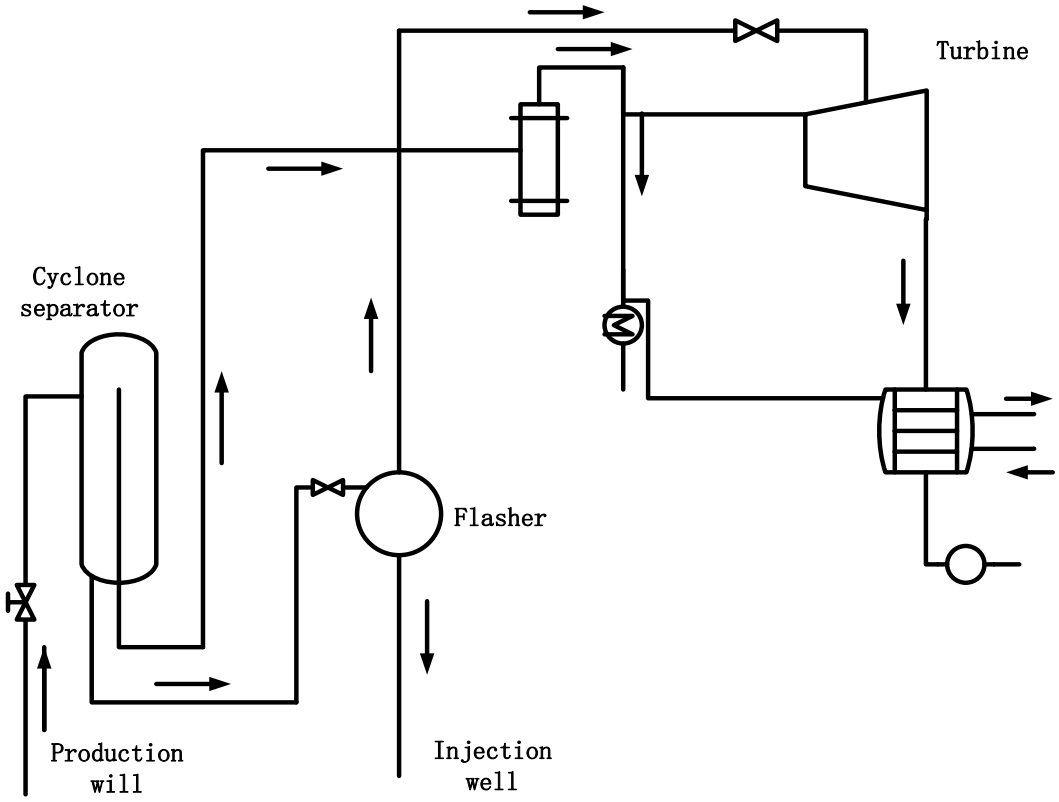

Figure 2.2 Simplified diagram of a double-flash power plant schematic (DiPippo 2008)

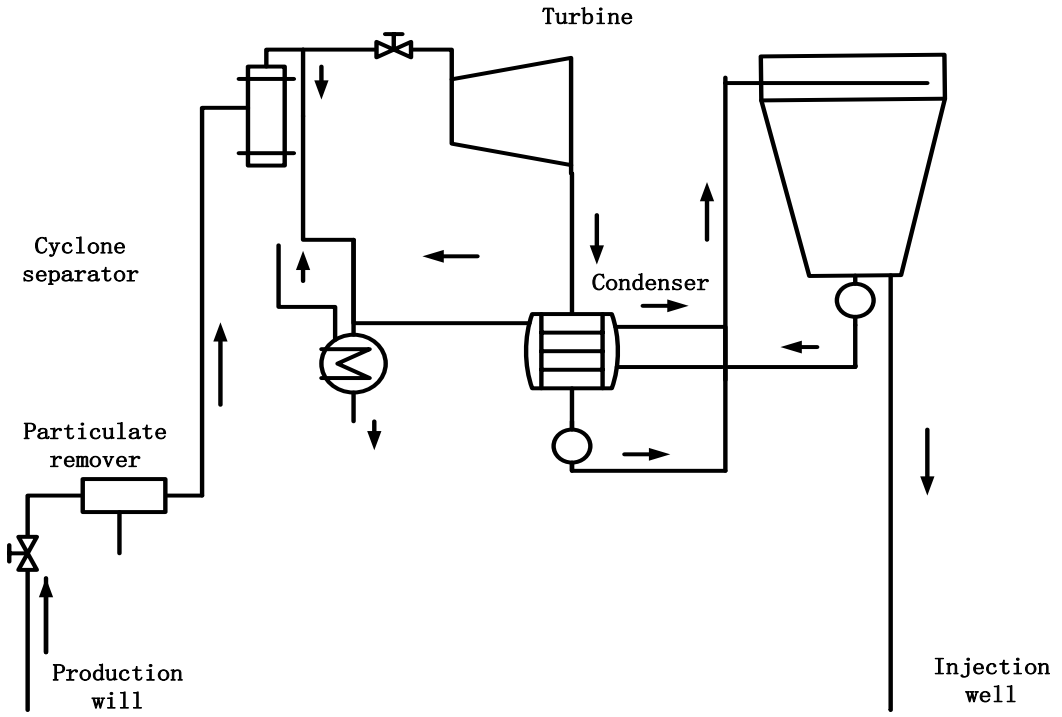

Figure 2.3 Simplified schematic flow diagram of a dry steam plant (DiPippo 2008)

NOTE:
This figure/table/image has been removed
to comply with copyright regulations.
It is included in the print copy of the thesis
held by the University of Adelaide Library.

Figure 2.4 Simplified schematic diagram of a basic binary geothermal power plant

(DiPippo 2008)

2.2 Hybrid geothermal fossil electricity power generation

According to the principles of thermodynamics, the efficiency of the steam cycle power plant is limited by the temperature of geothermal fluid and the temperature of the condensing temperature (Cengel, Boles 2002). Due to the limitation of the temperature of the geothermal fluid, directly using geothermal fluid to produce the electricity leads to a low efficiency. Instead, integrating the geothermal energy and fossil fuels' electricity generation, which is called hybrid power generation, is an approach that can provide significant thermodynamic advantages.

Three principal concepts of integrating the geothermal fluid into the fossil fired power generation have been discussed previously (Bruhn 2002).

- Fossil superheating of geothermal steam (DiPippo *et al.* 1978). Fossil superheating of geothermal steam involves the geothermal fluid being superheated by the flame to increase the temperature of geothermal fluid. and he superheater geothermal fluid then entering the steam turbine to produce the electricity. Beside the fossil fired power plant, fossil superheating of geothermal steam can also be used in the gas turbine power plant (Khalifa 1978). Kingston Reynolds Thom &Allardice Ltd. (1980) analyse the benefit of fossil superheating of geothermal steam used in the gas turbine power plant. Some other research of fossil superheating of geothermal steam used in the gas

turbine power plant has been analysed by Bettocchi et al (1992) and Bidini et al (1998).

- Compound geothermal fossil power plants (DiPippo, Kestin & Khalifa 1981).These plants have been analysed by DiPippo. They combine the features of a fossil superheating system and a geothermal preheating system.
- Geothermal feedwater preheating (Bruhn 2002). This system, called the geothermal aided power generation (GAPG) in this study, uses the geothermal fluid to preheat the feedwater system of fossil fired power generation. Geothermal aided power generation cannot be used in gas steam turbine power generation and it has advantages over using low temperature geothermal resources (Bruhn 2002).

The focus of this study is utilization of geothermal fluid to preheat the feedwater system of fossil fired Rankine steam cycle power generation. To the author's knowledge, the idea of using geothermal energy to preheat the feedwater of conventional fossil fired Rankine steam cycle power generation was first presented in the late 1970s by DiPippo (Kestin, DiPippo & Khalifa 1978).

A thermodynamic analysis shows that the hybrid fossil geothermal power plant in which low-grade geothermal energy is used has an overall improvement in the utilization of the low-grade geothermal resources and the fossil energy (Khalifa 1978). For geothermal fluid at 200℃ a geothermal aided power plant can produce 4% more

work than conventional fossil-fired power plant and 60% more work than a geothermal power plant. The criterion of choosing a geothermal utilization strategy was also studied by Kestin, DiPippo and Khalifa (1978).

Recently, the idea of using geothermal resources to preheat the feedwater has been analysed by Matthias Bruhn (Bruhn 2002) and J. Butcha (Buchta 2009). In order to estimate the potential of geothermal preheating the feedwater of conventional fossil fired power generation, two modern coal fired power planst are used as case studies (Bruhn 2002). In Bruhn's paper, energy output and economic efficiency calculations have been undertaken to estimate the benefit of geothermal energy. In Buchta's paper, the influence of the geothermal fluid temperature on the power plant performance is analysed. In Bruhn and Buchta's paper, the mathematical modelling of the use of geothermal fluid to preheat the feedwater of conventional fossil fired power plant has been carried out.

2.3 Integrating other thermal resources into power generation

Solar thermal energy is another kind of renewable energy that can also be integrated into fossil power generation to improve the efficiency of utilization of solar energy. Some previous studies have analysed the use of solar energy to aid the power generation.

Zoschak and Wu(1975) studied seven methods of integrating solar thermal energy into the steam power plant. An 800 MW conventional fossil-fired power plant was chosen as a case study to estimate the potential of using solar energy to preheat the feedwater of steam cycle, superheat the steam, reheat the steam, preheat the air to the boiler, combined the evaporation and superheating of the steam of steam cycle, and combined to preheat the air of boiler and feedwater of steam cycle. The results show that combination of evaporation and superheat the steam to be the preferred method.

You and Hu (1999) have studied integrating solar energy into conventional fossil-fired power generation. You and Hu (1999) analysed regenerative reheat Rankine power generation using solar energy as the heat source to preheat the feedwater of power plants. The paper reported the thermodynamic advantages of the solar aided power system. It shows that solar aided power systems can be more efficient than the conventional fossil-fired regenerative Rankine power plants. The solar aided power system has advantages of being easier to make the heat carrier function at different

temperatures by using the different types of collectors. You and Hu (2002) assessed the optimum saturation temperature of boilers and the optimum temperature of the solar collectors. Eric Hu in another study analysed the use of solar energy to preheat the feedwater of power plant for the purpose of promoting the output of the steam turbine. The result shows that a solar aided power system is an effective method of utilization of low-temperature solar thermal energy (Hu, *et al*, 2003). The recent paper of Eric Hu studied the advantages of using solar energy to preheat the feedwater of power plants in terms of energy and exergy analysis. The result shows that the exergy efficiencies of the power plant can be improved by using solar energy to replace the extraction steam to preheat the feedwater of regenerative reheat Rankine power plants (Hu, *et al*, 2010).

Yang *et al.* (2011) studied solar aided power generation for a 200 MW coal-fired thermal power plant. Four different schemes were studied. They found that solar aided power generation is the more efficient way to make use of solar heat, in the medium and low temperature range for power generation, by replacing the bled-off steam in the regenerative Rankine steam cycle.

Yan et al. (2010) studied the overall efficiencies of using solar energy to replace the extraction steam for the purpose of preheating the feedwater of regenerative reheat Rankine power plants at multi-points and multi-levels. They point out that integrating the solar energy into the fossil fired power plant can reduce the fossil consumption or increase the power output. They also find that the solar to electricity efficiency is higher

than the geothermal alone power plant with the same temperature.

Gupta and Kaushik (2009) analysed exergy characteristics for the different components of a proposed conceptual DSG solar-thermal power plant. Steam generated by Parabolic Trough Collector (PTC) is integrated with the thermal power plant to enter the steam turbine. They concluded that heating feedwater of a thermal power plant using solar energy is more advantageous than using the same (solar energy) in stand-alone solar thermal power plants

2.4 Previous models of the use of geothermal fluid to preheat feedwater for power generation

Buchta (2010) employed the following assumptions to calculate the performance of using geothermal fluid to preheat the feedwater of steam cycle:

- The temperature, pressure and enthalpy of water and steam in a steam cycle keep constant when geothermal fluid is used to preheat the feedwater of steam cycle.
- The turbine internal efficiency is independent from the turbine outlet stem flow.

Similarly, Bruhn (2002) employed the flowing assumption to estimate the benefit of geothermal energy:

- The internal efficiency of steam turbine keeps constant when the geothermal fluid is used to preheat the feedwater of power plant (Bruhn, 2002).

However, when a geothermal fluid is used to preheat the feedwater of the steam cycle, the mass flow rate of steam at each stage of the steam cycle must change; this means that the steam turbine is run under off-design conditions. Under an off-design condition the mass flow rate through and the exit pressure for the turbine stage change,

thereby changing the inlet conditions for the following turbine stages. Stodola's Law, which is attributed to Aruel Stodola, provides a method to calculate these changes (Stodola 1927).

Chapter 3

Modelling Descriptions

A mathematical model is developed to simulate and analyse the technical and economic characteristics of the GAPG technology in detail. The structure, methods and functions of the mathematical modelling are described in this chapter.

3.1 Introduction

Mathematical modelling aims to establish the mathematical expressions to characterise physical processes, and it requires assumptions. As the GAPG system is based on a conventional steam Rankine plant, a thermodynamic model of the conventional Rankine plant should be developed first, in which the mass and energy balance of the plant would be simulated mathematically. To this, a mathematical model of GAPG is added.

In order to analyse the thermodynamic advantages and the economic advantages of

the GAPG technology, the GAPG model consists of two sub-models, namely:

- a technical sub model
- an economic sub model.

The technical sub model calculates the mass flow rates in each part of the plant, the power outputs of each stage of the steam turbine and the whole plant, and the boiler (thermal) loadings, with or without the implementation of GAPG. This occurs both for the power boosting and the fuel saving modes. Using these outputs from the technical sub model, overall plant efficiencies and geothermal (to power) efficiencies can be calculated. Input information required for the technical sub model includes the mass flow rate, temperature and silicon dioxide content of the geothermal fluid.

The economic sub model is used to calculate the economic benefit of the GAPG system, which includes calculating the capital and operational costs and the economic benefits of the GAPG system at different operational conditions.

Figure 3.1 shows the inputs and outputs of the technical sub model and the economic sub model.

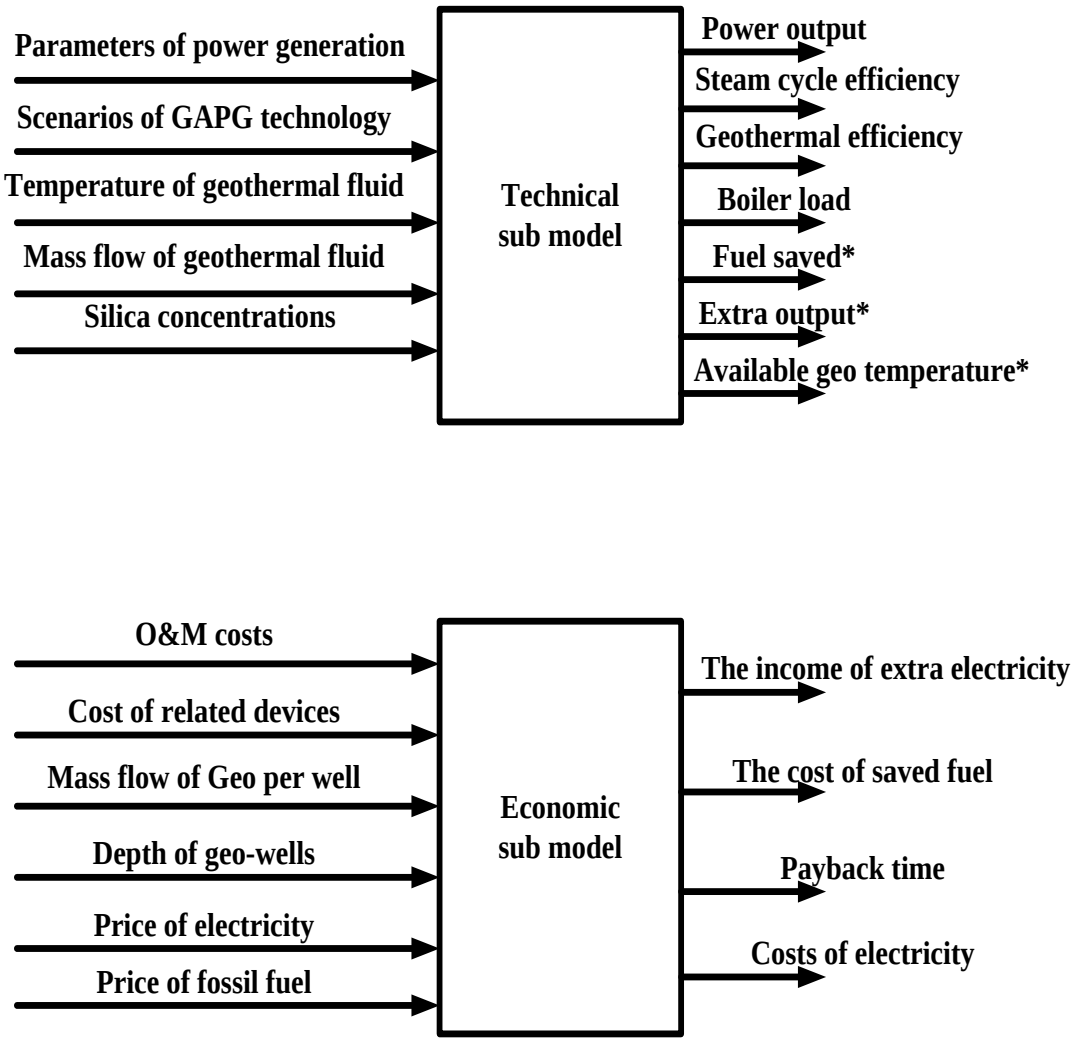

Figure 3.1 Structure of correlations of the technical sub model and the economic sub model

3.2 The physical model of GAPG technology

Figure 3.2 shows a schematic diagram of a typical coal fired power plant (with two closed feedwaters and one deaerator) with GAPG technology. In the system the high pressure superheated steam from the boiler enters the high pressure (HP) stage of the turbine first. This steam is typically sent back to the boiler for the (first) stage of reheating. In addition, part of the steam is typically extracted before being returned to the boiler, at point A shown in Fig. 3.2. The extraction steam goes to the high pressure feed heater ie. FWH3, to heat the feed water to the boiler. After re-heating, at point 3, the steam enters the intermediate pressure (IP) turbine and then the low pressure (LP) turbine to continue expansion and generate work. In the IP and LP stages of the turbine, part of the steam is also extracted at points B and C, to heat the feed water in the various stages of feed heaters. There are up to 8 stages of extraction in a typical Rankine regenerative power plant. The exhaust steam from the LP turbine, after passing the condenser and feed pump, becomes the main stream of the feed water for the boiler, which would be/is pre-heated in the feed heaters by the extracted steams before reaching the boiler.

In a GAPG plant, as shown in Fig. 3.2 ,a geothermal fluid heat exchanger exists parallel with each closed feedwater heater, eg. FWH3, FWH1. If the geothermal fluid is available at the right temperature, by adjusting the valves at the various stages of the feed heater (eg. valves 1 and 2) part or all the feed water can be heated in the

geothermal heat exchanger, to reduce or eliminate the extraction steam required for that stage of the feed heater. In other words, the geothermal fluid is used to replace the extraction steam to pre-heat the feedwater. In so doing, the saved extraction steam is used in the steam turbine to generate work in the turbine, and the temperature of the feed water (at point 1) entering the boiler does not change. The reason for targeting the closed feed heaters only is that this approach has least influence on the power plant and requires minimal plant modification.

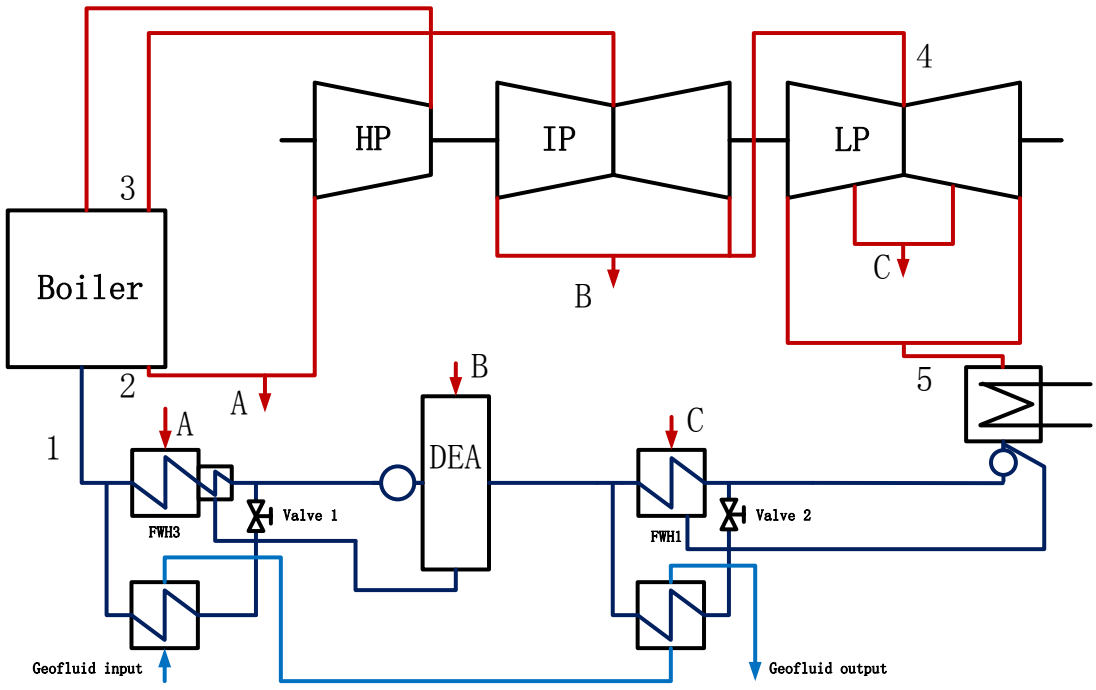

Figure 3.2 Schematic diagram of a typical coal fired power plant (with two closed feedwater and one deaerator) with GAPG technology

The percentages of extracted steam that can be replaced by the geothermal fluid at each stage depends on the temperature, flow rate and silicon concentration of the

geo-fluid. To maximize the benefit, the geothermal fluid should be first used to replace the highest possible (temperature) extracted steam, and then sent to the next lowest feedwater heat exchanger, if it is not limited by the temperature or silicon concentration.

The GAPG model can be used for two types of calculations: one is based on the given/known percentage of extraction steam to be replaced to calculate the mass flow rate of the geothermal fluid required; the other is based on the mass flow rate of geothermal fluid available, to determine the percentage of extraction steam that can be replaced by the geothermal fluid.

In most geothermal reservoirs, silicon dioxide is present in the quartz. The solubility of silicon dioxide mainly depends on the temperature of the geothermal fluid (Rournier, Rowe 1966). If precipitation occurs due to the low temperature, it will diminish the performance of the heat exchangers. The precipitate temperature of geothermal fluid needs to be calculated. In mathematical modelling, the net precipitation rate of carbon dioxide is calculated as a function of geothermal temperature, following Brown and Bacon (2009).

In the GAPG modelling, each component of the system, ie., steam turbine, boiler, feedwater heater, deaerator, condenser and geo-fluid, is simulated through a separate module.

3.3 Technical sub model of GAPG technology

For the technical sub model, each component of the power plant is simulated by a simple module. The modules of the technical sub model include:

- Steam turbine stage modules
- Feedwater modules
- A deaerator module
- A condenser module
- A boiler module
- A geothermal fluid module

When modelling the GAPG system, normally the whole power plant is treated as a closed system, with each individual component (eg. turbine and feedheater etc) treated as an open system at steady state (Cengel, Boles 2002). The energy and exergy balance equations for an open system at steady state are given as below:

$$\dot{Q} - \dot{W} = \sum \dot{m}_{in}\left(h_{in} + \frac{v_{in}^2}{2} + gz_{in}\right) - \sum \dot{m}_{out}\left(h_{out} + \frac{v_{out}^2}{2} + gz_{out}\right) \quad 3.1$$

$$\sum(1 - \frac{T_0}{T_k})\dot{Q} - \dot{W} + \sum \dot{m}_{in}\psi_{in} - \sum \dot{m}_{out}\psi_{out} - \dot{I} = 0, \quad 3.2$$

where $\dot{Q}$ (kW) is the rate of heat to be transferred to the steady-flow system,;

$\dot{W}$ (kW) is the rate of work produced by the steady-flow system,;

$\sum \dot{m}_{in}\left(h_{in}+\frac{v_{in}^2}{2}+gz_{in}\right)-\sum \dot{m}_{out}\left(h_{out}+\frac{v_{out}^2}{2}+gz_{out}\right)$ is the net change of the energy of the flow steam,

ψ_{in} (kJ/kg)andψ_{out} (kJ/kg) are the specific flow exergy,

$\dot{I}$ (kW) is the exergy destruction,

T_0 (K) is the environmental temperature, and

T_k (K) is the temperature of the heat that is transferred to the system.

Eq. 3.1 is the energy balance equation and eq 3.2 is the exergy balance equation used to calculate the heat capacity of each part of steam Rankine power plant and GAPG technology.

In eq. 3.2, the flow exergy is given by (Moran 1986):

$$\psi = h - T_o s \qquad 3.3$$

where s (kJ/kg K) is the entropy of steam, and

T_o (K) is the environment temperature.

Equation 3.2 can be used to calculate the exergy destruction of each component in the steam Rankine power plant.

3.3.1 Steam turbine module

The steam turbine is the device that converts the thermal energy of steam to the mechanical work by rotating the shaft of the steam turbine. Figure 3.3 shows the schematic structure of the steam turbine which is used in the mathematical modelling of GAPG technology. The steam turbine comprises a high pressure stage (HP stage of steam turbine), intermediate pressure stage (IP stage of steam turbine) and low pressure stage (LP stage of steam turbine). Each has five points of steam extraction.

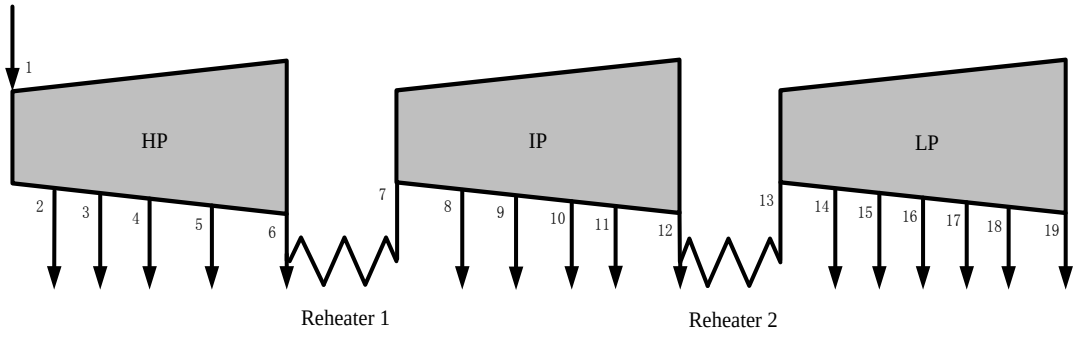

Figure 3.3 Schematic diagram structure of the steam turbine with extraction points for steam used in the mathematical model

The high pressure supercritical or subcritical steam from the boiler enters the HP stage of steam turbine. In the ideal process, the steam expands isentropically and produces the work by rotating the shaft of steam turbine. The pressure and temperature drop during this process. In practice, due to the irreversibility caused by friction and heat losses from the steam to the surroundings, the entropy increases during the expansion process. The steam leaves the HP stage of steam turbine at point 6 and enters

the boiler to be reheated to supercritical or subcritical steam again to enter the IP stage of steam turbine. Points 2 to 5 of the HP stages of steam turbine are extraction points, from which some of the steam is bled from the steam turbine to preheat the feedwater heater of the power plant.

The steam turbine stage module is used to calculate the power output from each stage of the steam turbine. The output of steam turbine is the sum of the output of each stage of the steam turbine. The output of one stage of the steam turbine is calculated by:

$$W_{\text{stage out}}(\text{kW}) = \dot{m}_{\text{in}}(h_{\text{in}} - h_{\text{out}}), \quad 3.4$$

where the $\dot{m}_{\text{in}}$ (kg/s) is the mass flow rate of steam entering the stage of the steam turbine,

h_{in} (kJ/kg) is the specific enthalpy of steam entering the stage of the steam turbine, and

h_{out} (kJ/kg) is the enthalpy of steam out of the stage of the steam turbine.

The exergy destruction in the steam turbine is given by:

$$I_{\text{stage destruction}} = m_{\text{in}}(\psi_{\text{in}} - \psi_{\text{out}}) - W, \quad 3.5$$

where $I_{\text{stage destruction}}$ (kW) is the exergy destruction in the steam turbine,

ψ_{in} (kJ/kg) is the specific exergy of steam entering the steam turbine,

ψ_{out} (kJ/kg) is the specific exergy of the steam output of the steam turbine, and

W (kW) is the work output from the steam turbine.

The total output of the steam turbine is the sum of each stage of the steam turbine so that equation 3.4 can be written as:

$$W_{out} = \sum_{i=1}^{n}(h_i - h_{i+1})m_{i,in} \quad 3.6$$

$$m_{i,in} = m_{i+1,in} + m_{i+1}, \quad 3.7$$

where n is the number of stages of steam turbine (as pointed in Fig. 3.3, in mathematical modelling, the maximum number of stages of steam turbine is 16 in equation 3.6),

the $\dot{m}_{i,in}$ (kg/s) is the mass flow rate of steam entering each stage of the steam turbine, and

$\dot{m}_{i+1}$ (kg/s) is the mass flow rate of steam extraction of each stage of the steam turbine (Equation 3.7 is used to calculate the steam flow rate entering each stage of the steam turbine, and "i+1" is the extraction point of steam turbine in Fig. 3.3, which means points 2 to 6, 8 to 12 and 14 to 19).

In the equation 3.6, h_i, h_{i+1} and $\dot{m}_{i,in}$ are known quantities and W_{out} is the unknown quantity.

In the steam turbine stages module of the technical sub model, the temperature and

pressure of steam entering into and out of the steam turbine and the temperature pressure and mass flow rate of extraction points of the steam turbine are inputs into the mathematical model; thus, the specific enthalpy of each point can be calculated. Equation 3.6 gives the output of the steam turbine when the special enthalpy of each point and mass flow rate of each stage of the steam turbine is calculated.

3.3.2 Feedwater heater module

In this project, the feedwater heater model is the model of the closed feedwater heater and the deaerator model is the open feedwater model. It is assumed that all the closed feedwater heaters are counter flow heat exchangers.

Figure 3.4 shows the structure of the closed feedwater heater that is modelled mathematically. A port of extraction steam is bled from the steam turbine and enters the feedwater heater at point 1 in Fig 3.4 to preheat the feedwater of the power plant, and outputs the feedwater heater at point 2 in Fig 3.4. The feedwater enters the feedwater at point 5 and leaves at point 4. In some of the feedwaters, drain steam from the high pressure feedwater heater enters at point 3 to mix with extraction steam. During this exchange process, it is assumed that the pressure is kept constant and the drain temperature at point 2 equals the saturation temperature of the extraction steam at point 1. The temperature change of the extraction steam and feedwater during the heat exchange process is shown at the bottom of Fig 3.4. During the heat exchange process,

the temperature of feedwater increases to the saturation temperature of the extraction steam at point 1 and the pressure of feedwater drops during the heat exchange process.

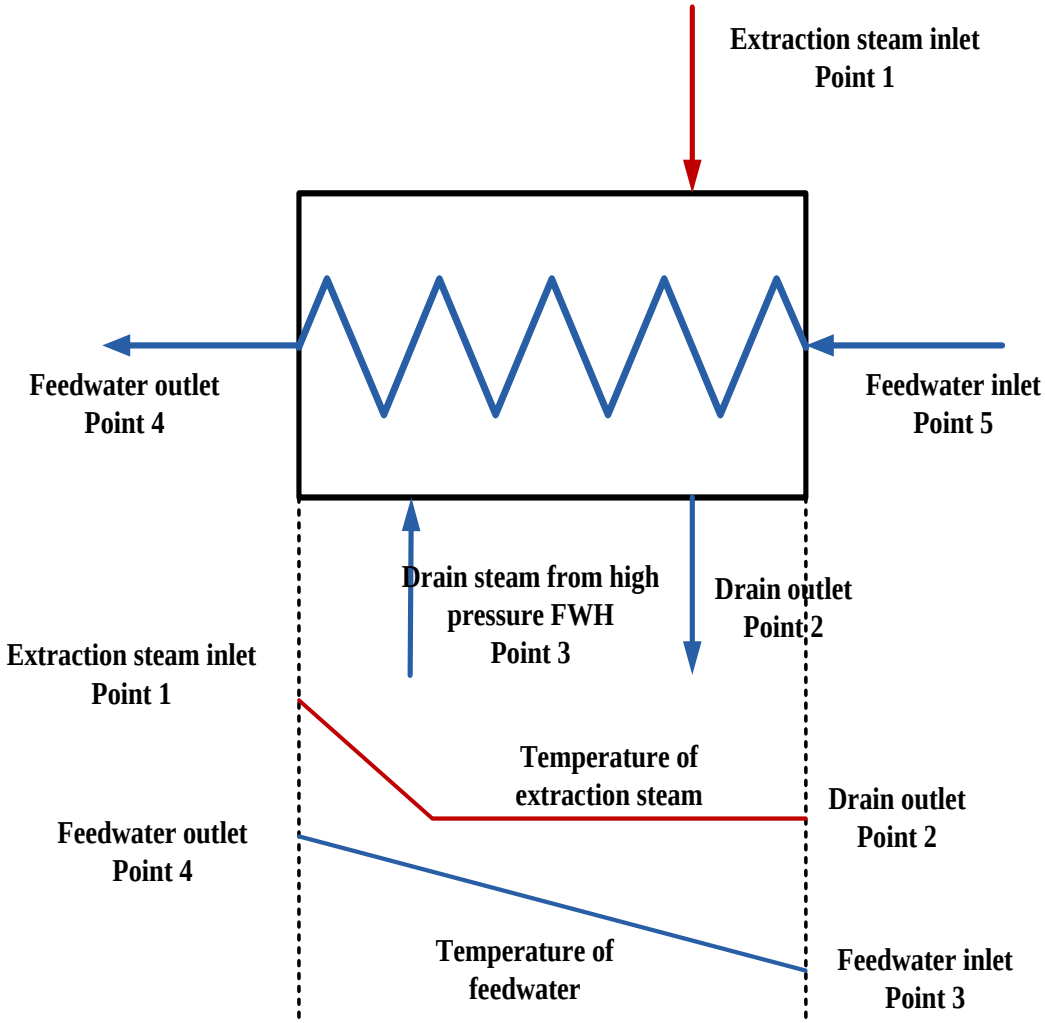

Figure 3.4 Schematic diagram of the model of the closed feedwater heater

The feedwater heater module is used to calculate the temperature of feedwater out from the feedwater heater. In the model, we make an assumption that the pressure of extraction steam during the heat exchange process keeps constant, and the drain steam output of the feedwater heater is at the saturation state of the extraction pressure.

The thermal formulas of the feedwater heater of Rankine cycle power plant without GAPG technology include:

$$\dot{m}_{feed}(h_{feedout} - h_{feedin}) = \dot{m}_{Ex}(h_{Exin} - h_{Drout}) + \dot{m}_{Dr}(h_{Drin} - h_{Drout}) \quad 3.8$$

$$P_{Extraction\ Inlet} = P_{Drain\ steam} \quad 3.9$$

$$P_{Feedwater\ Inlet} = P_{Feedwater\ Outlet} + \Delta P_{loss} \quad 3.10$$

$$\sum \dot{m}_{in}\psi_{in} - \sum \dot{m}_{out}\psi_{out} = \dot{I}, \quad 3.11$$

where the $\dot{m}_{feed}$ (kg/s) is the mass flow rate of feedwater (point 5 in Fig. 3.4),

the $\dot{m}_{Ex}$ (kg/s) is the mass flow rate of extraction steam (point 1 in Fig. 3.4),

the $\dot{m}_{Dr}$ (kg/s) the mass flow rate of drain steam (extraction steam of higher pressure closed feedwater heater) from higher pressure feedwaters (point 3 in Fig. 3.4),

ΔP_{loss} (Bar) is the pressure loss of the feedwater heater,

$\sum \dot{m}_{in}\psi_{in}$ is the flow exergy enter into the feedwater heater, which includes the extraction steam and feedwater, and

the $\sum \dot{m}_{out}\psi_{out}$ is the flow exergy output from the feedwater heater.

3.3.3 Deaerator module

In the mathematical model, the deaerator module is calculated as an open feedwater heater. Figure 3.5 shows the schematic structure of the deaerator (open feedwater heater). The figure shows that the extraction steam, feedwater and drain

steam from the high pressure feedwater heater enter the deaerator at points 1, 3 and 2, with a mixture output from the deaerator at point 4.

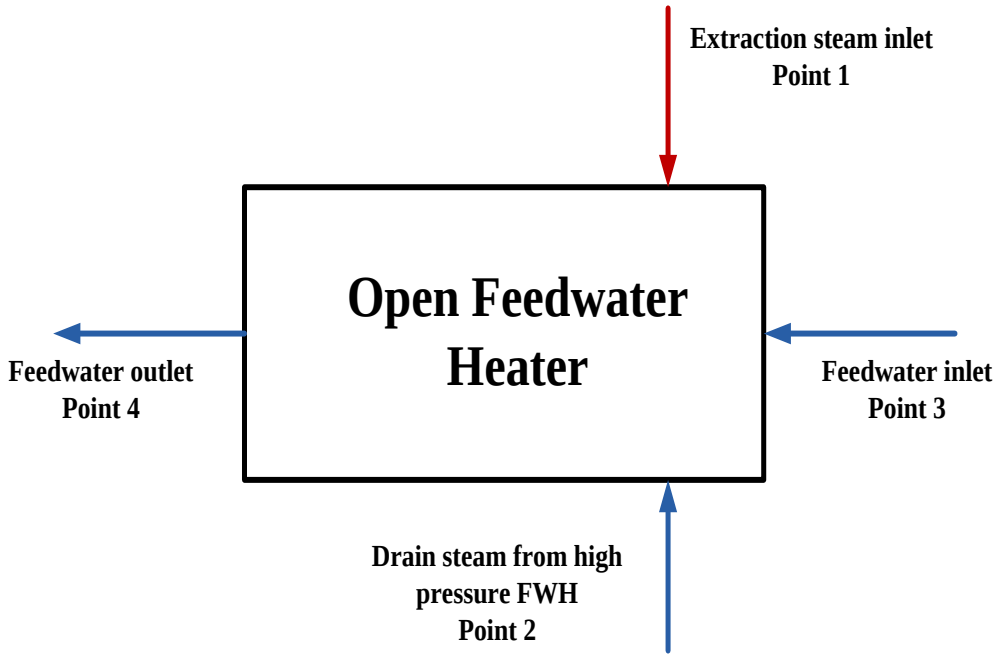

Figure 3.5 Schematic diagram of the structure of the Open Feedwater Heater used the in mathematical model

The deaerator module is used to calculate the temperature of feedwater from the deaerator. The deaerator in GAPG technology is not replaced by geothermal fluid. The equations used to model the deaerator include:

$$m_{feedin}\dot{h}_{feedin} + m\dot{}_{ex}h_{ex} + m_{drain}\dot{h}_{drain} = m_{feedout}\dot{h}_{feedout} \quad 3.12$$

$$\sum \dot{m}_{ex}\psi_{ex} + \sum \dot{m}_{feedin}\psi_{feedin} + \sum \dot{m}_{Drain}\psi_{Drain} - \sum \dot{m}_{feedout}\psi_{feedout} = \dot{I}_{Dea}, \quad 3.13$$

where the $\dot{m}_{feedin}$ (kg/s) and h_{feedin} (kg/s) are the mass flow rate and enthalpy of feedwater entering the deaerator (point 3 in Fig 3.5),;

$\dot{m}_{ex}$ (kg/s)and h_{ex} (kJ/kg) are the mass flow rate and enthalpy of the extraction steam (point 1 in Fig. 3.5),;

$\dot{m}_{drain}$ (kg/s)and h_{drain} (kJ/kg) are the mass flow rate and enthalpy of the drain steam (point 2 in Fig. 3.5), and

$\dot{m}_{feedout}$ (kg/s)and $h_{feedout}$(kJ/kg) are the mass flow rate and enthalpy of the feedwater output of the deaerator (point 4 in Fig. 3.5).

3.3.4 Condenser module

The condenser is the equipment that maintains the backpressure of the steam turbine, condensing the steam through a heat exchanger. The cooling water from the environment flows through the cooling pipes and carries the thermal energy away from the steam to the environment.

Figure 3.6 shows the arrangement of the structure of the condenser. Steam enters the condenser at point 1, is condensed at constant pressure and leaves the condenser as saturated liquid at point 2. Cooling water from the environment enters the condenser at point 3 and leaves the condenser at point 4. In the mathematical model, it is assumed that the pressure of steam which is cooled by the cooling water keeps constant and the quality of the steam output of the condenser is zero.

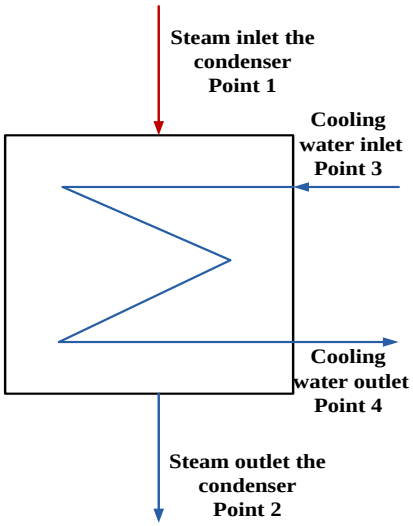

Figure 3.6 Schematic diagram of the condenser here modelled

The condenser module is used to calculate the enthalpy of feedwater from the condenser. This enthalpy of feedwater is calculated from the temperature and quality of feedwater. For the calculation of exergy of the destruction, the exergy of cooling water is not considered, and only the exergy destruction from steam to environment is calculated.

The heat equations of the condenser are:

$$P_{\text{steam inlet}} = P_{\text{steam outlet}} \quad 3.14$$

$$T_{\text{steam inlet}} = T_{\text{steam outlet}} \quad 3.15$$

$$\sum \dot{m}_{\text{steam in}} \psi_{\text{steam in}} - \sum \dot{m}_{\text{steam out}} \psi_{\text{steam out}} = \dot{I}_{\text{Con}} \quad 3.16$$

3.3.5 Boiler module

Figure 3.7 shows a schematic diagram structure of the boiler that consists of a furnace and two reheaters. The feedwater from the feedwater system enters the boiler at point 1. A constant pressure heat addition process is assumed, from the burning of fossil fuel, to heat the steam to the subcritical steam or supercritical condition. The heated steam from the boiler at point 2 is sent to the steam turbine. In practice, due to the fluid friction in boiler, there is a pressure drop through the boiler.

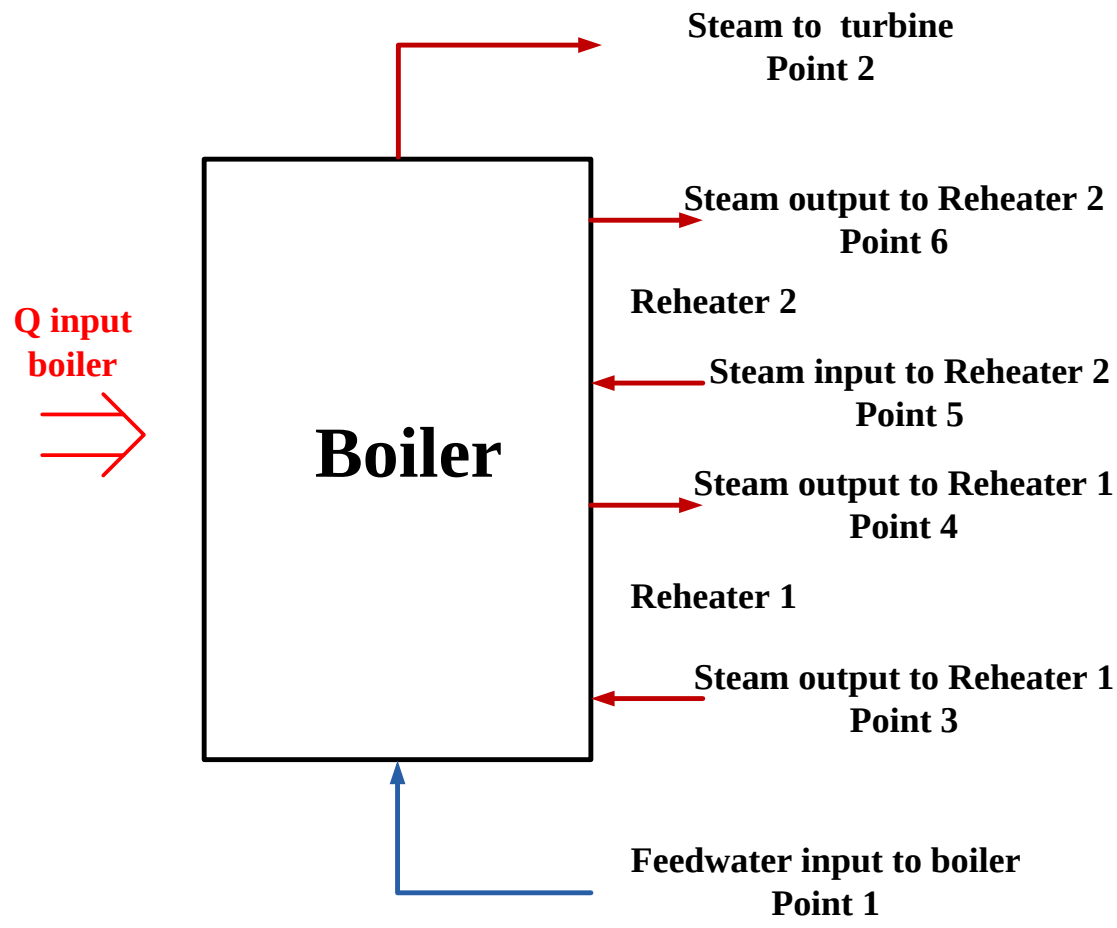

Figure 3.7 Schematic diagram of the boiler modelled.

In figure 3.7, steam from the HP stages of the steam turbine enters the boiler at point 3 and at a constant pressure and outlet the boiler to the IP stage of the turbine. The steam from the IP stage of the steam turbine enters the boiler again at point 5 and leaves at point 6 for the LP stage of the steam turbine. Because the double reheat of steam would cause the superheated exhaust, which leads to a decrease in the cycle's efficiency, most power plants only have one reheater (Cengel, Boles 2002).

The boiler module is used to calculate the fuel demand of the power plant for the furnace and reheaters. The calculation of exergy destruction does not include the exergy of the fossil fuel, only the exergy destruction from the steam. The heat balance equations of boiler include:

$$\dot{m}_{coal} q_{coal} = \dot{m}_{feedwater}(h_{feedwater\ out} - h_{feedwater\ in}) + \sum \dot{m}_{reheater}(h_{reheater\ out} - h_{reheater\ in}) \quad 3.17$$

$$\sum \dot{m}_{steam\ out}\psi_{steam\ out} - \sum \dot{m}_{feedwater\ in}\psi_{feedwater\ in} = \dot{I}_{Boiler}. \quad 3.18$$

where the $\dot{m}_{coal}$ (kg/s) is the coal consumption rate of the boiler,

q_{coal} (kJ/kg) is the standard coal thermal value,

$\dot{m}_{feedwater\ in}$ (kg/s) is the mass flow rate of feedwater entering into the boiler (point 1 in Fig 3.7),

$\dot{m}_{reheater\ in}$ (kg/s) is the mass flow rate of steam entering into the reheater (point 3, 5 in Fig. 3.7),

$h_{\text{feedwater out}}$ (kJ/kg), $h_{\text{feedwater in}}$ (kJ/kg) are the enthalpy of feedwater inlet and outlet boiler (point 2 in Fig. 3.7), and

$h_{\text{reheater out}}$ (kJ/kg), $h_{\text{reheater in}}$ (kJ/kg) are the enthalpy of steam inlet and outlet reheater (point 4, 6 in Fig. 3.7).

3.3.6 Geothermal aided module

A geothermal aided module is used to simulate the steam Rankine power plant performance after geothermal replacement. The performance of two operational modes of GAPG technology is calculated. Stodola's law is used to calculate the turbine performance under off-design conditions. The concentration of the silica dioxide is used to calculate the minimum geothermal fluid temperature.

Feedwater heater with geothermal fluid

Figure 3.8 shows the schematic structure of the geothermal preheater of the GAPG system. At the bottom of the figure is the geothermal preheater into which the geothermal fluid enters at point Geo1 and leaves at point Geo2. Two valves (Valve 1 and Valve 2) control the percentage of extraction steam that is replaced by geothermal heat. Valve 1 controls the mass flow rate of feedwater entering the feedwater and valve 2 control the mass flow rate of feedwater entering the geothermal preheater. The geothermal preheaters are counter flow heat exchangers and are assumed to transfer the heat at constant pressure. By controlling the mass flow rate of feedwater entering the

feedwater heater and geothermal preheater, the temperature of the feedwater output the feedwater heater would be controlled.

The mathematical model assumed that the integrated geothermal fluid has no impact on the temperature of feedwater entering the entering and output the feedwater heater. The formulas used to calculate the performance are:

$$\dot{m_{feedwater}}(h_{\text{feedwater out}}-h_{\text{feedwater in}})=$$

$$(100-X)\%\dot{m_{Extraction}}(h_{\text{Extraction in}}-h_{\text{Drain out}})+\dot{m_{Dr}}(h_{\text{Drain in}}-h_{\text{Drain out}})+\dot{m_{Geo}}(h_{\text{Geo in}}-h_{\text{Geo out}}) \quad 3.19$$

where X is the percent of extraction steam that be replaced by geothermal fluid,

$\dot{m_{feedwater}}$ (kg/s) is the mass flow rate of feedwater input into the feedwater heater (point 5 in Fig. 3.8),

$h_{\text{feedwater out}}$ (kJ/kg) and $h_{\text{feedwater in}}$(kJ/kg) are enthalpy of feedwater output from (point 4 in Fig. 3.8) and input (point 5 in Fig. 3.8) into the feedwater heater,

$\dot{m_{Extraction}}$ (kg/s) is the mass flow rate of extraction steam input into the feedwater heater (point 1 in Fig. 3.8),

$h_{\text{Extraction in}}$ (kJ/kg) is the enthalpy of extraction steam input into the feedwater heater (point 1 in Fig. 3.8),

$h_{\text{Drain in}}$ (kJ/kg)and $h_{\text{Drain out}}$(kJ/kg) is the drain steam input into(point 3 in Fig. 3.8) and output (point 2 in Fig. 3.8) from the feedwater heater,

$\dot{m_{Geo}}$ (kg/s) is the mass flow rate of geothermal fluid input into the geothermal

preheater (point Geo1 in Fig. 3.8), and

$h_{Geo\ in}$ (kJ/kg)and $h_{Geo\ out}$(kJ/kg) are enthalpy of geothermal fluid input into (point Geo1 in Fig. 3.8) and output (point Geo2 in Fig. 3.8) from the geothermal preheater.

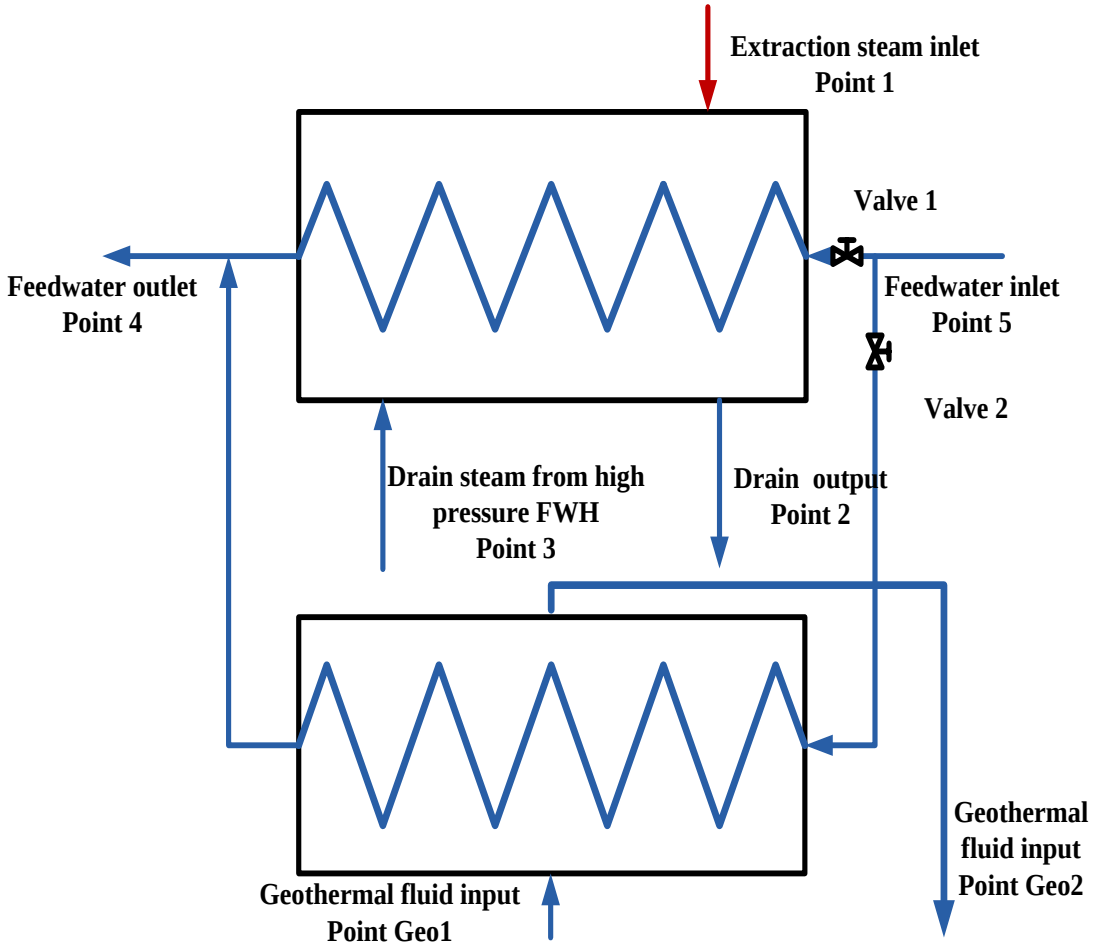

Figure 3.8 Schematic diagram of the model of the Closed Feedwater Heater with Geothermal preheater

In equation 3.19, in order to keep the temperature of the feedwater heater system constant, the $h_{feedwater\ out}$ is from the calculation result of the feedwater heater module. The temperature, pressure and enthalpy of feedwater to the feedwater heater are from

the previous feedwater module or the condenser module.

Power boosting mode and Fuel saving mode

Two basic operational scenarios, which are a power boosting mode and a fuel saving mode, would be calculated in the technical sub model. For the power boosting mode, as the mass flow rate of steam entering the steam turbine does not changes, the focus is to calculate the increased power output of the steam turbine. For the fuel saving mode, the power output of the steam turbine keeps constant, while the mass flow rate of steam of steam cycle is decreased due to the geothermal fluid is used to replace the extraction steam.

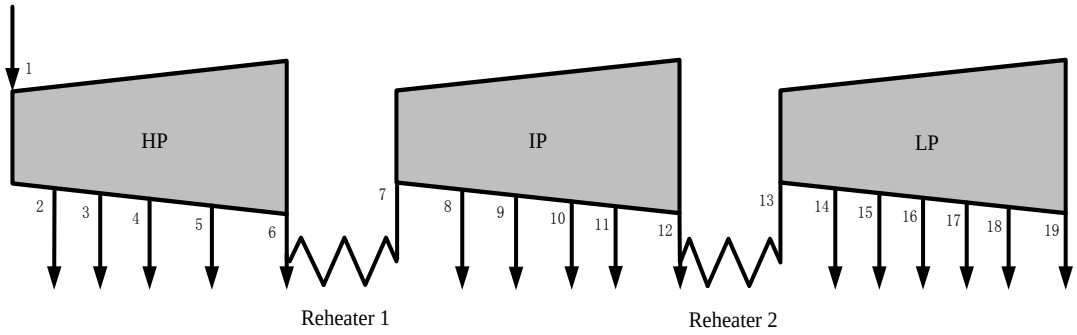

Figure 3.3 Schematic diagram of the structure of the steam turbine with extraction points for steam used in mathematical model

As shown previously, the equations of the steam turbine are as follows:

$$W_{out} = \sum_{i=1}^{n}(h_i - h_{i+1})\dot{m}_{i,in} \quad 3.6$$

$$\dot{m}_{i,in} = \dot{m}_{i+1,in} + \dot{m}_{i+1}, \quad 3.7$$

In the power boosting mode, when the extraction point a (a is the extraction point in Fig.3.3) is fully replaced by geothermal fluid, the equation 3.7 changes from $\dot{m}_{a,in} = \dot{m}_{a+1,in} + \dot{m}_{i+1}$ to $\dot{m}_{a,in} = \dot{m}_{a+1,in}$. This means that the mass flow rate of steam entering the next stage of steam increases by m_{i+1}. The increased power output after the geothermal replacement is as follows:

$$\Delta W_{out} = f(\dot{m}_a) = \sum_{i=a}^{n-1} \dot{m}_a (h_i - h_{i+1}), \qquad 3.20$$

where a is the extraction point of the steam turbine (points 2 to 6, 8 to 12, 14 to 18 in Fig. 3.3), and $\dot{m}_a$ is the mass flow rate of extraction steam that is replaced by geothermal fluid. If the extraction steam at point a, is fully replaced by geothermal fluid, the power output of the steam turbine is: $\Delta W_{out} = f(\dot{m}_a) + f(\dot{m})$, where the $f(\dot{m}_a)$ is the output of the steam turbine which from extraction steam replaced by geothermal fluid and $f(\dot{m})$ is the basic output of the steam turbine ($f(\dot{m})$ means the output of the steam turbine when the geothermal fluid is not used to replace extraction steam of the power plant). In the power boosting mode, when the operational mode is confirmed, the mass flow rate of steam for each stage of the steam turbine is calculated and the power output of the steam turbine is calculated by equations 3.6 and 3.20.

In the fuel saving mode, in order to keep the output of the steam turbine constant, the mass flow rate of steam entering the steam turbine would decrease. Equation 3.6 can

then be rewritten as:

$$W_{out} = \sum_{i=1}^{n} \dot{m}_1(h_i - h_{i+1}) - \sum_{i=2}^{n-1} \dot{m}_ı(h_{i+1} - h_{i+2}) \quad 3.21$$

where the $\sum_{i=1}^{n} \dot{m}_1 * (h_i - h_{i+1})$ is the output of all the steam expanded through the steam turbine ($\dot{m}_1$ is the mass flow of steam at point 1 in Fig. 3.3), $\sum_{i=2}^{n-1} \dot{m}_ı * (h_{i+1} - h_{i+2})$ is the output of extraction steam in the steam turbine if the extraction steam expands through the steam turbine and $\dot{m}_ı$ is the mass flow rate of extraction steam through each stage of the steam turbine. In equation 3.21, h_i, W_{out} and $\dot{m}_ı$ are known quantities and $\dot{m}_1$ is the unknown number. Hence $\dot{m}_1$ can be calculated from equation 3.21.

In the fuel saving mode, when some points (i.e. point i in Fig. 3.3) of extraction steam are replaced by geothermal fluid, the mass flow rate of other points of extraction steam remain constant. Hence the output from the steam turbine W_{out} is a function of $\dot{m}_ı$. As the power output and mass flow of extraction steam at no replaced point remain constant, when the extraction steam is replaced by geothermal fluid, the mass flow rate of steam entering the steam turbine m_1 can be calculated from equation 3.21.

Stodoal's Law

Integrating the geothermal fluid into the regenerative Rankine cycle affects not only the feedwater flows, but also the steam mass flows through the various stages of

the steam turbine and the reheater of the boiler. The changes of the mass flow rate through the steam turbine mean that the steam turbine is run under off-design conditions. Under the off-design conditions, due to the change of the mass flow rate, the exit pressure of the turbine stage would change, and thus the inlet conditions of the turbine stages following. Stodola's Law which is attributed to Aruel Stodola, provides a method to calculate these changes (Stodola 1927). According to the Stodola's Law (also called Ellipse Law) the exit pressure for a multistage turbine would change when the mass flow rate of the turbine changes.

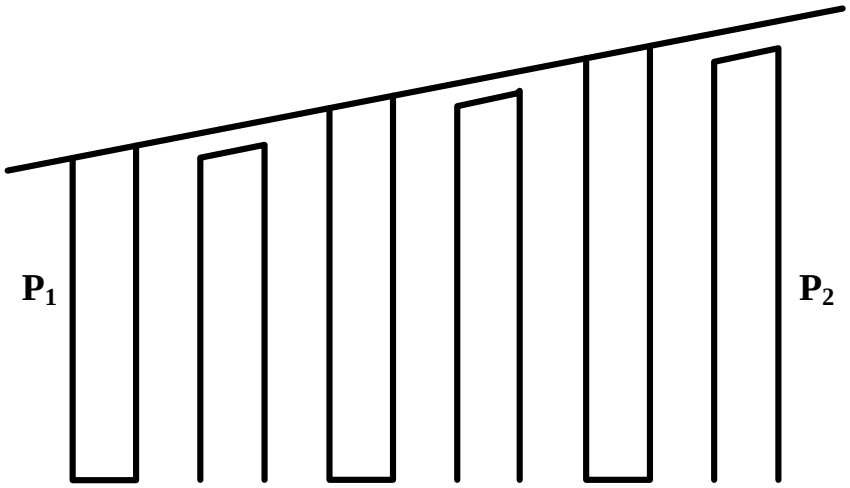

Fig 3.9 Typical schematic diagrams of one stage of steam turbine

Figure 3.9 shows a schematic diagram of a typical turbine stage. Point 1 is the inlet to the stage of the steam turbine, while point 2 is the outlet from the stage. For P_1 and P_2, Stodola's Law provides that:

$$\frac{D_1}{D_{10}} = \sqrt{\frac{p_1^2 - p_2^2}{p_{10}^2 - p_{20}^2}} \sqrt{\frac{T_{10}}{T_1}}, \qquad 3.22$$

where D_1 (kg/s) is the design or original flow rate,

D_{10} (kg/s) is the changed ie. the off-design flow rate,

p_1 (Bar) is the design inlet pressure,

p_2 (Bar) is the design outlet pressure,

p_{10} (Bar) is the inlet pressure under off design conditions,

p_{20} (Bar) is the outlet pressure under off-design conditions, and

T_1 (K) and T_{10} (K) are the inlet temperatures under the design and the off-design conditions, respectively.

In equation 3.22, D_1, D_{10}, p_1, p_2,p_{20} are known quantities and p_{10} is the unknown parameter. In the mathematical modelling, T_{10} and T_1 are assumed to be the same.

In the off-design conditions, the mass flow rate through each stage of the steam turbine ($m_{i+1,in}$) in equation 3.6 is calculated first, then equation 3.22 is used to calculate the extraction pressure (p_i). As the back pressure of the steam turbine is assumed to be kept constant, the extraction pressure is calculated from the last stages to the first stages of the turbine. Then the output of the steam turbine would be calculated under the off-design condition by using the equation 3.6.

Calculation of minimum geothermal fluid temperature

In geothermal reservoirs, silica is present in the geothermal fluid as quartz which mainly consists of silicon dioxide. The concentration of silicon dioxide in the geothermal fluid ranges from 300 to 700 mg/kg (Rournier and Rowe 1966). When the geofluid flow up the geothermal well and quench to a lower temperature, the silica dioxide becomes supersaturated (Chan 1989). Polymerization occurs when silica is in a supersaturated concentration, and polymerization continues until the silica scaling (Gunnarsson and Arnorsson 2005). The silica scaling occurs in geothermal wells (both production wells and injection wells), pipes of well field and geothermal feedwater system. In geothermal fluid, the rates of silica deposition and polymerization is determined by the PH and salt concentration of geofluid, the residence time and temperature of geofluid (Gunnarsson and Arnorsson 2005). The rate of silica deposition can be controlled by adjusting PH through the addition acid of by adding salt (Gunnarsson and Arnorsson 2005). In this case study, it is simply assumed that the solubility of silicon dioxide is controlled by the temperature of the geothermal fluid (Rournier and Rowe 1966) and the silica scaling occurs in the heat exchanger system of GAPG technology.

When the temperature drops, the dissolved silicon dioxide would precipitate from the fluid. In other words, the temperature of the geothermal fluid with the dissolved silicon dioxide would not be allowed to drop below a (low) temperature, at which the precipitation would occur. If used in GAPG, the temperature of the geothermal fluid out of the geothermal pre-heater is not allowed to reach the low temperature. The aim of the

geothermal sub model is to calculate the minimum geothermal fluid temperature, based on the concentration of silicon dioxide in the fluid. Bhuana *et al.* (2009) in their paper analyse the precipitation rate of silica as a function of temperature and silica concentration, as shown in Fig.3.10. It can be seen that the precipitation rate of silica in the geothermal fluid changes with the temperature of the geothermal fluid. In the technical sub model, a reference net precipitation rate of silica is chosen, and the temperature of the geothermal fluid at reference net precipitation is deemed as the minimum geothermal fluid temperature .The geothermal information that should be keyed into the geothermal module includes:

- Mass flow rate of geothermal fluid
- Mass flow rate per geothermal well
- Temperature of geothermal fluid
- Silica concentrations in the geothermal fluid
- Reference net precipitation rate of silica

The output of the geothermal module includes:

- Minimum geothermal fluid temperature
- Number of geothermal wells

In order to calculate the minimum allowed temperature for the geothermal fluid,

the net precipitation rate of silicon dioxide should be calculated. The approaches taken to calculate the silica precipitation and deposition rate of silicon dioxide are quite complex and poorly understood (Brown, Bacon 2009). A simplified approach using experimental data from Brown and Bacon (2009) is used in the geothermal sub model to calculate the deposition rate of silicon dioxide. For this approach, the precipitation rate of amorphous silica is shown in Fig. 3.10.

Figure 3.10 Precipitation rate of amorphous silica as a function of temperature and silica concentration (Bhuana, Ashman & Nathan, 2009).

For geothermal fluid at temperatures ranging from 0-300℃the kinetics of amorphous silica precipitation have been determined by the Rimstidt and Barnes study (Rimstidt and Barnes, 1980). The reversible reaction of silicon dioxide is:

$$SiO_2(S)+2H_2O(l) \leftrightarrow H_4SiO_4(aq)$$

For this reversible reaction, $H_4SiO_4(aq)$ is the precipitation of silicon dioxide. The net precipitation rate can be expressed as (Bhuana, Ashman & Nathan, 2009):

$$r'_{SiO_2} = -k_+\left(1 - {}^{Q}/_{K}\right)\frac{mol}{L.s}, \qquad 3.23$$

where the k_+ is the forward rate constant, K is the equilibrium constant and Q is the activity quotient. The Q/K is the degree of saturation (S).

Q is then calculated by

$$Q = {}^{a_{H_4SiO_4}}\Big/_{(a_{SiO_2})(a_{H_2O})^2}, \qquad 3.24$$

here a_i is the activity of species *i*. In the mathematical model, a_i is calculated as the silica concentration. As SiO_2 and H_2O are present as a solid and a liquid, then a_{SiO_2} and a_{H_2O} can be calculated as "1".

Rimistidt and Barnes (1980) provide a method to calculate k_+ and K as a function of temperature. The forward rate constant k_+ and the equilibrium constant are given by:

$$\log K = a_1 + b_1 T + c_1/T \qquad 3.25$$

$$\log k_+ = (a_1 + a_2) + b_1 T + (c_1 + c_2)/T \qquad 3.26$$

Rimistidt and Barnes (1980) provide the a_1, a_2, b_1, c_1, c_2 which is shown in table 3.1.

Table 3.1 Temperature functions of the rate constants for silica-water reactions (Rimistidt Barnes 1980)

$\log k_+ = 1.174 - 2.028 \times 10^{-3} T - 4158/T$
$a_2 = -0.707$, $c_2 = -2598$

For equation 3.23 to 3.26, the net precipitation rate of silica can be expressed as functions of temperature and silica concentration, as follows:

$$r'_{SiO_2} = 10^{(a_1+a_2)+b_1T+\frac{c_1+c_2}{T}}\left(1-\frac{a_{H_4SiO_4}}{10^{a_1+b_1T+\frac{c_1}{T}}}\right)\frac{mol}{L.s} \qquad 3.27$$

In the technical sub model, the r'_{SiO_2} is first calculated by the geothermal reservoir temperature. The result is compared with the reference silica precipitation. If the calculated silica precipitation is greater than the reference silica precipitation, the geothermal reservoir temperature is the minimum geothermal fluid temperature. If the silica precipitation is less than the reference silica precipitation, then the r'_{SiO_2} is then calculated by the geothermal reservoir temperature minus 10 ℃ until the calculated silica precipitation is greater than the reference silica precipitation.

3.3.7 Assessment of GAPG technology

The efficiencies of converting geothermal energy to power in two modes of the GAPG system are defined below.

In the power boosting mode:

$$\eta_{Boosting} = \frac{\Delta W_{Out}}{Q_{Geo} \pm \Delta Q_{Boiler}} . 100\% \quad 3.28$$

In the fuel saving mode:

$$\eta_{Saving} = \frac{\Delta W}{Q_{Geo}} . 100\% \quad 3.29$$

In the power boosting mode, the ΔW_{Out} (kW) is the increase in power output generated by the geothermal replacement, Q_{Geo} (kW) is the geothermal added to the power generation, ΔQ_{Boiler} (kW) is the change to the thermal energy load in the boiler (eg. the reheating load) due to the addition of geothermal heat.

As pointed out in part 3.3.1, Fig. 3.3 shows the schematic structure of the steam turbine which is used in the technical sub model. The ΔW_{Out} is calculated from the equation 3.20 and the extra power output caused by avoiding the extraction steam, where a is the extraction point (points 2 to 6, 8 to 12, 14 to 18 in Fig. 3.3) and $\dot{m}_a$ is the mass flow rate of the extraction steam that is avoided by the geothermal fluid.

$$\Delta W_{out} = f(m_a) = \sum_{i=a}^{n-1} m_a(h_i - h_{i+1}), \quad 3.20$$

In the fuel saving mode, to maintain the plant power output unchanged at the design value, the boiler flow rate needs to be reduced. Therefore the ΔW is the difference between the plant power output at this reduced boiler flow rate without any geothermal input and the designed plant output, which is:

$$\Delta W = W_{out} - \sum_{i=1}^{n}(h_i - h_{i+1})m'_{i,in}, \quad 3.30$$

where $m'_{i,in}$ (kg/s) is the mass flow rate of steam across each stages of steam turbine in fuel saving mode, and h_i (kJ/kg) is the enthalpy of steam at each point.

An exergy analysis of the system with and without geo-fluid input has been undertaken. The system boundary to be analysed is defined by the dotted lie shown in Fig. 3.11. The exergy efficiency of this system is defined below:

$$\eta_{exergy} = \frac{W+\Delta W_{out}}{X_{In}-X_{Out}+\Delta X_{Geo}}, \quad 3.31$$

where W (kW) is the output from the steam turbine without geothermal input, and ΔW_{out} is the increased output in the power boosting mode when the geothermal fluid is input into the system. The parameter X_{In} (kW) is the total exergy rate entering the system at locations 2, 4, and 6 of Fig 3.11, while X_{Out} is the total exergy output at locations 1, 3 and 5. Therefore ΔX_{Geo} (kW) is the total exergy change of the geo-fluid

into and out from the dotted boundary.

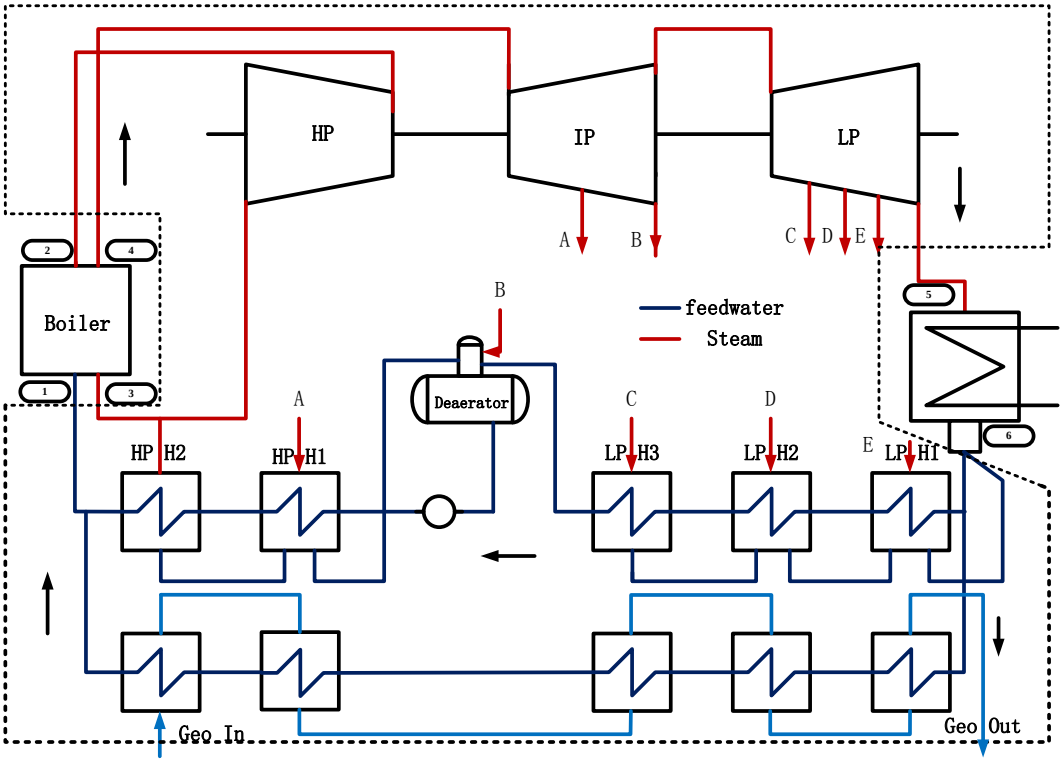

Figure 3.11 Schematic diagram of a GAPG power generation with full replacement of all closed feedwater heaters (the dotted line indicates the boundary for exergy analysis)

Referring to Fig. 3.11, the exergy into the system boundary (X_{in}) is calculated by

$$X_{In} = \dot{m}_2\psi_2 + \dot{m}_4\psi_4 + \dot{m}_6\psi_6, \quad 3.32$$

The exergy out of the system boundary is calculated by

$$X_{Out} = \dot{m}_5\psi_5 + \dot{m}_1\psi_1 + \dot{m}_3\psi_3, \quad 3.33$$

The exergy change of the geofluid is calculated from

$$\Delta X_{Geo} = \dot{m_{Geo}}(\psi_{Geo\ In} - \psi_{Geo\ Out}), \quad 3.34$$

where $\dot{m_{Geo}}$ (kg/s) is the mass flow rate of geothermal fluid and $\dot{\psi_{Geo\ In}}$ (kJ/kg) and $\dot{\psi_{Geo\ Out}}$ (kJ/kg) are the specific exergy flows of geofluid input to and output from the preheater.

3.4 Economics sub model

The economics sub model is used to calculate the economics of the GAPG system. The capital costs of geothermal wells and related devices and the economic benefit at different operational conditions are calculated in this sub model. The input parameters and output of the economics sub model is shown below.

Input parameters to the economics sub model

- O&M costs of power generation
- Costs of related geothermal devices
- Price of electricity
- Price of fossil fuel
- Mass flow rate per geothermal wells
- Depth of geothermal wells

Parameters taken from other sub models

- Fuel saved
- Extra output of electricity
- Available temperature of geothermal fluid

Outputs of economic sub model

- Income from extra electricity

- Costs of the saved fossil fuel
- Payback time
- Cost of electricity (COE)

3.4.1 Cost of electricity (COE)

The cost of electricity (COE) per kWh ($/kWh) takes into consideration such factors as the initial capital costs of the power plant, discount rates, the cost of operation and maintenance and the cost of fossil fuel (Sanyal 2004). The value that is ensured by discounting future income at a discount rate equals the return that might be gained from the investment.

The COE is calculated as (Kreith and Goswami, 2007):

$$COE = \frac{\sum_{t=0}^{t=N} \frac{C_t}{(1+a)^t}}{\sum_{t=1}^{t=N} \frac{Q_t}{(1+a')^t}} \quad 3.35$$

where N is the analysis period, which is the power plant life,

Q_t is the amount of (electrical) energy production in the period t ,

C_t is the investment cost of the power plant in the year t; the operations and maintenance cost in the year t and the fuel cost in the year t,

d' is the opportunity cost of capital which means the rate that investors could earn in

the financial markets with the capital, and

d is the discount rate which is an interest rate that an eligible depository is charged to borrow short term funds from a central bank.

3.4.2 Capital cost and O&M costs of GAPG technology

The capital cost includes drilling costs and other equipment costs. The factors that influence the drilling costs include (Entingh, 2006a):

- Design factors, which include the depth, trajectory and casing profile (diameter) of wells
- Location factors, which include the lithology of well fields, temperature of fluid and thermal gradient of well field
- Drilling problems.

Historically geothermal well costs have been estimated from the costs of oil and gas wells (Carson and Lin, 1981) and as a function of depth. However, these approaches do not consider the difference between geothermal wells and oil and gas wells (Mansure, 2005a) and are not reliable.

The geothermal drilling costs in this study were estimated using the formula of Dept. of Energy Geothermal Electricity Technology Evaluation Model, which has been

derived from geothermal wells (Entingh, 2006a). The formula of geothermal well costs is based on the well cost database from Mansure (Mansure, 2005b) which is the function of the depth of geothermal wells. The expression of the "average" line is given by (Entingh, 2006a):

$$C_{drill} = 0.58e^{0.0001491d} \ \$M \ (2004U\$), \quad 3.36$$

where d is the depth in feet and is based on 2000 U.S dollars.

Given the different lithologies of well fields, the low drilling costs and high drilling costs of geothermal wells are estimated from (Entingh 2006a):

$$\text{Low Drilling Costs} = 0.58e^{0.0001088d} \ \$M \ (2004U\$), \quad 3.37$$

$$\text{High Drilling Costs} = 0.58e^{0.0001893d} \ \$M \ (2004U\$), \quad 3.38$$

The capital costs of geothermal well fields also include the capital costs of other equipment for geothermal well fields. In this study, three kinds of equipment are considered:

- Geothermal surface equipment (pipes of well fields)
- Well stimulation
- Geothermal fluid pumps.

The O&M costs of geothermal well fields include the annual costs for the maintenance and the repair of equipment of the geothermal well field and the costs of staffing per year. In the economic sub model, the O&M costs for staffing of the facility is a user input and the O&M costs for maintenance and repair equipment costs of geothermal well field is a fraction of the capital costs of the geothermal well field which is also a user input.

In GAPG technology, each feedwater heater (except the deaerator) requires one geothermal preheater. Here it is assumed that the capital costs of the geothermal preheater equal that of the fossil fired Rankine plant feedwater heater.

3.4.3 Costs of a stand-alone geothermal alone power plant

The COE of a geothermal alone power plant involves three components of the power plant costs:

- The capital costs, which includes all interest payments and the financing cost
- The O&M costs of the power plant
- The capital costs of geothermal well fields and related devices.

Two kinds of geothermal alone power plant are considered: (a) a binary cycle power plant and (b) a flash cycle power plant. The estimation of the capital costs and

O&M costs of a geothermal alone power plant are based on the data in the Geothermal Electric Technologies Evaluation Model (Entingh, 2006b and Sanyal, 2004). The geothermal power plant with 50MW power capacity is used as a base case to calculate the capital costs and O&M costs of the geothermal alone power plant (Sanyal, 2004).

Capital costs of a binary cycle power plant

The capital costs of a binary cycle power plant depends on the performance of the geothermal plant, which is calculated based on the Geothermal Electric Technologies Evaluation Model (Entingh, 2006b). The plant costs are calculated as $ per KW, where the KW is the output of power plant.

The estimated cost of the binary cycle power plant is based on the 50MW plant as a function of geothermal resource temperature (Entingh, 2006a):

Geothermal resource temperature ＜190 ℃

$$Cost_{50WM} = K_0 + K_1 * T + K_2 * T^2 + K_3 * T^3, \qquad 3.39$$

where $Cost_{50WM}$ is for a 50MW index in $/kW

T is fluid temperature , ℃

K_0 = 21520.78

K_1= -331.34

K_2= 1.854876

K_3= -0.003491132

Geothermal resource temperature ＞190 ℃

$$Cost_{50WM} = Cost_{50WM,190\,℃} - 3.08 * (T - 190) \quad 3.40$$

Equations 3.39 and 3.40 are used for a 50MW binary power plant. For binary power plants with outputs other than 50MW, the plant cost ($/kW) is calculated by (Entingh, 2006a):

$$Cost = \left[50000 * Cost_{50WM} * \left({Inputted\ Plant\ Size}/{50}\right)^{0.8}\right]/(Input\ Plant\ Size * 1000) \quad 3.41$$

As pointed out by GETEM, equations 3.39 to 3.40 for the calculation of the capital costs of a geothermal plant include some uncertainty in respect of the plant size and resource temperature (Entingh, 2006a). So, in the economic sub model, the minimum power output of the binary cycle is 5 MW and the resource temperature is between 120℃ and 200℃.

Capital costs of a flash cycle power plant

Like the binary plant, the cost of the flash plant used in this study is based on the resource temperature, following the Geothermal Electric Technologies Evaluation Model (Entingh, 2006b). Each component of the power plant is calculated as $ per KW output of power plant, based on the gross binary effectiveness. The gross binary effectiveness (used to calculate the cost of the power plant) is calculated as (Entingh,

2006b):

$$be = C_0 + C_1 * T + C_2 * T^2, \quad 3.42$$

where T is the fluid temperature, ℉, and

(1) For a dual flash cycle:

C_0=-0.406848

C_1=-0.01166551

C_2=0.000101009

(2) For a single flash cycle:

C_0=2.6718

C_1=0.027828

C_2=0.000104

Based on the gross binary effectiveness, the cost of the geothermal fluid handling equipment, turbine generator, heat rejection, plant auxiliary and other equipment is calculated (Entingh, 2006b) as follows:

Geothermal fluid handling equipment:

$$\$/_{kW} = 85 * be^{-0.91} \quad 3.43$$

Turbine generator:

$$\$/_{kW} = 588 * output(MW)^{-0.29} \quad 3.44$$

Heat rejection

Surface condenser:

$$\$/_{kW} = 37 * be^{-0.17} \quad 3.45$$

Direct contact condenser:

$$\$/_{kW} = 102.5 * be^{-0.13} \quad 3.46$$

Plant auxiliary:

$$\$/_{kW} = 10.5 * be^{-0.17} \quad 3.47$$

Other equipment:

$$\$/_{kW} = 13.5 * be^{-0.005} \quad 3.48$$

O&M costs of a geothermal alone power plant

The O&M costs of such a geothermal power plant include the annual costs for maintenance and repair, equipment and staffing. Based on the GeothermEx's experience, the O&M costs of the geothermal power plant depend on the power output of the power plant, and ranges from 2cent/kWh to 1.4cent/kWh (Sanyal, 2004). The O&M costs of the geothermal power plant are calculated as (Sanyal, 2004):

$$c_0 = 2.0 * e^{-0.0025(P-5)} \text{ cent/kWh (US dollar in 2004),} \quad 3.49$$

where P (MW) is the power output of the power plant.

Chapter 4

Programming and model Validation

The GAPG model presented in Chapter 3 is coded by a computer programming language presented in Visual-Basic ie. Excel. The program is named GAPGEM which stands for “Geothermal Aided Power Generation Evaluation Model”. Real data from a subcritical Rankine steam cycle power plant has been used to validate the outputs of the model.

4.1 Programming of the mathematical modelling

4.1.1 Introduction

GAPGEM is able to simulate the technical performance of Rankine steam cycles and the Rankine steam cycle with geofluid replacement (GAPG technology), and the economic performance of GAPG technology. A main feature of GAPGEM is that it simulates various Rankine power plants with different structures and different

operational conditions for the GAPG technology. The thermodynamic data of GAPGEM is calculated by the WinSteam software which is copyrighted by Techware Engineering Application, Inc. Thus, when using the program (GAPGEM), users can:

- identify the structure of the power plant by choosing the number of stages of the steam turbine, the number of feedwater heaters of each stage of the steam turbine and the number of reheaters of the power plant;
- determine at which stages or locations, and by how much, geothermal energy is to be inputted into the plant. The GAPGEM can then calculate both the technical and economic performance of the GAPG technology for different operational conditions.

4.1.1.1 Structure of GAPGEM

GAPGEM consists of two sub programs which correspond to the technical sub model and economic sub model. Each subprogram can calculate the performance of the GAPG technology for two operational modes: the power boosting mode and the fuel saving mode.

Figure 4.1 shows the flow chart of GAPGEM. The GAPGEM program simulates the steam Rankine power plant under design conditions without geothermal replacement. The simulated results are used as a reference case. The geothermal information and the

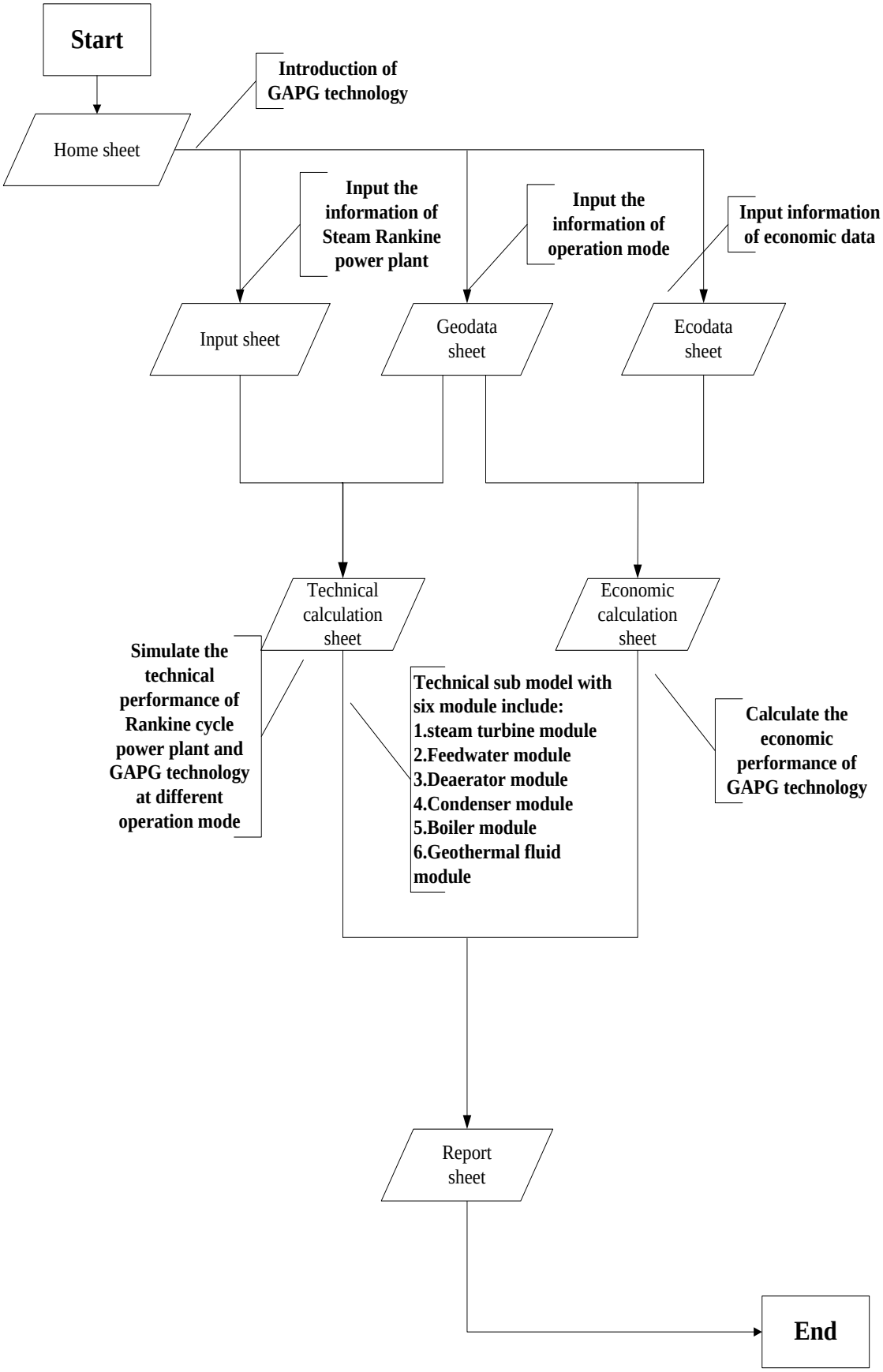

Figure 4.1 Flow chart of the software program of GAPGEM

operational condition of the GPAG technology is then input into the GAPGEM program. The technical performance and economic benefits of the GAPG plant under different operational conditions are then calculated by GAPGEM. Two operational modes, power boosting and fuel saving, are calculated, and for each mode, the users can choose between two scenarios, partial replacement or full replacement.

4.1.1.2 Steam cycle structure type

In order to run the GAPGEM program the structure of the power plant is required to input into the program by selecting the number of re-heating and turbine stages, the number of extractions in each stage of the turbine and their corresponding feed heater type (ie. open or close). There are up to 2 reheating stages, 3 turbine stages and 5 extraction points for each stage that can be selected in GAPGEM.

4.1.2 Operation Layout and Usage

GAPGEM is a spread sheet program and can be run in Microsoft Excel 2007 or a later version.

4.1.2.1 List of Sheets of GAPGEM programming

GAPGEM consists of 9 sheets, which include:

- Home sheet: to introduce the functions of GAGPEM.
- Power plant input sheet: to specify the physical arrangement of the steam Rankine power plant. The information about the steam Rankine power plant, which includes the pressure, temperature and mass flow rate of the steam turbine, the feedwater heater, the boiler and condenser is keyed into the input sheet to identify the structure of the power plant.
- Geodata sheet: to choose the operating conditions of a GAPG system. In the Geodata sheet, the stages and locations of the feedwater heater to be replaced by geothermal energy can be specific by the user. The GAPGEM can then calculate both the technical and economic performance of the GAPG technology for different operational conditions using these data.
- Ecodata sheet: to input the economic information about the geothermal well fields, the GAPG technology and the geothermal alone power plant (the binary cycle power plant, the flash cycle power plant).
- Report sheet: the technical performance and economic benefit of the GAPG plant under different operational conditions is given in a report sheet. The technical performance of the reference plant without geothermal fluid replacement is also shown on this sheet.
- Technical calculation sheets: technical calculations include three sheets: the CalculateFWH sheet, the GeoFWHboost sheet and GeoFWHsaving sheet. Each sheet is used to simulate different operating conditions of the GAPG

technology. The CalculateFWH sheet is used to simulate the steam Rankine power plant without geothermal replacement. The GeoFWHboost sheet is used to simulate the technical performance of GAPG technology for power boosting operations. The GeoFWHsaving sheet is used to simulate the technical performance of the GPAG technology for fuel saving operational conditions. The parameters from the power plant input sheet and Geodata sheet are used to simulate the technical performance of the Rankine cycle plant and the GAPG technology.

- Economic calculation: the capital costs, O&M costs of the geothermal well fields and the geothermal alone power plant, and the COE of the GAPG technology are calculated in this sheet.

4.1.2.2 An example case for GAPGEM

A 580MW subcritical power plant is used as a case study to show how to work a case using the GAPGEM.

Home sheet

This part of GAPGEM provides the information about the GAPG concept and the introduction of GAPGEM programming. A description of how to use the GAPGEM is also included in the home sheet.

Input sheet

The input sheet allows the user to specify the details of the power plant, up to three stages of the steam turbine, each of which can accommodate up to five feedwater heaters (open or closed feedwater heaters). Next, the temperature, pressure and flow rate of the steam cycle can be specified.

The specifics of the structure of the power plant include:

- Type and number of feedwater heaters
- Number of reheaters

The operational parameters of the specified power plant are:

- Mass flow rate, pressure and temperature of steam i let into the steam turbine
- Mass flow rate, pressure and temperature of steam coming out of the steam turbine
- Mass flow rate, pressure and temperature of extraction steam coming out of the steam turbine.
- The pressure, temperature and mass flow rate of steam under design conditions coming out of the boiler.
- The pressure and temperature of steam coming out of the reheater.

- Heat value of fossil fuel.
- Pressure loss of extraction steam
- Mass flow rate loss from the steam turbine
- Pressure loss through the feedwater heater system

Once the operational parameters of the power plant has been inputted, the GAPGEM is ready to run for the conventional power plant, ie. the Rakine steam power cycle; the enthalpy and entropy of each points of the power plant can be calculated by the WinSteam software. The simulation result of the power plant is shown in the Report sheet.

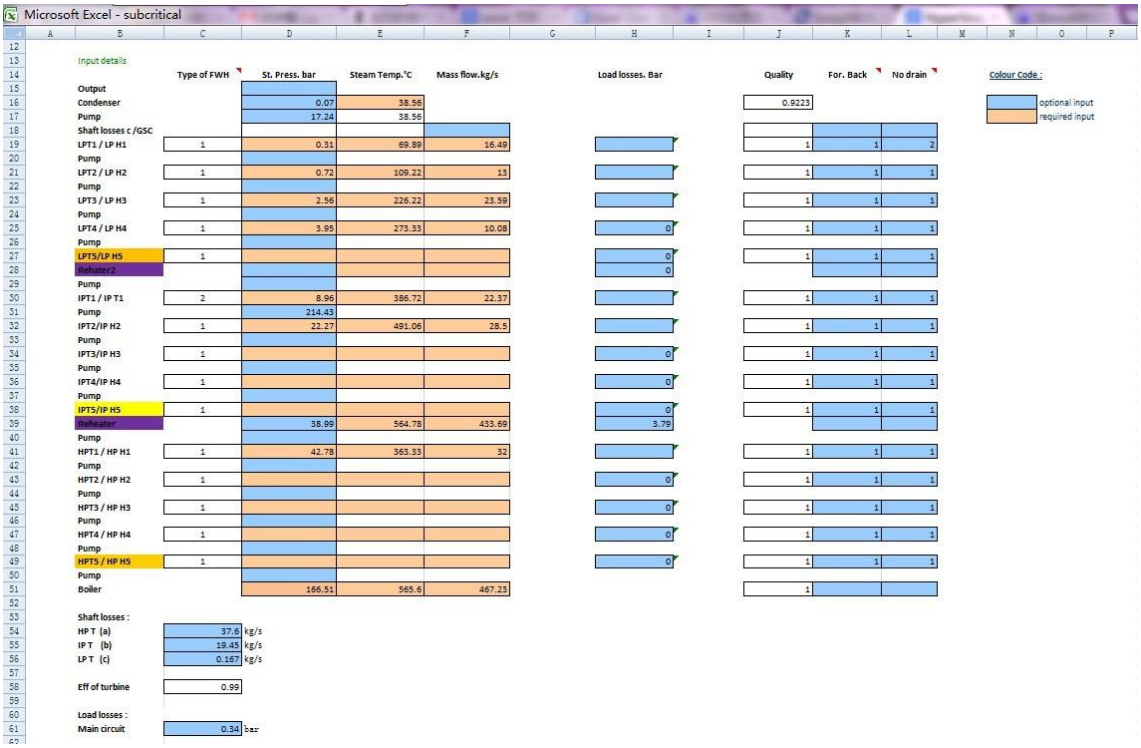

Figure 4.2 Input sheet of GAPGEM

Figure 4.2 shows the Input sheet of GAPGEM. The users are able to enter the details of the Rankine cycle power plant structure which include the types and number of feedwater heaters and the number of reheater stages. In GAPGEM, the types of feedwater heater include the closed feedwater heater ("1" represents closed feedwater heater), open feedwater heater ("2" represents open feedwater heater),. When the structure of the power plant is confirmed, the operational parameters which include pressure, temperature and mass flow rates of steam at various points of cycle can be entered.

Geodata sheet

The information about the geothermal fluid can be entered into the program in this page. Figure 4.3 shows a Geodata sheet of GAPGEM. Specific geothermal information required is:

- Silica concentrations in the geothermal fluid
- Feedwater heaters that are replaced by geothermal fluid
- Percentage of extraction steam to be replaced by geothermal fluid

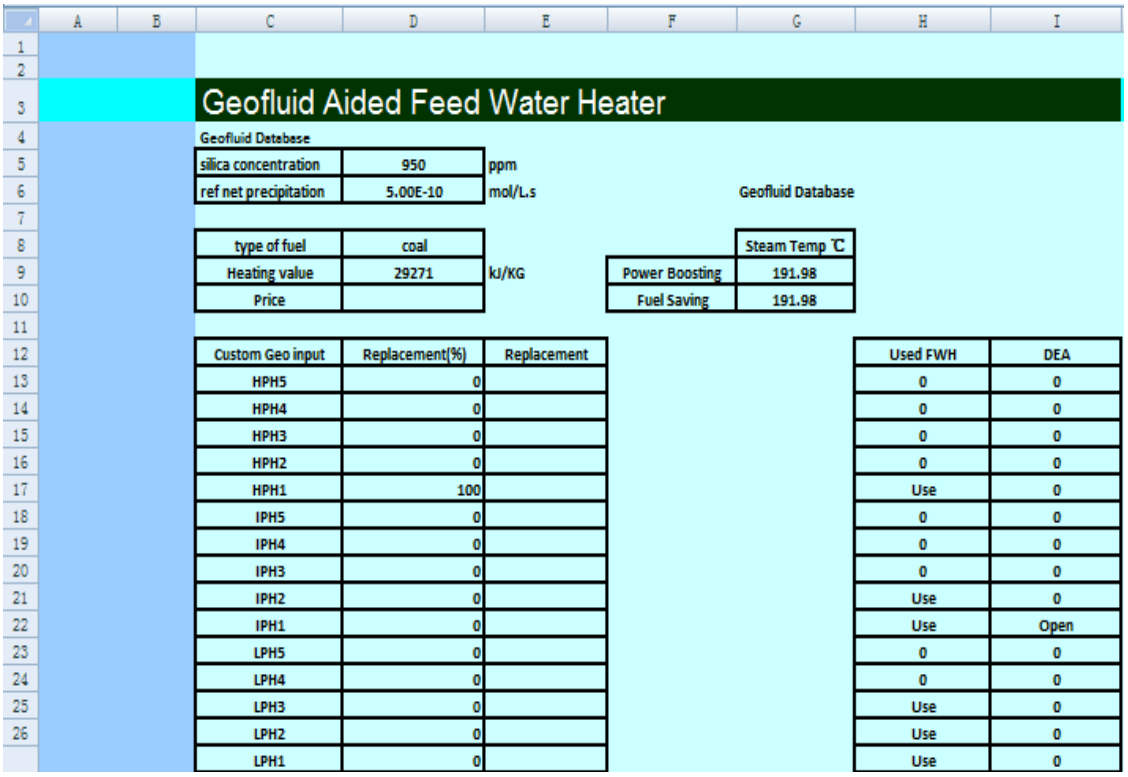

Geofluid Aided Feed Water Heater

Geofluid Database		
silica concentration	950	ppm
ref net precipitation	5.00E-10	mol/L.s

Geofluid Database

type of fuel	coal
Heating value	29271 kJ/KG
Price	

	Steam Temp ℃
Power Boosting	191.98
Fuel Saving	191.98

Custom Geo input	Replacement(%)	Replacement	Used FWH	DEA
HPH5	0		0	0
HPH4	0		0	0
HPH3	0		0	0
HPH2	0		0	0
HPH1	100		Use	0
IPH5	0		0	0
IPH4	0		0	0
IPH3	0		0	0
IPH2	0		Use	0
IPH1	0		Use	Open
LPH5	0		0	0
LPH4	0		0	0
LPH3	0		Use	0
LPH2	0		Use	0
LPH1	0		Use	0

Figure 4.3 Geodata sheet of GAPGEM

Ecodata sheet

The economic data concerning geothermal well fields, the GAPG technology and geothermal stand alone power plants (the binary cycle power plantand the flash cycle power plant) can be input through the Ecodata sheet to calculate the economics of the GAPG plant,the fossil fired power plant and the geothermal alone power plant. Three kinds of economic data can be input into the Ecodata sheet: the information about geothermal well fields, economic data about the geothermal alone power plant and economic data about the fossil fired power plant.

Input of geothermal wells		
Well Cost Curve	Low	
	Med	1
	High	
Tempter of Geothermal fluid	℃	180
Production Well Depth	Feet	4000
Injection Well Depth	Feet	5000
Injection to Producer	Ratio	1.1
Mass flow of Geo Power boosting	kg/s	385.66
Mass flow of Geo Fuel saving	kg/s	373.14
Mass flow per Well	kg/s	91
Number of Pro Wells Power boosting	Count	5
Number of Pro Wells Fuel saving	Count	5
Number of inj Wells Power boosting	Count	6
Number of inj Wells Fuel saving	Count	6
Surface Equipment Cost per well	$k/well	100

Figure 4.4 Input data required of geothermal wells

Figure 4.4 shows an example of the geothermal well fields information. The cells coloured white denote an input for the user to specify, the cells coloured yellow denote the data from other sheets and the cells coloured red denote the calculated result by input data. As shown in figure 4.4, the information required about the geothermal wells that should be input into Ecodata sheet includes:

- Well costs curve: As pointed out in Chapter 3, three formulas (equation 3.36 to 3.38) can calculate the capital cost of geothermal wells. Users of GAPGEM are able to choose one formula to calculate the cost of geothermal wells under different geologic conditions.
- Temperature of geothermal fluid;

- Depth of geothermal wells (production well, injection well) and injection to production ratio;
- Mass flow rate per well;
- Surface equipment cost of geothermal wells.

Figure 4.5 shows the input information required for the geothermal power plant to calculate the plant cost for the power boosting and fuel saving modes. Figure 4.6 shows the input information required for the combustion power plant and GPAG technology. These are used to calculate the COE of the GAPG technology.

Input of Binary power plant		
Plant size Power Boosting	MW	24.00
Plant size Fuel Saving	MW	24.00
Brine Effiectiveness(PB)		
Brine Effiectiveness(FS)		
Calculated Plant Costs(PB)	$/kW	1873.00
Calculated Plant Costs(FS)	$/kW	1873.00

Input of Flash power plant		
Plant size(PB)	MW	24.00
Plant size(FS)	MW	24.00
Number of flash		2
Condenser typy	Surface	
	Direct contact	1
NCG Removal	Jet	
	Vac pmp	
Calculated Plant Costs(PB)	$/kW	880.34
Calculated Plant Costs(FS)	$/kW	880.34

Input of Geo power well		
Number of production(binary)	count	4
Number of injection(binary)	count	5
Number of production(flash)	count	10
Number of injection(flash)	count	11
Surface Equipment Cost per well	$k/well	100

Figure 4.5 Input data required of geothermal power plant

Input of power plant and GAPG technology		
Plant size	MW	581.20
Plant size of GAPG(PB)	MW	22.26
Plant size of GAPG(FS)	MW	21.74
Total Plant Cost	K$	892433.00
Cost of Feedwater	K$	74674.00
O&M material cost	K$/year	21078.35
O&M labor cost	K$/year	0.00
Discount rate	%	3.00
Opportunity rate	%	3.00
Price of fossil fuel	$/ton	38.18
Fuel	ton/day	5248.00
Cost of Fuel	k$/year	62175.76
Labor cost	k$/year	0.00

Figure 4.6 Input of combustion power plant and GAPG technology

Report sheet

The simulation result of the technical performance and economic benefit of the power plant and GAPG technology is presented in the report sheet. Two levels of the analysis of GAPG technology are shown in this report:

- Power boosting mode,
- Fuel saving mode.

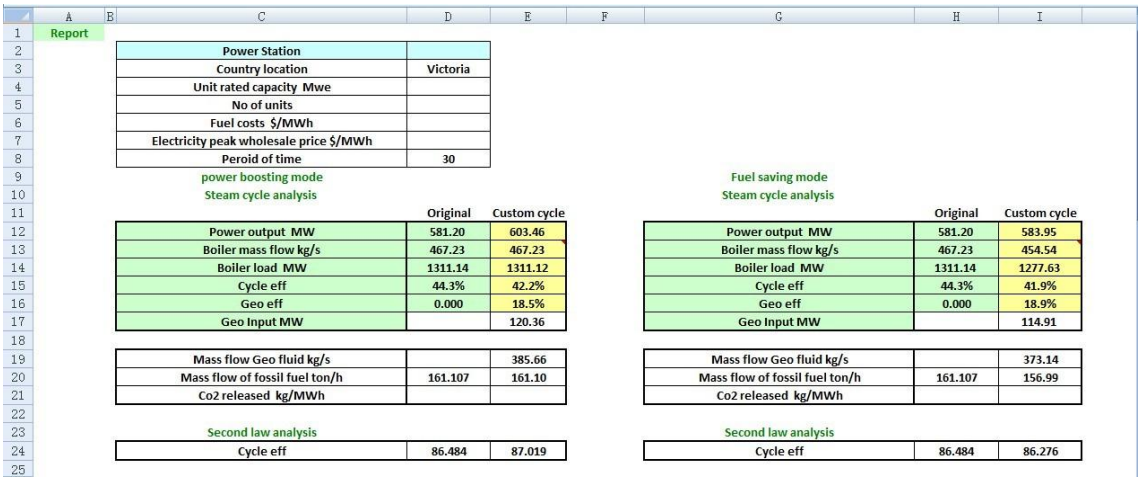

Report

Power Station	
Country location	Victoria
Unit rated capacity Mwe	
No of units	
Fuel costs $/MWh	
Electricity peak wholesale price $/MWh	
Peroid of time	30

power boosting mode
Steam cycle analysis

	Original	Custom cycle
Power output MW	581.20	603.46
Boiler mass flow kg/s	467.23	467.23
Boiler load MW	1311.14	1311.12
Cycle eff	44.3%	42.2%
Geo eff	0.000	18.5%
Geo Input MW		120.36
Mass flow Geo fluid kg/s		385.66
Mass flow of fossil fuel ton/h	161.107	161.10
Co2 released kg/MWh		

Second law analysis

Cycle eff	86.484	87.019

Fuel saving mode
Steam cycle analysis

	Original	Custom cycle
Power output MW	581.20	583.95
Boiler mass flow kg/s	467.23	454.54
Boiler load MW	1311.14	1277.63
Cycle eff	44.3%	41.9%
Geo eff	0.000	18.9%
Geo Input MW		114.91
Mass flow Geo fluid kg/s		373.14
Mass flow of fossil fuel ton/h	161.107	156.99
Co2 released kg/MWh		

Second law analysis

Cycle eff	86.484	86.276

Figure 4.7 Technical output of Report sheet

Figure 4.7 shows an example of the technical output of GAPG technology from a report sheet for power boosting and fuel saving modes. Figure 4.8 shows an example of the economic output of the GAPG technology from the report sheet. The calculated costs of electricity of the GAPG technology, the geothermal alone power plant and the fossil fired power plant are presented. In relation to the technical output, the left column presents the power boosting mode and the right column the fuel saving mode.

GAPG

Well field Capital	Cent/KWh	0.237
Well field O&M	Cent/KWh	0.065
Field Non well Capital	Cent/KWh	
Field Non well O&M	Cent/KWh	
Plant Capital	Cent/KWh	0.563
Plant O&M	Cent/KWh	1.575
GAPG Capital	Cent/KWh	0.129
GAPG O&M	Cent/KWh	0.065
COE	Cent/KWh	2.569

Binary power plant

Well field Capital	Cent/KWh	0.237
Well field O&M	Cent/KWh	0.065
Field Non well Capital	Cent/KWh	0
Field Non well O&M	Cent/KWh	0
Plant Capital	Cent/KWh	0.725
Plant O&M	Cent/KWh	1.917
COE	Cent/KWh	2.944

Rankine cycle power plant

capital cost	Cent/KWh	0.584
O&M cost	Cent/KWh	1.635
COE	Cent/KWh	2.219

GAPG

Well field Capital	Cent/KWh	
Well field O&M	Cent/KWh	
Field Non well Capital	Cent/KWh	
Field Non well O&M	Cent/KWh	
Plant Capital	Cent/KWh	
Plant O&M	Cent/KWh	
GAPG Capital	Cent/KWh	
GAPG O&M	Cent/KWh	
COE	Cent/KWh	

Binary power plant

Well field Capital	Cent/KWh	
Well field O&M	Cent/KWh	
Field Non well Capital	Cent/KWh	
Field Non well O&M	Cent/KWh	
Plant Capital	Cent/KWh	
Plant O&M	Cent/KWh	
COE	Cent/KWh	

Rankine cycle power plant

capital cost	Cent/KWh	
O&M cost	Cent/KWh	
COE	Cent/KWh	

Figure 4.8 Report sheet for the economic calculations

Technical calculation sheet and economic calculation sheet

The technical calculation and economic calculation sheets include 5 sheets which suit the technical and economic sub models. The input parameters from the power plant input sheet, the Geodata sheet and the Ecodata sheet are used to simulate the technical performance and COE of the Rankine cycle power plant and the GAPG technology for two operational modes and for the silica precipitation of the geofluid. Winsteam Software is used in these sheets to calculate the enthalpy and entropy of each point of the power plant by using the input from the power plant input sheet.

4.2 Model validation

The validation of the mathematical model is performed for the fossil fire power plants cases only. As the modelling of the power plant and the modelling of using geothermal fluid to preheat use the same principle to keep the heat and mass balance of the steam cycle, the validation of the mathematical modelling can be simplified to use mathematical modelling to simulate the fossil fired power generation. The results of the simulation can be compared to the operational results.

Two coal fired power plants, a subcritical coal fired power plant and a supercritical coal fired power plant, are claimed as case studies to verify the first phase of the mathematical modelling:

- **Subcritical power generation**: LOY YANG power plant is a 500 MW sub critical fossil fired power generation which is located in Victoria, Australia. Data are obtained from Baziotopoulos (2002).

- **Supercritical power generation:** The case study of a 580 MW supercritical power generation is from the report for national Energy Technology Laboratory (NETL, 2007).

Figure 4.9 Heat and steam balance of the 500 MW LOY YANG unit at design conditions (Baziotopoulos, 2002)

Figure 4.9 shows the operation parameters of the extraction steam when the subcritical power plant is running at design conditions The parameters in Fig. 4.9 are measured parameters at design conditions. The extraction steam from points A, B, C, D, E, and F is used to preheat the feedwater. The extraction steam from the points A, B, D, E, and F enters the closed feedwater heaters. The extraction steam from the point C enters into the deaerator which is also used to remove oxygen from the feedwater.

Table 4.1 compares the measured with the simulated parameters of the subcritical LOY YANG power plant. The result shows that the difference between the simulated result and the designed operational conditions is less than 5%.

Table 4.1 Comparison result of operational parameters and simulated parameters of the subcritical power plant

	Measured Parameters	Simulated Parameters	Difference
Output of steam turbine	500 MW	501.7MW	0.34%
Feedwater temperature enter into the boiler	251.1 ℃	250.9 ℃	0.08%
Feedwater temperature at point A	251.1 ℃	250.9 ℃	0.08%
Feedwater temperature at point B	202.0 ℃	206.8 ℃	2.38%
Feedwater temperature at point C	157.1 ℃	164.9 ℃	4.96%
Feedwater temperature at point D	118.3 ℃	118.0 ℃	0.25%
Feedwater temperature at point E	90.6 ℃	90.6 ℃	0
Feedwater temperature at point F	53.9 ℃	53.5 ℃	0.74%
Feedwater temperature of GSC	45.6℃	45.2 ℃	0.88%

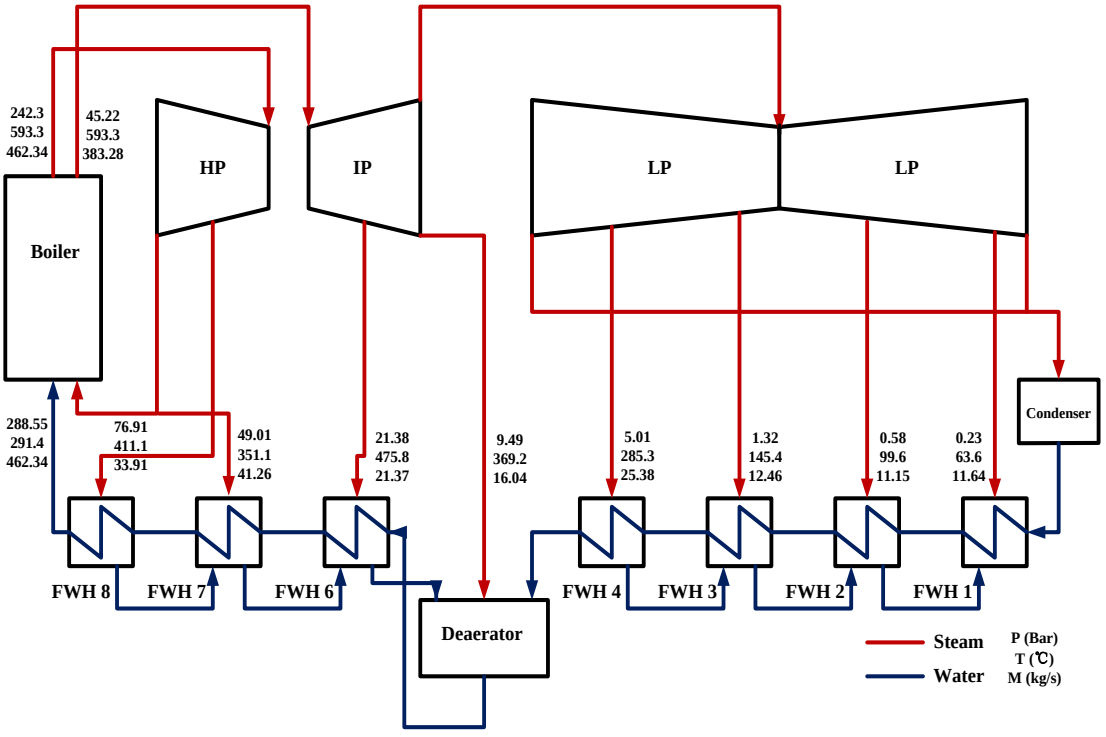

Figure 4.10 Heat and steam balance of the supercritical unit at design conditions (NETL, 2007)

Figure 4.10 shows the operational parameters of the extraction steam when the supercritical power plant is running at design conditions. The parameters in Fig. 4.10 are measured parameters at design conditions. The supercritical power plant has seven closed feedwater heaters which are used to preheat feedwater and one deaerator.

Table 4.2 shows the comparison result between the measured and calculated parameters of a supercritical power plant. The result shows that the difference between the simulated result and the designed operational conditions is less than 2%.

Table 4.2 Comparison result of operational parameters and simulated parameters of supercritical power generation

	Measured Parameters	Simulated Parameters	Difference
Output of steam turbine	580 MW	580.5MW	0.09%
Feedwater temperature enter into the boiler	291.4℃	287.7℃	1.27%
Feedwater temperature at FWH8	291.4℃	287.7℃	1.27%
Feedwater temperature at FWH7	260.8℃	259℃	0.69%
Feedwater temperature at FWH6	215.3℃	218.7℃	1.58%
Feedwater temperature at DEA	181.9℃	184℃	1.15%
Feedwater temperature at FWH4	147.2℃	144.4℃	1.9%
Feedwater temperature at FWH3	103.3℃	103.7℃	0.38%
Feedwater temperature at FWH2	81.3℃	80.8℃	0.62%
Feedwater temperature at FWH1	60.9℃	60.6℃	0.49%
Feedwater temperature at Condenser	39.2℃	38.8℃	1.02%

Tables 4.1 and 4.2 show that the difference between the measured parameters and simulated parameters is less than 5%, so it can be concluded that the mathematical modelling is correct. Because of the validation of the mathematical modelling for both

the case studies of the subcritical coal fired power plant and the supercritical coal fired power plant at design conditions, the bugs and the errors of the mathematical modelling would be cleared. Since the function of using geothermal fluid to preheat feedwater is to maintain the energy and mass balance of the steam cycle, also applies to the functions of the steam power generation, the simulated result of the power plant with the GAPG system can be considered to be correct.

Chapter 5

Technical Case Study

5.1 Introduction

In this chapter, a detailed technical evaluation is performed, using the model of GAPG in a subcritical power plant to assess the merits of the GAPG under various conditions. The 500MW subcritical power plant (LOY YANG power plant in Victoria, Australia) has been selected as the case study; the heat and steam balance for this power plant is shown in Fig. 5.1.Some parameters of the LOY YANG power plant are shown in Table 5.1.

Table 5.1 Parameters of LOY YANG power plant

Power output	500MW
Boiler mass flow rate	407.71 kg/s
Boiler load	1113.203 MW
Cycle efficiency	45.1%
Mass flow rate of fossil fuel	136.785 ton/h

The LOY YANG power plant is a subcritical power plant with five closed feedwater heaters and one deaerator. The extraction steam at point A is bled from the high pressure steam turbine, the extraction steam at points B and C are bled from the intermediate pressure steam turbine, and the extraction steam at point D, E and F are bled from the low pressure steam turbine.

Figure 5.1 Heat and steam balance of the 500 MW unit at design condition

The technical performance of the GAPG technology is assessed for four scenarios of the geofluid temperature. In this case study, it is assumed that the silica concentrations of the geofluid is 900 ppm at 260℃, 700ppm at 210℃ and 130℃.

Table 5.2 lists the scenarios assessed here. In the first scenario, the geothermal fluid was assumed to enter the power plant at the temperature of 260℃. According to equation 4.27, the silica precipitates at about 195℃, the geofluid can only be used to replace extraction steam at point A. So, in the first scenario, geothermal fluid at a temperature of 260℃is used to replace 100% of the extraction steam at point A (in Figure 5.1), and then returned at 195℃. Figure 5.2 shows the schematic diagram for scenario 1.

Table 5.2 Replacing scenarios and numbers of subcritical power plant

Scenarios No.	Geothermal Temperature in	Geothermal Temperature out	Replacing scenarios
Scenario 1	260℃	195℃	Replacing the extraction steam at point A
Scenario 2	210℃	170℃	Replacing the extraction steam at point B
Scenario 3	260℃	55℃	Replacing all the extraction steam at point A, B, D, E, F
Scenario 4	130℃	55℃	Replacing the extraction steam at point D, E and F

In the second scenario, the geofluid temperature is 210℃ and the silica is to precipitate at about 170℃. Here the geofluid can be used to replace the extraction steam at point B. So, in the second scenario, geothermal fluid at a temperature of 210℃ can be used replace 100% of the extraction steam at point B (in Figure 5.1) and then returned at 170℃ (Figure 5.3 shows the schematic diagram of scenario 2).

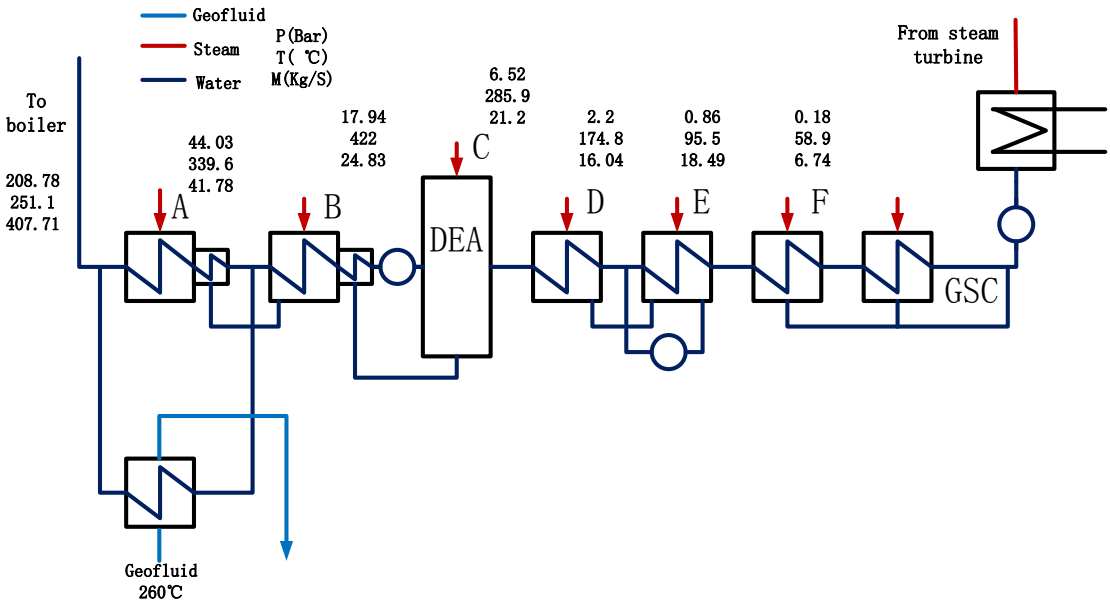

Figure 5.2 Schematic diagram of the subcritical power plant feedwater system with GAPG technology, scenario 1, replacing the extraction steam at point A.

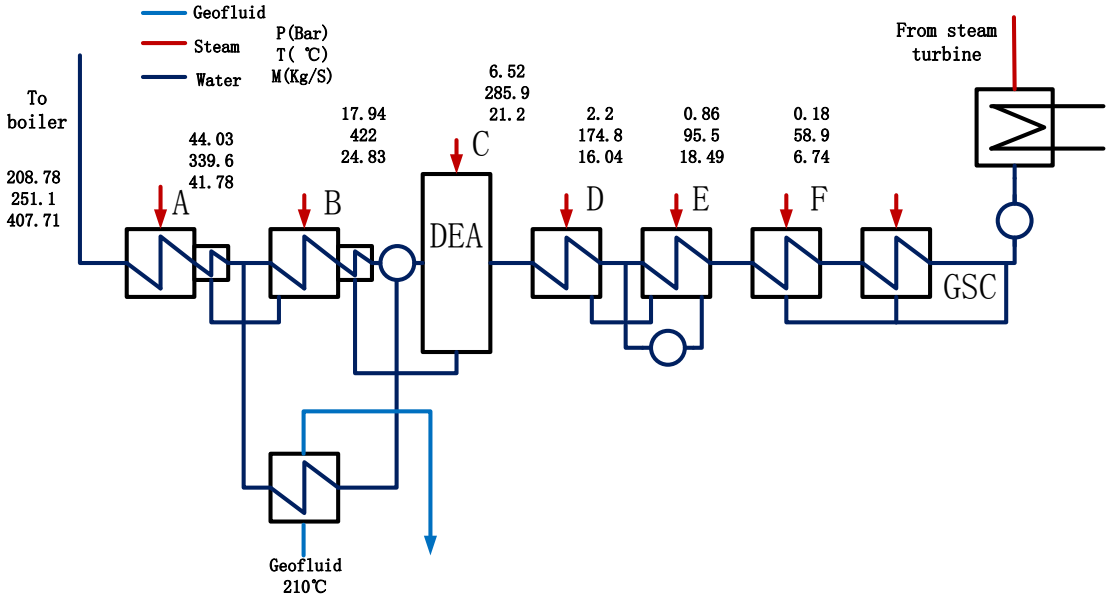

Figure 5.3 Schematic diagram of subcritical power plant feedwater system with GAPG technology (scenario 2, replacing the extraction steam at point B)

In the third scenario (assuming no silica in geofluid, so all FWH can be replaced by geofluid), the same temperature of the geothermal fluid as in scenario one was used to replace all the extraction steam points in Fig. 5.1 (Figure 5.4 shows the schematic diagram of scenario 3).

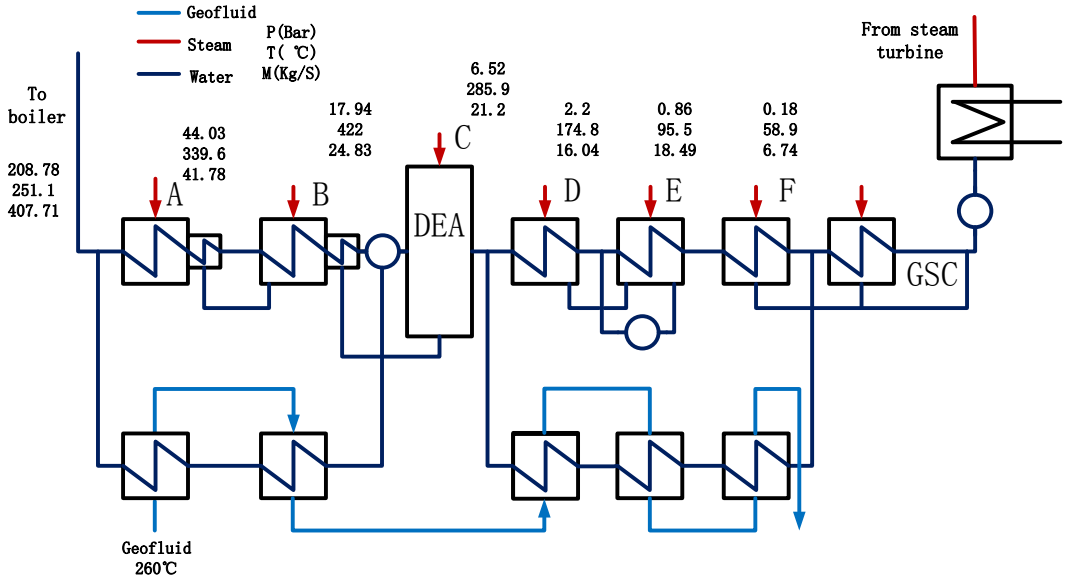

Figure 5.4 Schematic diagram of the subcritical power plant feedwater system with GAPG technology, scenario 3, replacing all the extraction steam at point A, B, D, E, F.

In the fourth scenario(assuming no silica in geofluid, so all FWH can be replaced by geofluid), it was assumed a lower temperature (130℃) geothermal fluid was available and could only be used to replace the extraction of low pressure heaters, which are D, E, F in Fig. 5.1 (Figure 5.5 shows the schematic diagram of scenario 4).

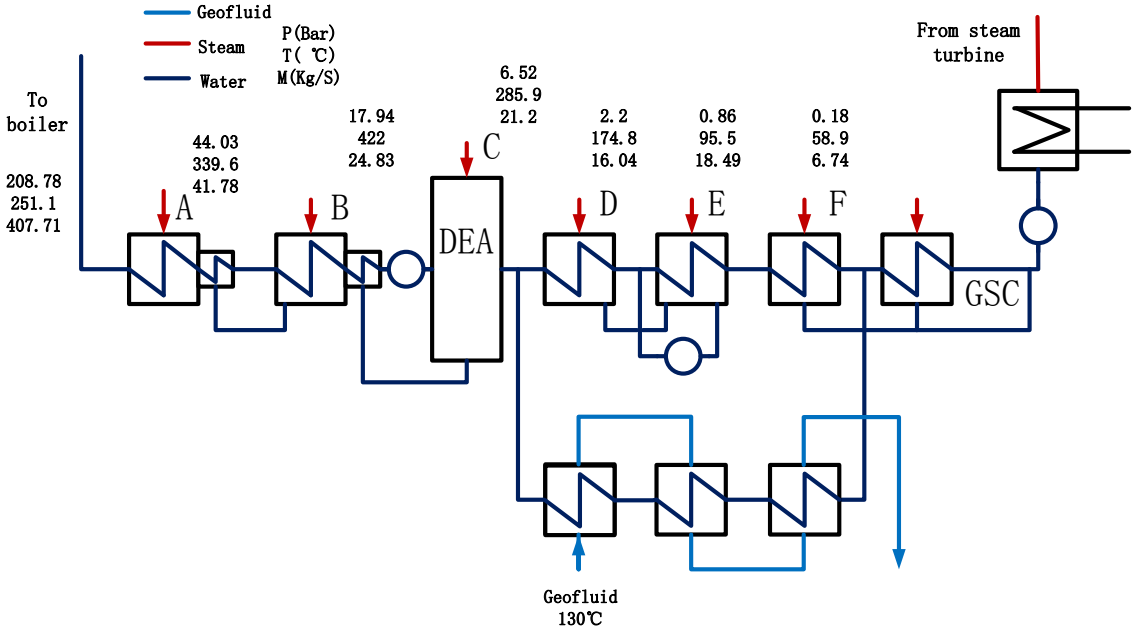

Figure 5.5 Schematic diagram of the subcritical power plant feedwater system with GAPG technology, scenario 4, replacing the extraction steam at point D, E and F.

5.2 Energy analysis of GAPG in the study case

For the GAPG technology, the geothermal replacement of extraction steam in a feedwater heater does not need to be carried out completely; instead, with a different mass flow rate of geofluid, the extraction steam can be replaced at any percentage from 0% to 100%. Figure 5.6 shows the simulated result of the extra power output from the geothermal fluid for the different proportions of replacement for the four scenarios while Fig. 5.7 shows the simulated result of saved fossil fuel for these four scenarios.

The results in Fig. 5.6 show that when the extraction steam at point A (scenario 1) is fully replaced by geothermal fluid the increased power output is nearly 50MW and the total power output of the power plant is 550MW. This means that when the extraction steam at point A is fully replaced by geothermal fluid, the power output of the steam turbine increases by nearly 10%.When the replacement of the extraction steam is at point B, the additional power from the geofluid is 22.16 MW. The lower output occurs because the quality, i.e. the temperature of geothermal fluid, is lower. In scenarios 3 and 4, when the geothermal fluid fully replaces the extraction steam the extra output of GAPG technology is 84.33 MW and 12 MW. The results of scenario 3 show when the closed feedwater heater is completely replaced by geothermal fluid, the extra output is the highest. However, this scenario requires the precipitation of silica to be addressed.

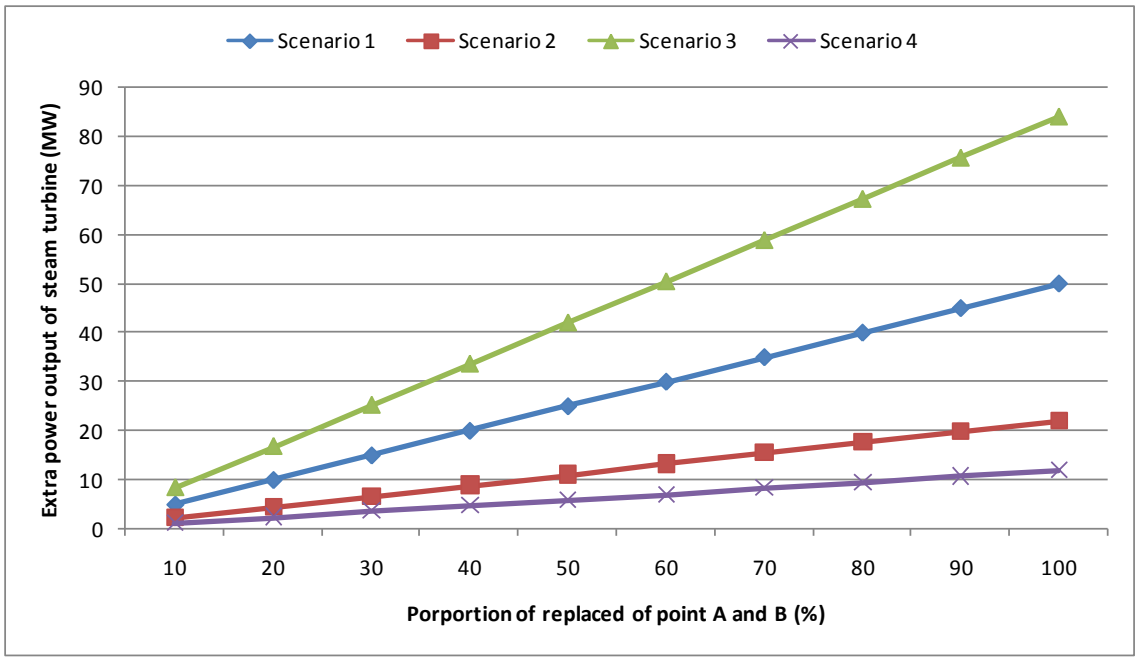

Figure 5.6 Extra power output for the steam turbine for the four scenarios of different proportions of replacement of bled steam in the power boosting mode.

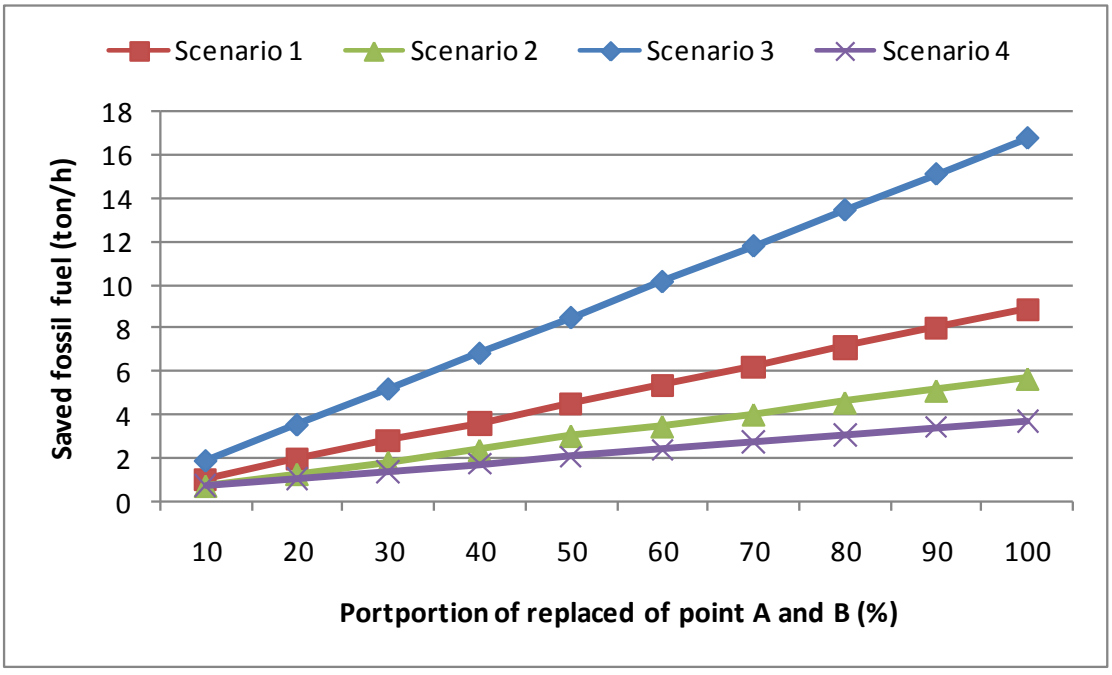

Figure 5.7 Saved coal of power plant for the four scenarios of different proportions of replacement of bled steam in the fuel saving mode.

The results shown in Fig. 5.7 indicates that when the geofluid is used to replace the extraction steam at point A, more coal would be saved than if geothermal fluid is used to replace the extraction steam at point B. When the extraction steam at point A is fully replaced by geothermal fluid, the saved fossil fuel is 9.37 ton/h. Compared with the mass flow rate of fossil fuel without geothermal fluid (136.785 ton/h in Table 5.1), about 6.85 % of the fossil fuel is saved when the extraction steam at point A is fully replaced by geothermal fluid and 4.77% of the fossil fuel is saved when the extraction steam at point B is fully replaced by geothermal fluid. For scenarios 3 and 4, when the geothermal fluid is fully replaced, the saved fossil fuel caused by the GAPG technology is 17.48 ton/h and 4.48 ton/h respectively.

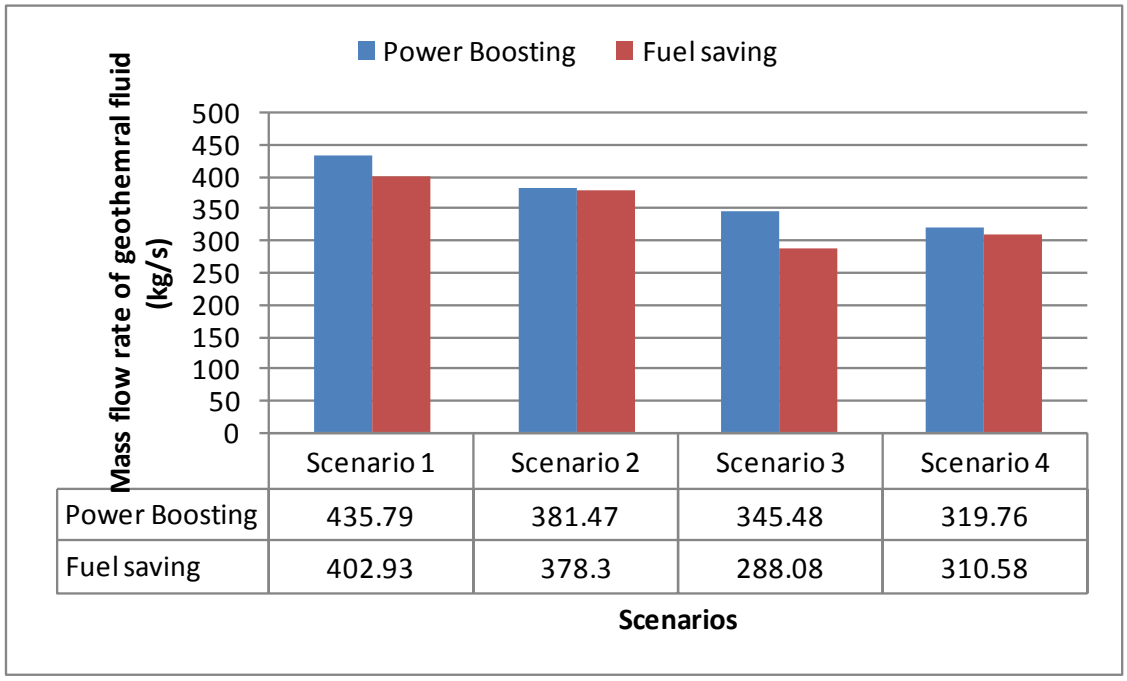

Figure 5.8 Mass flow rate of geothermal fluid required in different operational modes for four scenarios

Figure 5.8 shows the mass flow rate of geofluid in different operational modes for four scenarios. It can be seen that the mass flow rate of geothermal fluid needed for the fuel saving mode is less than that needed for the power boosting mode. The reason is that, in the fuel saving mode, the mass flow rate of feedwater is less than in the power boosting mode, which means that less energy from the geofluid is needed in the fuel saving mode. This means that when the extraction steam of the single feedwater heater is replaced by geofluid, the feedwater heater with higher extraction steam requires more geofluid than that with lower extraction steam. However, at the same temperature of geofluid (scenarios 1 and 3), the mass flow rate of geofluid needed for scenario 1 (435.79kg/s power boosting mode, 402.93 kg/s fuel saving mode) is more than for scenario 3 (345.48 kg/s power boosting mode, 288.08 kg/s fuel saving mode). This means that when the geofluid is used to replace the extraction steam from more than one feedwater heater, a lower flow rate of geofluid is needed than for the replacement of one stage of the feedwater heater.

From the thermodynamic point of view, the efficiency of a geothermal power plant is capped by the temperature of the geothermal fluid from the ground in geothermal alone power plants. The maximum efficiency of a steam cycle is called Carnot efficiency. The efficiency of the GAPG technology which does not directly use geothermal energy to produce electrical power is not capped by the Carnot efficiency. The GAPG technology has the advantage of the utilization of geothermal energy. The efficiency of geothermal energy converting to electricity in the GAPG has been defined

in chapter 3, as follows:

For power boosting mode

$$\eta_{Boosting} = \frac{\Delta W_{Out}}{Q_{Geo} \pm \Delta Q_{Boiler}} . 100\% \quad 5.1$$

For fuel saving mode:

$$\eta_{Saving} = \frac{\Delta W}{Q_{Geo}} . 100\% \quad 5.2$$

Figure 5.9 shows the efficiencies in the GAPG system for different scenarios. It can be seen that the scenario 1 has the highest efficiency of geothermal energy to convert to power. And at the same geothermal temperature, the efficiency of replacing the extraction steam of the single feedwater heater (scenario 1) is higher than the efficiency of replacing the extraction steam of all the feedwater heaters (scenario 3).

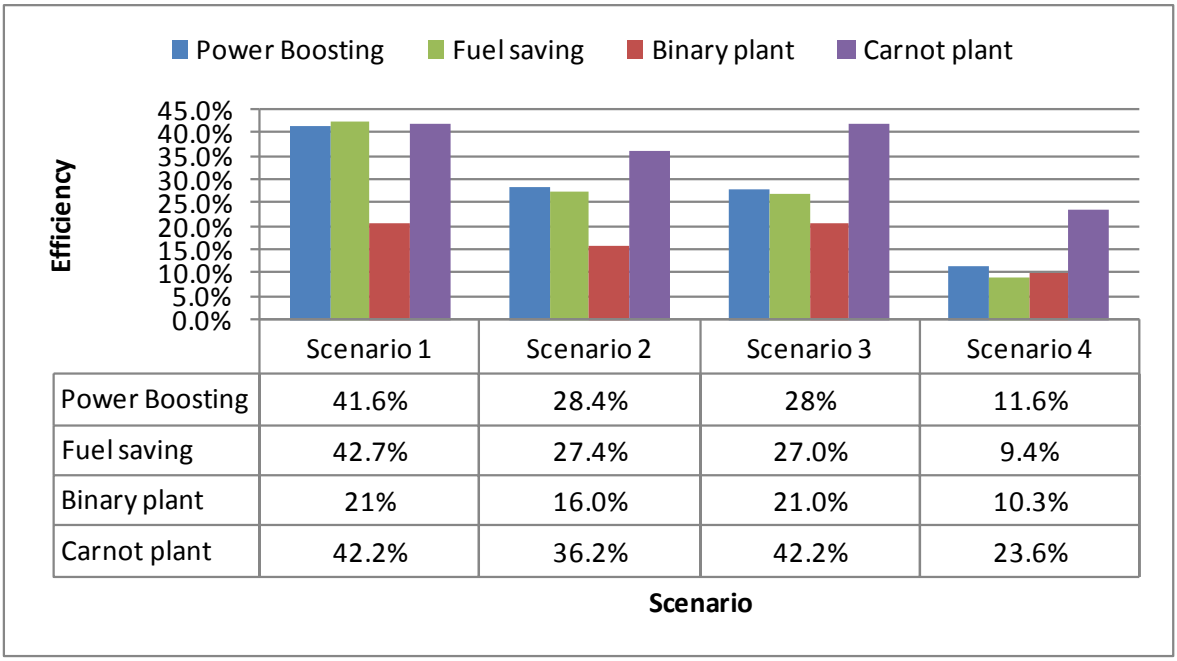

	Scenario 1	Scenario 2	Scenario 3	Scenario 4
Power Boosting	41.6%	28.4%	28%	11.6%
Fuel saving	42.7%	27.4%	27.0%	9.4%
Binary plant	21%	16.0%	21.0%	10.3%
Carnot plant	42.2%	36.2%	42.2%	23.6%

Figure 5.9 Efficiencies of the geothermal component of the power in the GAPG system for different scenarios

In Fig. 5.9, the efficiency of the binary cycle power plant is calculated based on the US Department of Energy GETEM model (Entingh, Mines 2006). The results in Fig.5.9 show that compared with the geothermal alone power plant (the binary cycle power plant), the GAPG technology has higher efficiency, especially for geothermal fluid with a high temperature. It has been shown that the efficiencies of the GAPG technology for scenario 1 are 41.6% for the power boosting mode and 42.7% for the fuel saving mode while the efficiency of the binary cycle power plant is 21 %. In scenario 2, the efficiencies of the GAPG technology are 28.4% for the power boosting mode and 27.4% for the fuel saving mode while the efficiency of the binary cycle power plant is 16 %.

Figure 5.9 also shows the efficiency of the GAPG technology compared with the Carnot plant at maximum geofluid temperature. The Carnot cycle is a reversible cycle which is composed of two isothermal processes and two adiabatic processes. Since the Carnot efficiency is the maximum theoretically possible efficiency for a heat engine working between the two temperatures, the Carnot efficiency of a steam cycle is capped by the hot reservoir temperature of that steam cycle. In the GAPG technology, the Carnot efficiency of the GAPG technology is not calculated by the maximum geothermal temperature, however, but is calculated by the combustion temperature in the boiler.

5.3 Exergy analysis of GAPG in the study case

The second law efficiency and the exergy destruction of each part of a power plant is calculated by mathematical modelling. The exergy efficiency of a power plant with the GAPG technology had been defined in chapter 3 as:

$$\eta_{\text{exergy}} = \frac{W+\Delta W}{\psi_{\text{In}}-\psi_{\text{Out}}+\Delta\psi_{\text{Geo}}} \quad 3.31$$

ψ_{In} is the total flow exergy entering the power plant. ψ_{Out} is the total flow exergy leaving the power plant. $\Delta\psi_{\text{Geo}}$ is the total exergy change of feedwater which absorbs heat from the geothermal fluid. Figure 5.10 shows the schematic diagram of a subcritical power plant (the LOY YANG power plant) for the exergy analysis. In this case study, for the steam cycle, the exergy flowing into the marked system is calculated by:

$$\psi_{\text{In}} = m_2\psi_2 + m_4\psi_4 + m_6\psi_6 \quad 3.32$$

The exergy output of the cycle marked with black-dotted lines is calculated by:

$$\psi_{\text{Out}} = m_5\psi_5 + m_1\psi_1 + m_3\psi_3 \quad 3.33$$

The exergy change of the geothermal fluid is calculated by:

$$\Delta\psi_{Geo} = m_{Geo}(\psi_{Geo\ In} - \psi_{Geo\ Out}) \quad 3.34$$

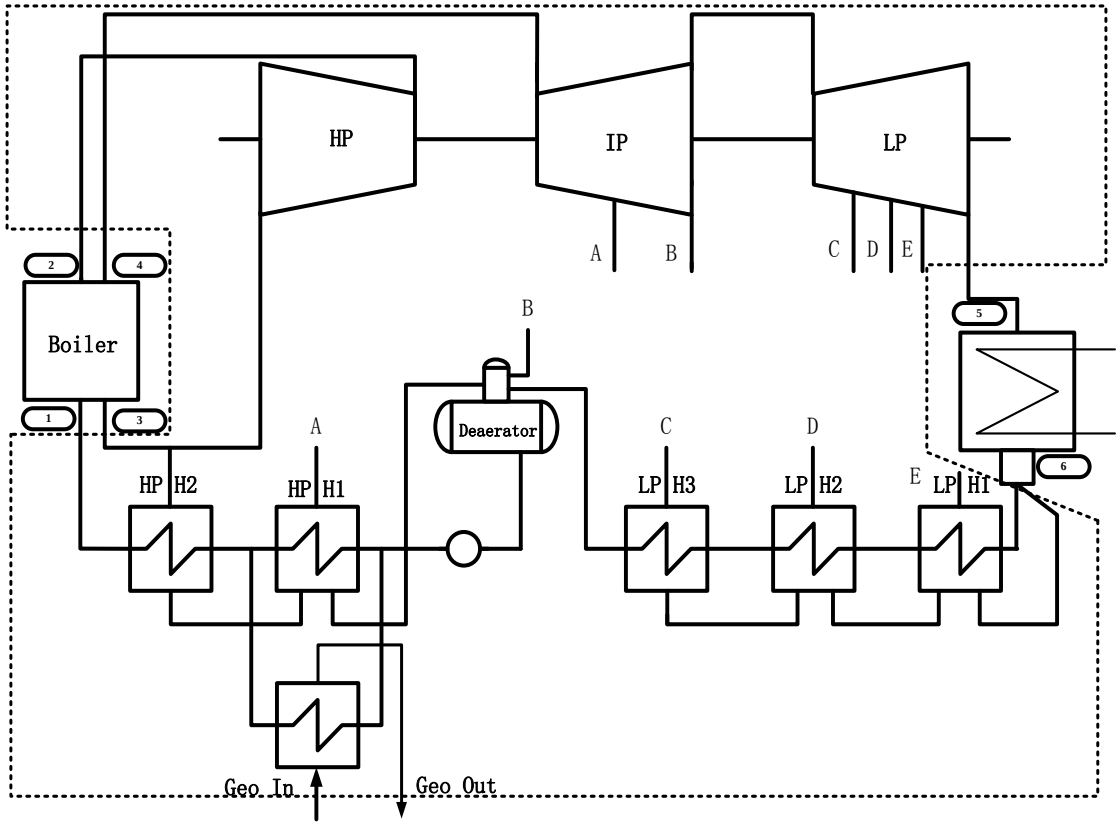

Figure 5.10 Schematic diagram of LOY YANG power plant (the dotted line indicates the boundary for exergy analysis, scenario 2)

Table 5.3 shows the exergy efficiency of LOY YANG power plant with and without geothermal fluid for the 4 scenarios. The results from table 5.3 show that when the geothermal fluid is integrated into the power plant, the efficiency of that power plant hardly changes. Compared with scenario 1 and scenario 4, the second efficiency of power plant at scenario 3 changes more than the other two scenarios; the reason is that at scenario 3, all the extraction steam is replaced by geothermal fluid; more geothermal

energy is integrated into the power plant, which has more influence on the power plant.

Table 5.3 Exergy efficiency of power plant without geothermal and four scenarios

Operational condition	Without geothermal	Scenario 1	Scenario 2	Scenario 3	Scenario 4
Power boosting	91.0%	90.9%	91.0%	91.8%	91.0%
Fuel saving		89.8%	89.8%	90.4%	89.7%

The exergy destruction is calculated by using mathematical modelling. Table 5.4 and 5.5 show the exergy input and output dotted line. Table 5.5 and 5.6 show the simulated result of the exergy destruction of each part of the power plant.

Table 5.4 Exergy input into the boiler

		Reference Condition	A is fully replaced	B is fully replaced	D is fully replaced	E is fully replaced
Exergy Input (MW)	Power Boosting	599.6	612.9	599.6	599.6	599.5
	Fuel saving		566.3	579.7	595.1	596.9

Table 5.5 Exergy destruction of condenser

Exergy destruction(MW)		Total	Special value (KJ/KG)
Reference condition		48.15	173.35
A is fully replaced	Power Boosting	55.4	173.35
	Fuel saving	49.6	173.35
B is fully replaced	Power Boosting	54.6	173.35
	Fuel saving	51.5	173.35
D is fully replaced	Power Boosting	53.0	173.35
	Fuel saving	51.8	173.35
E is fully replaced	Power Boosting	53.4	173.35
	Fuel saving	52.5	173.35

In mathematical modelling, the boiler and condenser are the components through which flow exergy enters and leave the power plant. Tables 5.4 and 5.5 show that the exergies are influenced by the utilization of the geothermal fluid. The reason is that when the geothermal fluid is integrated into the power plant, the mass flow rate of steam (of the feedwater) is changed, so that the exergy entering and outputted from the power plant also changes.

Table 5.6 Exergy destruction of a steam turbine

Exergy destruction(MW)		Total	HP	IP	LP
Reference condition		40.1	6.9	7.5	25.7
A is fully replaced	Power Boosting	49.9	6.9	7.8	35.2
	Fuel saving	47.2	11.8	7.8	27.5
B is fully replaced	Power Boosting	42.8	6.9	4.6	31.2
	Fuel saving	48.5	16.9	4.0	27.5
D is fully replaced	Power Boosting	41.4	6.9	7.5	27
	Fuel saving	48.5	15.4	7.8	25.4
E is fully replaced	Power Boosting	41.1	6.9	7.5	26.8
	Fuel saving	48.6	15.2	7.7	25.6

Tables 5.6 and 5.7 show the exergy destruction in the steam and feedwater. They show that, when the geothermal fluid is used to replace the extraction steam of the steam turbine, there is an increase in the exergy destruction in the steam turbine. The reason is that the replaced extraction steam expands through the steam turbine, which causes the exergy destruction in the steam turbine. However, the result in table 5.7 shows that there is a decrease in the exergy destruction in the feedwater heater. The reason is that extraction steam is the steam with a higher temperature, which means

more exergy destruction in the heat transfer process.

Table 5.7 Exergy destruction for each feedwater heater (except deaerator)

Exergy destruction(10^3kJ/s)		
Reference condition		27.1
A is fully replaced	Power Boosting	15.7
	Fuel saving	11.3
B is fully replaced	Power Boosting	14.7
	Fuel saving	12.8
D is fully replaced	Power Boosting	25.9
	Fuel saving	24.8
E is fully replaced	Power Boosting	24.8
	Fuel saving	23.9

Chapter 6

Economic case study

The economic performance of the GAPG technology is analysed in this chapter for a subcritical and a supercritical power plant. In this chapter, it is assumed that the geothermal well field is in close proximity to the power plant. The cost of electricity (COE) for the GAPG technology in the two power plants is calculated and compared with that of a flash cycle geothermal only power plant and a binary cycle geothermal only power plant.

6.1 Introduction

6.1.1 Geothermal well field and geothermal power plant

Geothermal Well field

A geothermal well field in Imperial County California, USA, is used as the Imperial case study by which to analyse the economic advantages of GAPG technology. The geothermal well field has 11 production wells which have an average depth of

1219m (4000ft) and a geothermal fluid temperature of 175-188℃, while the mass flow rate per production well is 91kg/s, and there are 13 rejection wells with an average depth of 2370m (4500ft) (DiPippo, 2008).

Binary cycle power plant

A binary cycle geothermal power plant was built in 1993 in the geothermal field. Table 6.1 summaries the geothermal power plant (DiPippo, 2008). According to Sones and Krieger (2000), only 7 wells of the geothermal well field were needed to meet the demand of the binary cycle power plant. .

Table 6.1 Technical performance of the binary cycle power plant (DiPippo, 2008)

Flash cycle power plant

A double flash geothermal power plant located in Cerro Prieto, Mexico, was chosen as the study case. The design specification for this plant is shown in Table 6.2 (Anon, 2000). It can be seen that, the geothermal flow rate of the geothermal fluid is 817.9 kg/s, and nine wells of geothermal well field were needed for the flash cycle power plant.

Table 6.2 Technical performance of flash cycle power plant (Anon, 2000)

6.1.2 Coal fired power plants

The coal fired power plants selected as case studies are a 580MW subcritical power plant and a 580 MW supercritical power plant, for which the design specifications and cost estimates of the power plant have been reported by the National Energy Technology Laboratory (NETL, 2007).

Subcritical coal fired power plant

The 580 MW subcritical steam cycle power plant has single reheater. Figure 6.1 shows the heat and steam balance of the 580 MW unit at design condition. From the information in Fig. 6.1, the capacity of the power plant, the efficiency of power generation and the consumption of coal are calculated and listed in Table 6.3.

Table 6.3 Simulated technical performance of subcritical power plant

Unit rated capacity	581.2MW
Efficiency of power generation	44.3%
Consumption of coal*	161.1ton/h

*The heat value of the coal is 29271 kJ/kg

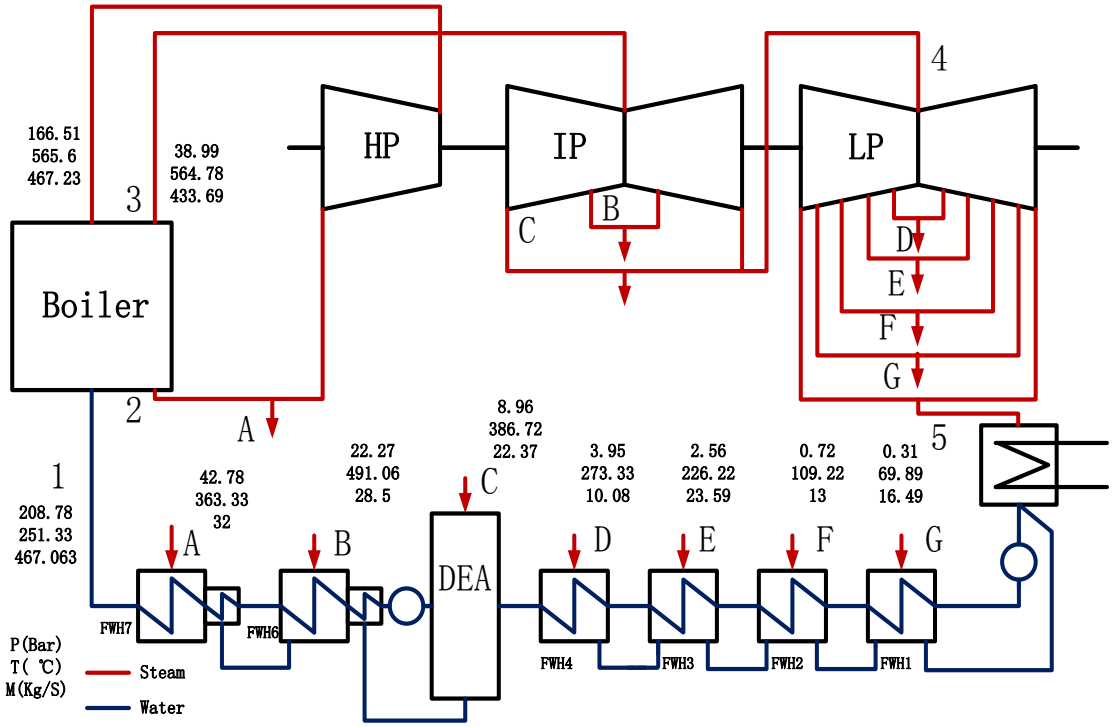

Figure 6.1 Heat and steam balance of the 580 MW unit at design conditions

The capital costs of the power plant are specific and include the capital costs of equipment, materials and the costs of labour. Estimation of the capital costs of the power plant were based on information from the National Energy Technology Laboratory (NETL, 2007), as given in Table 6.4, which shows that, including the cost of labour, the total capital costs of the power plant was $ 892,433,000 (US) in 2007.

The O&M costs of the power plant were provided by the National Energy Technology Laboratory (NETL, 2007). The cost of fuel and consumables is included. Table 6.5 shows the O&M costs of the power plant (NETL, 2007).

Table 6.4 Capital costs of the 580MW subcritical power plant (NETL, 2007)

Item	Total plant cost ($ 2007)
Coal & Sorbent handling	39,970,000
Coal & Sorbent prep & Feed	18,855,000
Feedwater & Misc. Bop Systems	74,674,000
PC Boiler	267,420,000
Flue Gas Cleanup	135,338,000
HRSG, ducting & Stack	39,104,000
Steam Turbine	114,004,000
Cooling Water system	40,003,000
Ash/Spent Sorbent Handling Sys	13,096,000
Accessory electric plant	52,203,000
Instrumentation & Control	21,371,000
Improvements to site	14,079,000
Buildings & Structures	62,315,000
Total	**892,433,000**

Table 6.5 Maintenance material costs (O&M Cost) of the subcritical power plant (NETL, 2007)

Consumables	Total Cost ($ 2007)
MU & WT Chem.	1,424,619
Limestone (ton)	1,103,371
Ammonia	3,496,290
SCR Catalyst	3,136,289
Fly Ash	592,641
Bottom Ash	512,385
Coal	62,175,757
Total	**83,254,111($ per year)**

Supercritical coal fired power plant

The second case study involved a 580 MW supercritical steam cycle power plant with a single reheater. Figure 6.2 shows the heat and steam balance of the plant at design conditions.

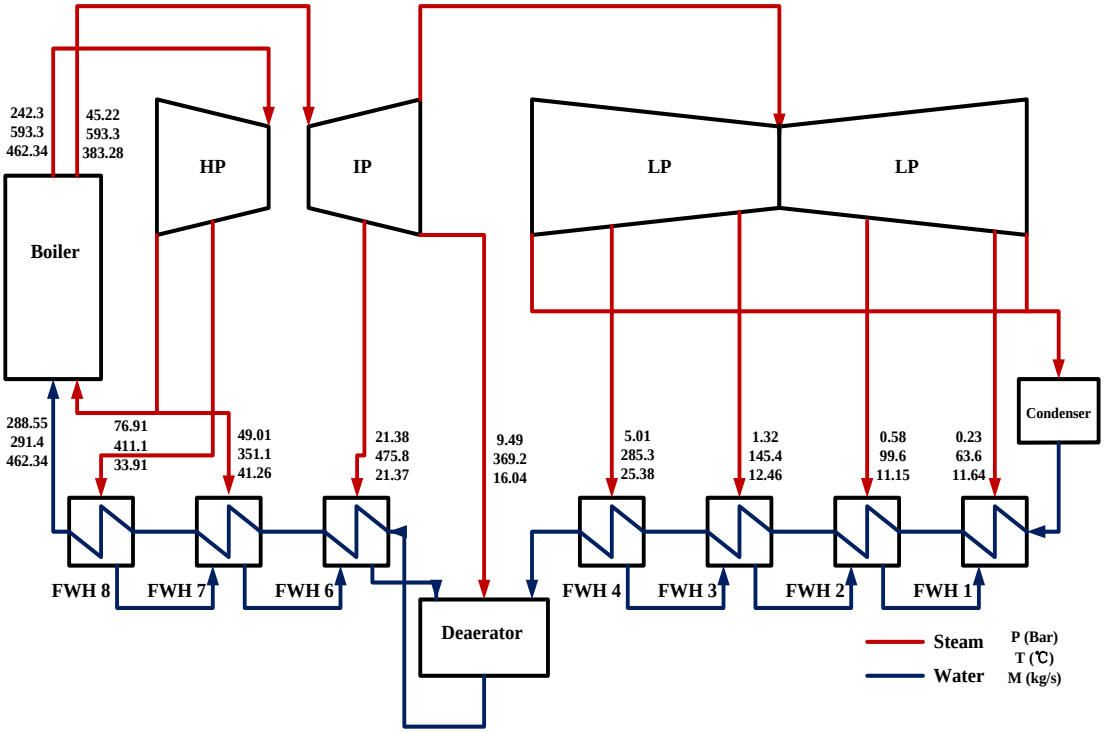

Figure 6.2 Heat and steam balance of the supercritical unit at design conditions

Table 6.6 Calculated technical performance of the supercritical power plant

Unit rated capacity	584MW
Efficiency of power generation	46.9%
Consumption of coal*	153.1ton/h

*The energy value of coal is 29271 kJ/kg

Table 6.6 shows the calculated performance of the supercritical power plant. The calculated output of the steam turbine is 580.5MW, the overall thermal efficiency of power plant is 46.6% and the consumption of coal is 153.1 ton/h.

Estimates of the capital costs of the power plant are shown in Table 6.7(NETL, 2007), including the cost of labour for construction. The total capital costs of the power plant were $905,901,000 (US) in 2007. The O&M costs of the power plant are shown in Table 6.8 (NETL, 2007).

Table 6.7 Capital costs of 580MW supercritical power plant (NETL, 2007)

Item	Total plant cost ($ 2007)
Coal & Sorbent handling	38,365,000
Coal & Sorbent prep & Feed	18,059,000
Feedwater & Misc. Bop Systems	79,149,000
PC Boiler	296,317,000
Flue Gas Cleanup	128,593,000
HRSG, ducting & Stack	37,291,000
Steam Turbine	115,948,000
Cooling Water system	37,370,000
Ash/Spent Sorbent Handling Sys	12,627,000
Accessory electric plant	51,068,000
Instrumentation & Control	21,555,000
Improvements to site	14,054,000
Buildings & Structures	55,506,000
Total	**905,901,000**

Table 6.8 Maintenance material costs (O&M Cost) of supercritical power plant (NETL, 2007)

Consumables	Total Cost ($ 2007)
MU & WT Chem.	1,009,427
Limestone (ton)	3,273,667
Ammonia	2,960,869
SCR Catalyst	553,798
Fly Ash	1,919,038
Bottom Ash	479,759
Fuel	68,217,892
Total	**78,414,450 ($ per year)**

6.1.3 Scenarios of the case study

In order to provide an economic comparison between the GAPG technology and traditional technologies (geothermal alone power plant), it is assumed that the subcritical coal fired power plant and supercritical coal fired power plant have been all built at Imperial County as has the geothermal only power plants (binary flash cycles). Four scenarios were examined in the case study to analyse the economic advantages of the GAPG technology. In these four scenarios, the silica concentration of geothermal fluid is concerned in this study.

Table 6.9 Four scenarios of economic case study

Scenario A	Geothermal resources is used to power the **binary cycle power plant**
Scenario B	Geothermal resources is used to power the **flash cycle power plant**
Scenario C	Geothermal fluid is used to replace the extraction steam of **FWH 4, 3, 2 in the subcritical power plant**
Scenario D	Geothermal fluid is used to replace the extraction steam of **FWH 4, 3 and 2 in the supercritical power plant**

Table 6.9 summarises the four scenarios. In scenario A, it is assumed that a binary cycle power plant is built in Imperial County using geothermal resources to produce electricity. In scenario B, it is assumed that a double flash cycle power plant is built in Imperial County using geothermal resources to produce electricity power. In scenario C, it is assumed that geothermal fluid (180℃) is used to replace the extraction steam of the subcritical power plant at points D, E, F as shown in Fig. 6.3. In scenario D, it is assumed that geothermal fluid(180℃) is used to replace the extraction steam of FWH 4,

3 and 2 for the supercritical power plant, as shown in Fig. 6.4.

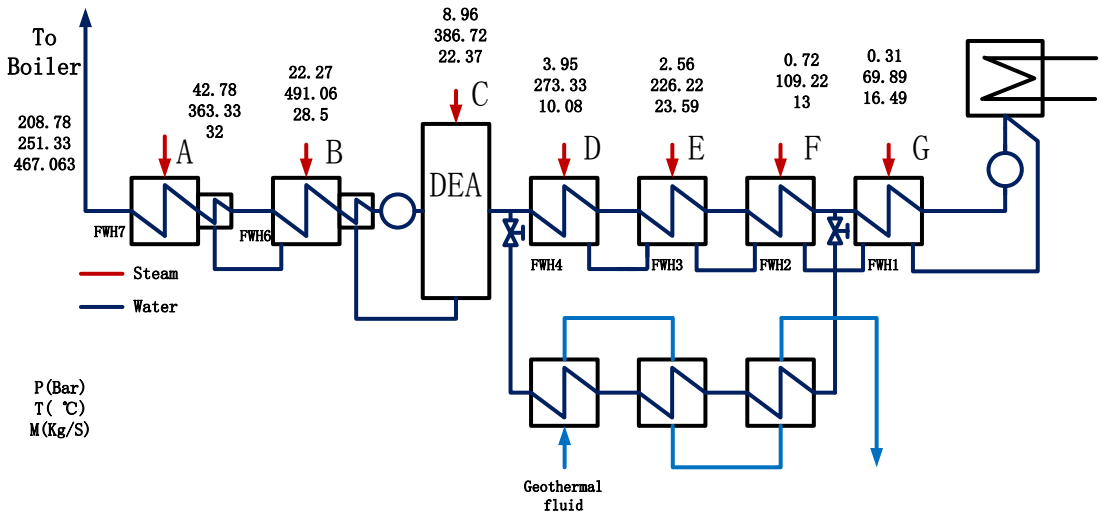

Figure 6.3 Schematic diagram of the subcritical power plant feedwater system with the GAPG technology in which FWH 4,3,2 are fully replaced by geothermal fluid.

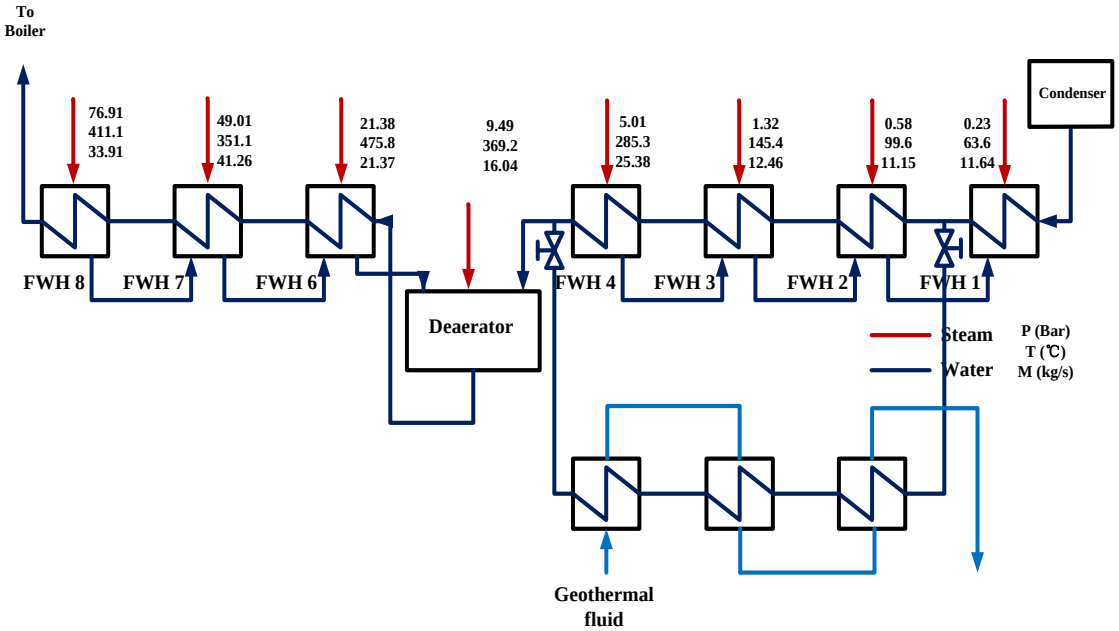

Figure 6. 4 Schematic diagram of the supercritical power plant feedwater system with the GAPG technology in which FWH 4,3,2 are fully replaced by geothermal fluid

6.2 Results

6.2.1 Technical performance of GAPG technology

In scenario C, the power boosting mode and fuel saving mode of the GAPG technology are both compared with the geothermal alone power plant. The technical performance of the GAPG in each case is shown in table 6.10. As shown, an extra power output of 22 MW was predicted with 385.7 kg/s geothermal fluid mass flow rate, in the power boosting mode. In the fuel saving mode, a total of 580MW power out remain the same, at which 21 MW is attributed to the 373.1 kg/s geothermal flow. As the production rate per geothermal well is 91kg/s, only 5 production geothermal wells and 6 injection wells were needed to meet the GAPG requirement in both the power boosting mode and fuel saving modes.

Table 6.10 Technical performance of the GAPG technology (for the subcritical power plant).

Power output of power plant (MW)	581
Extra power output of GAPG, power boosting (MW)	22
Power output caused by GAPG, fuel saving (MW)	21
Mass flow rate of geothermal fluid (kg/s) (power boosting)	385.7
Mass flow rate of geothermal fluid (kg/s) (fuel saving)	373.1

In scenario D, the power boosting mode and fuel saving mode of the GAPG technology are compared with the geothermal alone power plant. The technical performance of the GAPG technology of each case is shown in Table 6.11. As shown in

Table 6.11, the power output attributed to the GAPG technology with the supercritical power plant is 23 MW for the power boosting mode and 22 MW for the fuel saving mode, the mass flow rate of geothermal fluid is 351.4 kg/s for power boosting mode and 348.4 kg/s for fuel saving mode. As the mass flow rate per production well is 91kg/s, only 4 production geothermal wells and 5 injection wells are needed to meet this load for both the power boosting and the fuel saving modes.

Table 6.11 Technical performance of the GAPG technology (for the supercritical power plant).

Power output of Power plant (MW)	584
Power output of GAPG, power boosting (MW)	23
Power output of GAPG, fuel saving (MW)	22
Mass flow rate of geothermal fluid (kg/s) (power boosting)	351.4
Mass flow rate of geothermal fluid (kg/s) (fuel saving)	348.4

6.2.2 Cost of geothermal power plant

Calculating the COE of the geothermal alone power plant includes calculating the capital costs of the power plant system and the O&M costs of the power plant. Chapter 3 has introduced the method to calculate the capital costs of geothermal well fields, a geothermal alone power plant, and the O&M costs of a geothermal alone power plant.

Tables 6.12 and 6.13 show the capital costs of geothermal well fields (binary cycle power plant) and the capital costs and O&M costs of the binary cycle power plant. For

the subcritical power plant with GAPG technology, the power output "produced" by GAPG technology is 22 MW for the power boosting mode and 21 MW for the fuel saving mode. For the supercritical power plant, the power output "produced" by the GAPG technology is 23 MW for the power boosting mode and 22 MW for the fuel saving mode, while the binary cycle power plant is 44MW with 12 units. It is assumed that the power output of the binary cycle power plant is 22 MW with 6 units and 4 production wells and 5 injection wells serving the binary power plant. The capital costs of geothermal wells are calculated by equation 3.36 and the O&M costs of geothermal wells are assumed to be 1% of the geothermal well capital costs per year. The capital costs of the binary cycle geothermal power plant is calculated as $ per kW (kW is the power output of the power plant) based on the Geothermal Electric Technologies Evaluation Model (Entingh, 2006b). As the temperature of the geothermal fluid is 180℃,the capital costs of the binary cycle power plant are calculated by equations 3.39 and 3.41. O&M costs of the power plant are calculated by an experimental formula provided by Sanyal (equation 3.49).

Table 6.12 Costs of geothermal well fields (for the binary cycle power plant, 2004$)

Number of production wells	4
Number of injection wells	5
Capital cost per production well (k$)	1,053
O&M cost per production well (k$/year)	10.5
Capital costs per injection well (k$)	1,222
O&M cost per injection well (k$/year)	12.2
Surface equipment cost per well (k$/Well)	100
Total Well capital (k$)	**11223**
Total O&M cost (k$/year)	**103**

Table 6.13 Capital cost and O&M cost of the binary cycle power plant (2004$)

Capital cost of power plant ($/kW)	1873
Total capital cost of power plant ($)	44,951,932
O&M cost of power plant (cent/kWh)	1.91

Table 6.14 Costs of geothermal well fields (for the double flash cycle power plant, 2004$)

Number of Production wells	10
Number of Injection wells	11
Capital cost per Production well (k$)	1,053
O&M cost per Production well (k$/year)	10.5
Capital costs per Injection well (k$)	1,222
O&M cost per Injection well (k$/year)	12.2
Surface equipment cost per well (k$/Well)	100
Total Well capital (k$)	26076
Total O&M cost (k$/year)	240

Table 6.15 Capital cost and O&M cost of the double flash cycle power plant (2004$)

Capital cost of power plant ($/kW)	880.34
Total capital cost of power plant ($)	21,128,144
O&M cost of power plant (cent/kWh)	1.91

Like the binary plant, the capital costs of the double flash cycle geothermal power plant are also calculated as $ per kW (the kW is the power output of power plant), and the plant costs are derived for major equipment in the power plant. The costs of each component of the power plant are based on the gross binary effectiveness, which is calculated by equation 3.42, and capital costs of each of the components of the power plant are calculated by equations 3.43 to 3.48. The O&M costs of double flash cycle

power plant are also calculated by equation 3.50. Tables 6.14 and 6.15 show the capital costs of the geothermal well fields (double flash cycle power plant) and the capital costs and O&M costs of the double flash cycle power plant.

Table 6.16 Costs of geothermal well fields (subcritical GAPG technology, 2004$)

Number of Production wells (Power boosting)	5
Number of Injection wells (Power boosting)	6
Capital cost per Production well (k$ Power boosting)	1,053
O&M cost per Production well (k$/year Power boosting)	10.5
Capital costs per Injection well (k$ Power boosting)	1,222
O&M cost per Injection well (k$/year Power boosting)	12.2
Surface equipment cost per well (k$/Well Power boosting)	100
Total Well Capital (k$ Power boosting)	13699
Total O&M cost (k$/year Power boosting)	125
Number of Production wells (Fuel saving)	5
Number of Injection wells (Fuel saving)	6
Capital cost per Production well (k$ Fuel saving)	1,053
O&M cost per Production well (k$/year Fuel saving)	10.5
Capital costs per Injection well (k$ Fuel saving)	1,222
O&M cost per Injection well (k$/year Fuel saving)	12.2
Surface equipment cost per well (k$/Well Fuel saving)	100
Total Well Capital (k$ Fuel saving)	13699
Total O&M cost (k$/year Fuel saving)	125

6.2.3 Costs of GAPG technology

Subcritical power plant

The costs of GAPG technology include the capital costs of geothermal well fields and the capital costs of geothermal preheaters. As pointed out previously, there are 5 production wells and 6 injection wells of a geothermal well that are needed to meet the GAPG technology of a subcritical power plant and 5 production wells and 6 injection

wells for the GAPG technology of a supercritical power plant. Table 6.16 shows the costs of the geothermal wells for the GAPG technology of the subcritical power plant while the costs of the geothermal wells of the GAPG technology for the supercritical power plant are shown in table 6.17. The capital costs of production, injection wells and the O&M costs of the geothermal well field are calculated. The surface equipment cost per well is assumed to be 100 K$ (US) in case study.

Table 6.17 Costs of geothermal well fields (supercritical GAPG technology, 2004$)

Number of Production wells (Power boosting)	4
Number of Injection wells (Power boosting)	5
Capital cost per Production well (k$ Power boosting)	1,053
O&M cost per Production well (k$/year Power boosting)	10.5
Capital costs per Injection well (k$ Power boosting)	1,222
O&M cost per Injection well (k$/year Power boosting)	12.2
Surface equipment cost per well (k$/Well Power boosting)	100
Total Well Capital (k$ Power boosting)	11223
Total O&M cost (k$/year Power boosting)	103
Number of Production wells (Fuel saving)	4
Number of Injection wells (Fuel saving)	5
Capital cost per Production well (k$ Fuel saving)	1,053
O&M cost per Production well (k$/year Fuel saving)	10.5
Capital costs per Injection well (k$ Fuel saving)	1,222
O&M cost per Injection well (k$/year Fuel saving)	12.2
Surface equipment cost per well (k$/Well Fuel saving)	100
Total Well Capital (k$ Fuel saving)	11223
Total O&M cost (k$/year Fuel saving)	103

6.2.4 COE of four scenarios

The COE for the four scenarios is calculated by equation 3.35. Calculating the COE includes information about initial capital costs, discount rates, opportunity cost of

capital, cost of operation and maintenance and cost of the power plant, power plant life and the amount of energy production in the power plant life. The initial capital costs and O&M costs of the GAPG technology, the geothermal well field and the geothermal alone power plant are shown in table 6.12 to 6.17. In this case study, the discount rate is assumed to be 4%, the opportunity cost of capital is assumed to be 9 %, and the power plant life span is assumed to be 30 years.

Table 6.18 shows the COE of four scenarios of the economic case study. The result shows that the COE of the GAPG technology is lower than the COE of the traditional power plant (geothermal alone power plant). Compared with the geothermal alone power plant, the GAPG technology has lower capital and O&M costs. The reason is that the GAPG technology is based on the coal fired power plant which can reduce the capital cost of the GAPG technology, As shown in table 6.1, the GAPG capital costs of subcritical power plant are 3.32 cent/kWh for the power boosting mode and 3.4 cent/kWh for the fuel saving mode, while the plant capital costs are 5.06 cent/kWh. A comparison of the COEs of the GAPG technology for the supercritical power plant and for the subcritical power plant finds the COE of the supercritical power plant to be lower than the COE of the subcritical power plant. The reason is that the geothermal well field cost of the GAPG technology integrated into the supercritical power plant and well field O&M cost is lower than the GAPG technology integrated into the subcritical power plant.

Table 6.18 COE of four scenarios for the economic case study (2007$)

Scenario A Binary cycle power plant (cent/kWh)	
Well field Capital	1.49
Well field O&M	0.26
Plant Capital	5.97
Plant O&M	2.25
COE	**9.97**
Scenario B Flash power plant (cent/kWh)	
Well field Capital	3.47
Well field O&M	0.60
Plant Capital	2.81
Plant O&M	2.25
COE	**9.13**
Scenario C GAPG technology (subcritical power plant) (cent/kWh)	
Well field Capital (Power Boosting)	1.96
Well field O&M (Power Boosting)	0.31
GAPG Capital (Power Boosting)	3.32
COE(Power Boosting)	**5.59**
Well field Capital (Fuel saving)	2.01
Well field O&M (Fuel saving)	0.32
GAPG Capital (Fuel saving)	3.40
COE(Fuel saving)	**5.73**
Scenario D GAPG technology(supercritical power plant) (cent/kWh)	
Well field Capital (Power Boosting)	1.50
Well field O&M (Power Boosting)	0.24
GAPG Capital(Power Boosting)	3.49
COE(Power Boosting)	**5.23**
Well field Capital(Fuel saving)	1.58
Well field O&M(Fuel saving)	0.25
GAPG Capital(Fuel saving)	3.7
COE(Fuel saving)	**5.53**

*The costs determined by using the Chemical Engineering Plant Cost Index.

Chapter 7

Conclusions

With the increase in demand for energy and the need for environmental protection, geothermal energy, as a renewable resource, is increasing in its attractiveness. Stand alone geothermal power stations have been established all over the world. Integrating a geothermal resource into a conventional fuel fired Rankine cycle power plant, through the so called Geothermal Aided Power Generation (GAPG) concept, can significantly increase the efficiencies and reduce the costs of geothermal energy required for stand alone geothermal power generation

A mathematical model and the Geothermal Aided Power Generation Evaluation Model (GAPGEM) software has been developed based on thermodynamic principles to simulate the technical and economic performance of the steam Rankine power plant and the GAPG technology at varying operational conditions.

Through the simulation using the GPAGEM software, this study draws the following conclusions:

- The GAPG technology has higher thermodynamic first law efficiency than the geothermal alone power plants. The results in chapter 5 show that, compared with the binary cycle power plant, the GAPG technology has higher first law efficiency, especially when using geothermal fluid with a high temperature. These results show that, when geothermal fluid at 260℃ is used to fully replace the high pressure feedwater heater (FWH) of the power plant (with a concern for the silica precipitation of the geothermal fluid), the efficiency of GAPG in the power boosting mode is 41.6% and that for the fuel saving mode is 42.7%, while the binary plant efficiency at 260℃ is about 21%. The results in chapter 5 also show that, when the geothermal fluid at 210℃ is used to fully replace one stage of the FWH of the power plant, the efficiency of the GAPG in the power boosting mode is 28.4% and that in the fuel saving mode is 27.4%, while the binary plant efficiency at 210℃ is 16%.
- In the GAPG technology, the geothermal fluid does not directly enter into the steam turbine to produce work but is used to replace the extraction steam to preheat the feedwater of the power plant. The efficiency of the GAPG technology is no longer limited by the temperature of geothermal fluid, but rather by the maximum temperature of the Rankine cycle power plant.
- Utilization of the existing infrastructure of conventional fossil fired

power plants can demonstrate the economic advantages of the GAPG technology. The results in chapter 6 show that compared with the geothermal alone power plant (both the binary cycle power plant, and the flash cycle power plant), the GAPG technology has the lower cost of electricity (COE). The reason is that the GAPG technology has lower capital plant and O&M costs. The COE of the subcritical power plant discussed in chapter 6 is 5.59 cent/kWh for the power boosting mode and 5.73 for the fuel saving mode. The COE of the supercritical power plant in chapter 6 is 5.23 cent/kWh for the power boosting model and 5.53 cent/kWh for the fuel saving mode. However, the COE of the binary cycle power plant and the flash cycle power plant is 9.97 cent/kWh and 9.13 cent/kWh, respectively.

- The GAPG technology is flexible in its utilization. Depending on the difference between geothermal temperature and silica concentration, the GAPG technology can be used to replace different stages of the feedwater heater. Different operational modes can be used to satisfy different levels of electricity demand.

- Low to medium temperature geothermal resources can be used in the GAPG technology to generate power efficiently.

Chapter 8

Future Work

As pointed in Chapter 3, in geothermal fluid, the rates of silica deposition and polymerization is determined by the PH and salt concentration of geofluid, the residence time and temperature of geofluid (Gunnarsson and Arnorsson 2005) and the silica scaling occurs in geothermal wells (both production wells and injection wells), pipes of well field and geothermal feedwater system. In this study, the silica precipitate rate is calculated as a function of temperature which is based on the report of Brown and Bacon (2009). In the future, the GAPGEM software will be improved by paying attention to concern the impact of the PH, salt concentration of geofluid and silica scaling on in geothermal wells (both production wells and injection wells), pipes of well field and geothermal feedwater system on the economic performance of the GAPG technology.

The technology performance of the fuel saving mode of the GAPG technology has been calculated by using the GAPGEM software. However, the mass flow of steam

entering into the steam has some deviation during the calculation process due to the mass flow loss of the turbine. Future work should concern itself with the mass flow loss of turbines so as to reduce the deviation in the technical performance of the fuel saving mode.

References

Anon 2000, *List of Geothermal Power Plant,* Mitsubishi Heavy Industries. Ltd., Yokohama.

Baziotopoulos, C. 2002, 'Utilising solar energy within conventional coal fired power stations', Master Thesis, Deakin University, Australia.

Bettocchi, R, Cantore, G, Gadda, E, Negri, D and Montenegro, G 1992, 'Thermodynamic and economic analysis on geothermal integrated combined cycle power plants,' in *Proceeding of 2nd Florence World Energy Research Symposium*, Florence, pp. 239-255.

Bertani, R. 2005, 'World Geothermal Power Generation in the period 2001-2005', *Geothermics*, Vol.34, no.6, pp.651-690.

Bhuana, SD, Ashman, PJ, Graham, N 2009, 'Silica deposition in enhanced geothermal systems', in *Proceeding of the Australia Geothermal Conference 2009*, Australian Geothermal Energy Association, Brisbane.

Bidini, G, Desideri, U, Di Maria, F, Baldacci, A, Papale, R and Sabatelli, F 1998, 'Optimization of an integrated gas turbine-geothermal power plant', *Energy Conversion*

and Management, vol. 39, pp. 1945-1956.

Brown, K.L. & Bacon, L.G. 2009, 'Pilot plant experiments at Wairakei Power Station', *Geothermics*, Vol.38, pp.64-71.

Bruhn, M 2002, 'Hybrid geothermal-fossil electricity generation from low enthalpy geothermal resource: geothermal feedwater preheating in conventional power plant', *Energy*, vol.27, pp. 329-346.

Buchta, J 2009, 'Green power from conventional steam power plant combined with geothermal wells,' in *Proceeding of the IEEE International Conference on Industrial Technology*, Monash University, Australia.

Carson, C.C & Lin, Y.T. 1981, 'Geothermal well costs and their sensitivities to changes in drilling and completion operations', in *Proceeding of the International Conference Geothermal Drilling and Completions Technology,* Albuquerque, NM.

Cengel, Y, Boles, MA 2002, *Thermodynamics: an engineering approach*, 4th edn, Mc-Hill Company, Columbus, OH.

Chan, S.H 1989, 'A Review on solubility and polymerization of silica', *Geothermics*, vol.18, No.1/2, pp. 49-56.

DiPippo, R, Khalifa, HE, Correia, RJ, Kestin, J 1978, 'Fossil superheating in geothermal steam power plants', in *Proceeding of the Intersoc Energy Convers Eng Conference 13th,* San Diego California, USA.

DiPippo, R, Kestin, J and Khalifa, HE 1981, 'Compound hybrid geothermal-fossil power plants', *Journal of Engineering for Power*, vol. 103, pp. 797-804.

DiPippo, R 2008, *Geothermal Power Plants: Principles, Applications, Case Studies*

and Environmental Impact, 2nd edn, Butterworth-Heinemann, Oxford.

Entingh, D.J. 2006, *Geothermal Electricity Technology Evaluation Model (GETEM): Volume I-Technical reference Manual*, US Dept. of Energy.

Entingh, D.J. 2006, *Geothermal Electricity Technology Evaluation Model (GETEM): Volume III-Detailed Technical Appendixes*, US Dept. of Energy.

Entingh, D.J. & Mines, G.L 2006, 'A framework for evaluating research to improve U.S geothermal power systems', *Geothermal Resources Council Transactions*, Vol. 29

Gupta, M.K. and Kaushik, S.C. 2009, 'Exergetic utilization of solar energy for feed water preheating in a conventional thermal power plant', *International Journal of Energy Research*, vol. 33, pp.593-604.

Gunnarsson, I and Arnorsson S. 2005, 'Impact of silica scaling on the efficiency of heat extraction from high-temperature geothermal fluids', *Geothermics*, vol. 34, pp.320-329

Hu, J.E, Mills, R.D, Morrison, L.G, Lievre, P. 2003, 'Solar power boosting of fossil fuelled power plants', In *Proceedings of ISES solar world congress 2003*, ISES ,Goteborg, pp. 14-19.

Hu, E., Yang, YP., Nishimura, A., Yilmaz, F. and kouzani, A 2010, 'Solar thermal aided power generation', *Applies Energy*, vol.87, no. 9, pp. 2881-2885.

Hu, E, Nathan, G & Battye, D 2010, 'An efficient method to generate power from low to medium temperature solar and geothermal resources', in *Proceeding of the Chemeca 2010 Conference*, Institution of Chemical Engineers in Australia (IChemE), Australia.

Kestin, J, DiPippo, R, Khalifa, HE 1978, 'Hybrid geothermal-fossil power plants', *Mechanical Engineering*, Vol. 100, pp. 28-35

Khalifa, HE 1978, 'Hybrid power plants for geo-pressured resources', in *Processing of 5th Annual Geothermal Conference and Workshop*, Electric power Research Institute, Washington D.C.

Khalifa, HE, DiPippo, R and Kestin, J 1978, 'Geothermal preheating in fossil-fired steam power plants', in *Processing of Intersoc Energy Convers Eng Conf 13th*, NASA Astrophysics Data System, San Diego, vol. 2, pp. 1068-1073.

Kolb, GJ 1978, 'economic evaluation of solar-only and hybrid power towers using molten salt technology', *Solar Energy*, Vol.62, no. 1, pp. 51-61.

Kingston Reynolds Thom & Allardice Ltd, 1980, An Investigation into hybrid geothermal / gas power plants, New Zealand Energy Research and Development Committee,

Kreith, F & Goswami, Y.D. 2007, Handbook of Energy Efficiency and Renewable Energy, Boca Raton, FL.

Mansure, A.J., Bauer,S.J. & Livesay, B.J. 2005a, 'Geothermal Well Cost Analyses 2005', GRC *Transactions*.

Mansure, A.J., Bauer,S.J. 2005b, 'Advances in Geothermal Drilling Technology: reducing cost while improving longevity of the well', GRC *Transactions*.

Moran, M.J. 1986, *Availability Analysis: A Guide Efficient Energy Use*, Prentice-Hall, New Jersey.

National Energy Technology Laboratory (NETL), 2007, *Cost and Performance*

Baseline for Fossil Energy Plants, Volume 1: Bituminous Coal and Natural Gas to Electricity Final Report, National Energy Technology Laboratory, Pittsburgh.

Rimstidt, J.D. & Barnes, H.L 1980, 'The kinetics of silica-water reactions', *Geochimica et Cosmochimica Acta*, Vol. 44, pp. 1638-1639.

Rournier, R.O. & Rowe, J.J. 1966, 'Estimation of underground temperatures from the silica content of water from hot springs and wet-steam wells', *American Journal of Science*, Vol. 264, pp.685-697.

Sones, R., Krieger, Z. 2000, 'Case Histroy of the Binary Power Plant Development at the Heber, California Geothermal Resources', in *Proceedings of World Geothemral Congress 2000,* International Geothermal Association, Morioka ,pp. 2217-2219.

Sanyal, S.K. 2004, 'Cost of geothermal power and factors that affect it', in *Proceeding of the Twenty-Nine Workshop on Geothermal Reservoir Engineering*, Stanford University, Stanford, California.

Stodola, A 1927, *Steam and gas turbines*, McGraw-Hill, New York.

U.S. Energy Information Administration, 2011, International *Energy Outlook 2011*, U.S. Energy Information Administration, Washington DC.

You, Y. and Hu, E. 1999, 'Thermodynamic advantages of using solar energy in the regenerative Rankine power plant', *Applied Thermal Engineering*, vol.19, pp.1173-1180.

You, Y. and Hu, E. 2002, 'A medium-temperature solar thermal power system and its efficiency optimization', *Applied Thermal Engineering*, vol.22, pp.357–364.

Yan, Q, Yang, Y, Nishimura, A, Kouzani, A & Hu, E 2010, 'Multi-points and

Multi-level Solar Integration into a Conventional Coal-Fired Power Plant', *Energy&Fuels*, Vol.24, pp.3733-3738.

Yang, YP, Yan, Q. Zhai, RR., Kouzani, A. and Hu, E. 2011, 'An efficient way to use medium-or-low temperature solar heat for power generation integration into a conventional power plant', *Applied Thermal Engineering*, vol. 31, no. 2-3, pp. 157-162.

Zoschak, R.J. and Wu, S.F. 1975, 'Studies of the direct input of solar energy to a fossil-fuelled central station steam power plant', Solar Energy, vol. 17, No.5, pp. 297-305.